ALMA MATER STUDIORUM
UNIVERSITÀ DI BOLOGNA

in cotutela con Università "**Iuliu Hatieganu" University of Medicine and Pharmacy, Cluj-Napoca, Romania**

DOTTORATO DI RICERCA IN

Scienze Mediche Generali e Scienze dei Servizi

Ciclo XXXVII

Settore Concorsuale: 06/B1 Medicina interna

Settore Scientifico Disciplinare: MEDS-05/A Medicina interna

METABOLIC DYSFUNCTION-ASSOCIATED STEATOTIC LIVER DISEASE: NON-INVASIVE ASSESSMENT OF DISEASE PROGRESSION

Presentata da: *MADALINA-GABRIELA INDRE*

Coordinatore Dottorato

Prof.ssa Susi Pelotti

Supervisore

Prof. Fabio Piscaglia

Prof.ssa Lucia Maria Procopciuc

Esame finale anno 2025

DOCTORAL THESIS SYNOPSIS

INTRODUCTION

This doctoral thesis is the result of a joint PhD program between the University of Medicine and Pharmacy "Iuliu Haţieganu", Cluj-Napoca, Romania, under the supervision of Prof. Dr. Lucia Maria Procopciuc, and Alma Mater Studiorum University of Bologna, Bologna, Italy, under the guidance of Prof. Fabio Piscaglia. The central focus of this thesis was the metabolic dysfunction-associated steatotic liver disease (MASLD), a liver condition that has seen rising prevalence and incidence in recent years, making it the most common type of liver disease today.

The progression of MASLD to more advanced stages, such as advanced fibrosis and cirrhosis, significantly increases the risk of developing important events in the course of the disease. Predicting disease progression through non-invasive methods represents a dynamic and highly relevant field of research with significant implications for patient care.

Therefore, a part of my clinical research focused on deepening our understanding of the progression of MASLD to the more advanced stages by using non-invasive ultrasound-based elastography techniques, including vibration-controlled transient elastography (VCTE), VCTE-based scores, and two-dimensional shear wave elastography (2D-SWE).

I validated the VCTE-based scores—Agile 3+, Agile 4, and FAST scores—within a cohort of individuals of Caucasian descent for the very first time. Utilizing a multi-level random effects model meta-analysis, I established standardized cut-off values for 2D-SWE that distinguish between different stages of liver fibrosis in patients with biopsy-proven MASLD, applicable at varying pre-test probabilities. These cut-off values are designed for use in both primary care and specialized healthcare settings.

Additionally, I investigated the benefits of the treatment with non-selective beta-blockers (NSBB) in patients with compensated cirrhosis, emphasizing its role in preventing the first decompensation event. Notably, I demonstrated that patients with small gastroesophageal varices and porto-systemic shunts can also derive significant benefits from this treatment. My research demonstrated that the presence of type 2 diabetes mellitus (T2DM) acts as an independent risk factor for the onset of the first decompensation event, regardless of etiology.

THE CURRENT STATE OF KNOWLEDGE

Metabolic dysfunction-associated steatotic liver disease (MASLD), previously known as non-alcoholic fatty liver disease (NAFLD), poses a growing challenge for healthcare systems due to its increasing prevalence. Recent data shows a rise from 25.5% in 2005 to 37.8% in 2016, with 25% of cases progressing to metabolic dysfunction-associated steatohepatitis (MASH) within three years. MASH accounts for 12% of liver transplants in Europe and can lead to severe liver complications, including cirrhosis and hepatocellular carcinoma. Historically diagnosed through liver biopsy, MASLD's multifactorial nature and biopsy limitations have spurred the need for non-invasive diagnostic methods. Fibrosis stage remains a critical predictor of mortality, highlighting the importance of early detection and monitoring. Advances in non-invasive tests,

particularly ultrasound elastography, are revolutionizing diagnostics by reducing biopsy reliance and enhancing surveillance strategies.
All liver diseases cause structural changes that affect biomechanical properties, measurable through elastography. This can be done using ultrasound-based techniques such as vibration-controlled transient elastography (VCTE) and two-dimensional shear wave elastography (2D-SWE).
Recently developed and validated VCTE-based scores, Agile 4 and Agile 3+, are designed to identify cirrhosis (F4) and advanced fibrosis (≥F3), respectively, in patients with MASLD, particularly within specialized liver clinics; yet they were not validated yet in specific populations, such as those of Caucasian descent. The FibroScan-AST (FAST) score was developed and validated in 2020 for the non-invasive identification of patients with MASH who have significant activity and fibrosis.

Even though the use of 2D-SWE for ton-invasive liver fibrosis assessment has rapidly increased, it still lacks cut-off standardization and robust validation.
Clinically significant portal hypertension (CSPH), a primary factor in cirrhosis decompensation, is characterized by a hepatic venous pressure gradient (HVPG) of 10 mmHg or higher. An HVPG value ≥10 mmHg identifies patients with compensated advanced chronic liver disease (cACLD) at elevated risk of decompensation, this being of outmost importance for disease management and prognosis. Recent observations suggest that patients with advanced MASLD may face a higher prevalence of portal hypertension-related decompensation events at any given hepatic venous pressure gradient (HVPG) compared to patients with other etiologies. Moreover, decompensation in advanced MASLD may occur at lower HVPG levels compared to patients with other liver disease etiologies.

The adaptation of this knowledge for advanced MASLD and MASH is currently an active area of research.

PERSONAL CONTRIBUTIONS

Study 1: FAST and Agile–the MASLD drift: Validation of Agile 3+, Agile 4 and FAST scores in 246 biopsy-proven NAFLD patients meeting MASLD criteria of prevalent Caucasian origin

Work hypothesis/ objectives: The study aimed to evaluate the effectiveness of Agile 3+, Agile 4, and FAST scores in distinguishing advanced fibrosis (≥F3), cirrhosis (F4), and fibrotic MASH (MASH + NAS ≥4 + F ≥2) within a cohort of biopsy-proven MASLD patients from a tertiary medical center in Cluj-Napoca, Romania. Our specific objectives were to assess the performance of Agile 3+ in predicting advanced fibrosis (≥F3), Agile 4 in predicting cirrhosis (F4), and the FAST score in identifying fibrotic MASH, and to determine whether these scores provide better diagnostic accuracy than the existing NITs in these scenarios.

Material and methods: A cohort of 246 patients with MASLD from the Medical 3 Clinic in Cluj-Napoca, Romania, was retrospectively followed during the period from January 2007 to July 2023. The diagnostic performance of Agile 3+, Agile 4, and FAST scores was assessed through AUROC curves, and the DeLong test was employed to compare the diagnostic performance of these indices. Concordance between "grey zones" was examined using McNemar's test, with statistical significance set at $p < 0.05$.

Results: Among 246 patients, 113 (45.9%) were women, and 75 (30.5%) presented diabetes. Agile 3+ and Agile 4 demonstrated excellent performance in identifying ≥F3 and F4, achieving AUROCs of 0.909 and 0.968, while the FAST score yielded acceptable results in distinguishing fibrotic NASH. When compared to FIB-4 and LSM-VCTE, both Agile 3+ and Agile 4 performed better than FIB-4 and had a similar performance to LSM-VCTE, but with higher diagnostic accuracy, hence reducing the grey zone.

Conclusions: Agile 3+ and Agile 4 are reliable, non-invasive tests for identifying advanced fibrosis or cirrhosis in MASLD patients, while FAST score demonstrated moderate performance in identifying fibrotic NASH.

Study 2: Diagnostic accuracy of two-dimensional shear wave elastography (2D-SWE) ultrasound for liver fibrosis assessment in metabolic dysfunction-associated steatotic liver disease (MASLD): A multi-level random effects model meta-analysis

Work hypothesis/ objectives: The aim of this study was to conduct a systematic review and meta-analysis using a multi-level random effects model to assess the diagnostic accuracy of 2D-SWE in patients with biopsy-proven MASLD. We aimed to establish reliable cut-off values for different stages of liver fibrosis that could be effectively applied in clinical practice.

Material and methods: The primary outcome was the diagnostic accuracy of 2D-SWE for different stages of liver fibrosis in MASLD patients. Subgroup analyses considered ultrasound manufacturer, patient demographics, and comorbidities. A bivariate logit-normal random effects model was used to estimate pooled sensitivity, specificity, and AUROC. A multiple threshold model facilitated the analysis of studies reporting more than one cut-off, while enabling the calculation of positive and negative predictive values for different pre-test probabilities.

Results: 20 observational studies (SuperSonic Imagine, General Electric Healthcare, Canon Medical Systems) fulfilled the inclusion criteria, comprising 2223 participants with biopsy-proven MASLD. The prevalence of mild fibrosis (F1), significant fibrosis (F2), advanced fibrosis (F3), and cirrhosis (F4) were 30.0%, 18,5%, 17.9%, and 10.9% , respectively. The sAUCs [95% CI] in detecting ≥F1, ≥F2, ≥F3, and F4 were 0.82 [0.16-0.98], 0.82 [0.76-0.88], 0.86 [0.77-0.93], and 0.89 [0.80-0.95], respectively.
The optimal cut-off values were 6.432 kPa for ≥F1, 8.174 kPa for ≥F2, 9.418 kPa for ≥F3, and 11.548 kPa for F4, respectively.

Conclusions: Our meta-analysis identified optimized cut-offs for fibrosis staging by 2D-SWE in etiology-specific chronic liver diseases (MASLD), with excellent diagnostic performance, underscoring the potential for standardizing cut-off values.

Study 3. The effectiveness of non-selective ß-blockers in preventing the first decompensation event in patients with compensated cirrhosis enduring clinically significant portal-hypertension (CSPH) after etiological treatment. Diabetes mellitus as independent risk factor for first decompensation event

Work hypothesis/ objectives: The study aimed to evaluate the impact of non-selective beta-blockers (NSBB) on the first occurrence of decompensation in patients with cirrhosis and clinical evidence of persistent clinically significant portal hypertension (CSPH) two years post-etiological treatment. We sought to identify independent risk factors contributing to the initial decompensation event in different etiologies, including MASLD, thus providing a clearer understanding of disease progression and potential intervention points.

Material and methods: A cohort of 406 patients with compensated liver cirrhosis from the Sant'Orsola Polyclinic in Bologna, Italy, was retrospectively followed during the period from 2017 to 2020. Multivariable Cox regression analyses were conducted to identify predictors of decompensation and bacterial infections, with hazard ratios and 95% confidence intervals reported. ROC curve analysis was used to evaluate the performance of continuous parameters, with statistical significance set at $p < 0.05$. Statistical analysis was conducted using IBM SPSS (version 29), and R software.

Results: During a mean follow-up of 32 months, 127 (31%) patients decompensated, with ascites being the most common (77%) decompensating event. Decompensation rates were lower in patients on NSBBs (16% vs 44%; $P < .0001$). At Cox regression analysis, hemoglobin, Child-Pugh, Model for End-Stage Liver Disease–Sodium, diabetes at baseline, and previous bacterial infections were independent predictors of decompensation, while NSBBs use had a protective effect (hazard ratio, 0.32; 95% confidence interval, 0.20–0.49; $P < .0001$).

Conclusions: NSBBs decrease the risk of first decompensation in patients with cirrhosis and enduring CSPH after etiological treatment.

GENERAL CONCLUSIONS

In conclusion, Study 1 provides a comprehensive evaluation of several non-invasive diagnostic tests (NITs) in the context of metabolic dysfunction-associated fatty liver disease (MASLD). The validation of Agile 3+, Agile 4, and FAST scores in distinguishing various stages of liver fibrosis in Caucasian patients with biopsy-confirmed MASLD highlights their potential utility in clinical practice, particularly in enhancing diagnostic accuracy and reducing indeterminate results. Additionally, Study 2 supports the broad applicability of two-dimensional shear wave elastography (2D-SWE) for assessing different stages of liver fibrosis in biopsy-proven MASLD, emphasizing the need for careful consideration of individual patient factors and machine performance variations to ensure accurate evaluations. The findings presented in Study 3 underscore the clinical significance of non-selective beta-blockers (NSBB) in preventing decompensating events in patients with compensated cirrhosis, including those with MASLD-related cirrhosis and persistent clinically significant portal hypertension (CSPH). Study 3 also underscores

the significance of factors included in the new definition of MASLD, such as type 2 diabetes mellitus, and their impact on disease progression and the risk of decompensation, regardless etiology. The interaction between NSBB and decompensation triggers, such as the presence of T2DM, or bacterial infections, suggest potential benefits that extend beyond their primary hemodynamic effects.

These conclusions collectively enhance our understanding of MASLD and its management, paving the way for improved patient outcomes through more informed clinical decision-making.

THE ORIGINALITY AND INNOVATIVE CONTRIBUTION OF THE THESIS

Validation of Diagnostic Scores: This research was the first to validate Agile 3+, Agile 4, and FAST scores for identifying liver fibrosis stages in biopsy-proven MASLD patients of Caucasian origin. The study confirmed and established new cut-off values, significantly reducing the "grey zone" compared to standard LSM-VCTE cut-offs.

Meta-Analysis of 2D-SWE: A multi-level random effects model meta-analysis of 2D-SWE in biopsy-proven MASLD (2,223 subjects) demonstrated excellent diagnostic accuracy and established standardized cut-off values.

Impact of Non-Selective Beta-Blockers (NSBB): NSBB significantly reduced the risk of first decompensation in compensated cirrhosis with CSPH, even after etiological treatment, including MASLD cases. Patients on NSBB had a lower decompensation rate (16%) compared to those off NSBB (44%). Type 2 diabetes mellitus was identified as an independent predictor of liver disease progression and decompensation, alongside bacterial infections.

UNIVERSITY OF MEDICINE AND PHARMACY "IULIU HAŢIEGANU" CLUJ-NAPOCA
ALMA MATER STUDIORUM UNIVERSITY OF BOLOGNA

DOCTORAL SCHOOL

CLUJ-NAPOCA 2025
BOLOGNA 2025

LIST OF PUBLICATIONS

Articles published in full text as a result of doctoral research, first author:

1. **Taru MG**, Neamti L, Taru V, Procopciuc LM, Procopet B, Lupsor-Platon M. How to Identify Advanced Fibrosis in Adult Patients with Non-Alcoholic Fatty Liver Disease (NAFLD) and Non-Alcoholic Steatohepatitis (NASH) Using Ultrasound Elastography—A Review of the Literature and Proposed Multistep Approach. Diagnostics. 2023 Feb 19;13(4):788. DOI:10.3390/diagnostics13040788 *(ISI IF 3, Q1; WOS:000939326200001) (Chapter 1, The current state of knowledge)*

2. **Taru MG**, Lupsor-Platon M. Exploring Opportunities to Enhance the Screening and Surveillance of Hepatocellular Carcinoma in Non-Alcoholic Fatty Liver Disease (NAFLD) through Risk Stratification Algorithms Incorporating Ultrasound Elastography. Cancers. 2023 Aug 14;15(16):4097. DOI:10.3390/cancers15164097 (ISI IF 4.5, Q1; WOS:001057069300001) (Chapter 1, The current state of knowledge)

3. **Taru MG,** Tefas C, Neamti L, Minciuna I, Taru V, Maniu A, Rusu I, Petrushev B, Procopciuc LM, Leucuta DC, Procopet B, Ferri S, Lupsor-Platon M, Stefanescu H. FAST and Agile–the MASLD drift: Validation of Agile 3+, Agile 4 and FAST scores in 246 biopsy-proven NAFLD patients meeting MASLD criteria of prevalent caucasian origin. PloS one. 2024 May 23;19(5): e0303971. DOI:10.1371/journal.pone.0303971 *(ISI IF 2.9, Q1; WOS:001231237700084) (Personal contribution, Chapter 3)*

4. Turco L*, **Taru MG***, Vitale G, Stefanescu H, Mirici Cappa F, Berardi S, Baldan A, Di Donato R, Pianta P, Vero V, Vizioli L, Procopciuc LM, Procopet B, Morelli MC, Piscaglia F. β-blockers lower first decompensation in patients with cirrhosis and enduring portal hypertension after etiological treatment. Clin Gastroenterol Hepatol. 2024 Aug 27:S1542-3565(24)00780-8. doi: 10.1016/j.cgh.2024.08.012. Epub ahead of print. PMID: 39209198 (ISI IF 11.6, Q1) **Observation: Turco L (Internal Medicine Unit for the Treatment of Severe Organ Failure, IRCCS Azienda Ospedaliero-Universitaria di, Bologna, Italy, and Taru MG (Faculty of Medicine, "Iuliu Hatieganu" University of Medicine and Pharmacy, Cluj-Napoca, Romania) share first authorship (Personal contribution, Chapter 5)*

5. **Taru MG,** Leucuta DC, Lupsor-Platon M, Turco L, Ferri S, Hashim A, Orasan OH, Procopet B, Stefanescu H, Morelli MC, Piscaglia F, Ravaioli F. Diagnostic accuracy of 2D-SWE ultrasound for liver fibrosis assessment in MASLD: A multi-level random effects model meta-analysis. Hepatology. 2024 Dec 16. doi:

10.1097/HEP.0000000000001190. Epub ahead of print. PMID: 39689354. (ISI IF 12.9, Q1) *(Personal contribution, Chapter 4)*

SUMMARY

ABBREVIATIONS USED IN TEXT

%	Percentage
2D-SWE	Two-dimensional shear wave elastography
AASLD	American Association for the Study of Liver Diseases
ACLD	Advanced chronic liver disease
ACLF	Acute on chronic liver failure
Alb	Albumin
ALP	Alkaline phosphatase
ALT	Alanine aminotransferase
APRI	AST to Platelet Ratio Index
ARFI	Acoustic radiation force impulse
AST	Aspartate aminotransferase
AUROC	Area under the receiver operating curve
BMI	Body mass index
cACLD	Compensated advanced chronic liver disease
CAP	Controlled attenuation parameter
CI	Confidence interval
CLD	Chronic liver disease
CRN	Clinical Research Network
CSPH	Clinically significant portal hypertension
CT	Computed tomography
DAA	Direct-acting antivirals
DM	Diabetes mellitus
EASL	European Association for the Study of the Liver
EFSUMB	European Federation of Societies for Ultrasound in Medicine and Biology
ELF	Enhanced Liver Fibrosis score
EVL	Endoscopic variceal ligation
F	Fibrosis
F0	Absence of fibrosis
F1	Mild fibrosis
F2	Significant fibrosis

F3	Advanced fibrosis
F4	Cirrhosis
FAST	FibroScan-AST score
FIB-4	Fibrosis 4 index
FLIP	Fatty liver inhibition of progression
FN	False negative
FP	False positive
GEV	Gastroesophageal varices
GE	General Electric Healthcare
GGT	Gamma glutamyl transpeptidase
Hb	Hemoglobin
HBV	Hepatitis B virus
HCC	Hepatocellular carcinoma
HCV	Hepatitis C virus
HE	Hepatic encephalopathy
HR	Hazard ratio
HVPG	Hepatic venous pressure gradient
Hz	Hertz
INR	International normalized ratio
IPD	Individual patient data
ITD	Intention to diagnose
IQR	Interquartile range
Kg	Kilogram
kPa	Kilopascals
LB	Liver biopsy
LDL	Low density lipoprotein cholesterol
LREs	Liver-related events
LS	Liver stiffness
LSM	Liver stiffness measurement
M	Mean
m	Meter / measurements
MASH	Metabolic dysfunction-associated steatohepatitis
MASLD	Metabolic dysfunction-associated steatotic liver disease
MELD	Model for end stage liver disease
MRI	Magnetic resonance imaging
m/sec	Meters per second
n	Number
NAFLD	Non-alcoholic fatty liver disease
NAS	NAFLD activity score
NASH	Non-alcoholic steatohepatitis
NITs	Non-invasive tests

NPV	Negative predictive value
NUC	Nucleos(t)ide analogue
PH	Portal hypertension
PPV	Positive predictive value
PVT	Portal vein thrombosis
Q1	Percentile 25
Q3	Percentile 75
QIBA	Quantitative Imaging Biomarkers Alliance
ROC	Receiver operating characteristics
sAUC	Summary area under the ROC curve
SD	Standard deviation
Se	Sensitivity
Sp	Specificity
SPSS	Spontaneous portosystemic shunt
SRU	Society of Radiologists in Ultrasound
SSI	SuperSonic Imagine
SVR	Sustained virological response
TB	Total bilirubin
Tg	Triglycerides
TIPS	Transjugular intrahepatic portosystemic shunt
TN	True negative
Tot Cho	Total cholesterol
TP	True positive
T2DM	Type 2 diabetes mellitus
US	Ultrasound
VCTE	Vibration-controlled transient elastography
WFUMB	World Federation for Ultrasound in Medicine and Biology

INTRODUCTION

This doctoral thesis is the result of a joint PhD program between the University of Medicine and Pharmacy "Iuliu Haţieganu", Cluj-Napoca, Romania, under the supervision of Prof. Dr. Lucia Maria Procopciuc, and Alma Mater Studiorum University of Bologna, Bologna, Italy, under the guidance of Prof. Fabio Piscaglia. The successful completion of this work was made possible through the invaluable support and mentorship of numerous persons.

I am deeply grateful for the financial support provided by various research grants, under the guidance of outstanding mentors, including Prof. Dr. Monica Lupşor-Platon, Dr. Horia Ştefănescu, Prof. Olga Hilda Orăşan, and Prof. Bogdan Procopeţ. Additionally, I was fortunate to receive funding from the Study Loans and Scholarships Agency, The Ministry of Education, Romania, through the H.G. no. 118/2023 scholarship, supervised by Prof. Fabio Piscaglia. This support allowed me to pursue a fellowship at Alma Mater Studiorum University of Bologna, where I conducted high-quality research alongside prestigious research groups and collaborated with brilliant clinicians and researchers, such as Dr. Maria Cristina Morelli, Dr. Laura Turco, Dr. Silvia Ferri, Dr. Federica Mirici Cappa, Dr. Sonia Berardi, and Dr. Federico Ravaioli.

The central focus of this thesis was the metabolic dysfunction-associated steatotic liver disease (MASLD), a liver condition that has seen rising prevalence and incidence in recent years, making it the most common type of liver disease today.

The progression of MASLD to more advanced stages, such as advanced fibrosis and cirrhosis, significantly increases the risk of developing important events in the course of the disease, such as clinically significant portal hypertension, the first decompensation event, the onset of hepatocellular carcinoma, a higher liver-related mortality, and a greater incidence of major cardiovascular events. While liver biopsy is considered the gold standard for diagnosing the stage of fibrosis, it is often impractical or impossible to perform on most MASLD patients. Therefore, predicting disease progression through non-invasive methods represents a dynamic and highly relevant field of research with significant implications for patient care.

Therefore, a part of my clinical research focused on deepening our understanding of the progression of MASLD to the more advanced stages by using non-invasive ultrasound-based elastography techniques, including vibration-controlled transient elastography (VCTE), VCTE-based scores, and two-dimensional shear wave elastography (2D-SWE).

In the course of a chronic liver disease in general, and of MASLD in particular, the occurrence of the first decompensation event is a critical milestone, as the disease

trajectory tends to deteriorate significantly following this event. In thes respect, another key aspect was to explore how critical events, such as the first decompensation event, can be predicted and potentially prevented through the use of currently available treatments, such as non-selective beta-blockers (NSBB). Additionally, I explored whether the indications for NSBB treatment can be expanded beyond the currently recognized guidelines. Furthermore, I aimed to investigate how various factors related to MASLD, such as the presence of type 2 diabetes mellitus (T2DM), impact the onset of the first decompensation event.

Building on the existing background and current understanding of MASLD, this research presents results that are notable for their novelty on an international scale.

I validated the VCTE-based scores—Agile 3+, Agile 4, and FAST scores—within a cohort of individuals of Caucasian descent for the very first time. Utilizing a multi-level random effects model meta-analysis, I established standardized cut-off values for 2D-SWE that distinguish between different stages of liver fibrosis in patients with biopsy-proven MASLD, applicable at varying pre-test probabilities. These cut-off values are designed for use in both primary care and specialized healthcare settings.

Additionally, I investigated the benefits of NSBB treatment in patients with compensated cirrhosis, emphasizing its role in preventing the first decompensation event. Notably, I demonstrated that patients with small gastroesophageal varices and porto-systemic shunts can also derive significant benefits from this treatment. My research demonstrated that the presence of type 2 diabetes mellitus (T2DM) acts as an independent risk factor for the onset of the first decompensation event, regardless of etiology. Furthermore, I identified key triggers for first decompensation, including bacterial infections and low hemoglobin levels.

Preliminary findings from this thesis were presented at esteem international hepatology conferences, both as oral and poster presentations. The complete results were published in reputable journals focused on hepatology.

These findings establish a solid foundation for future research, providing valuable insights that can guide subsequent initiatives. Specifically, they contribute to the standardization of ultrasound-based elastography, enhance our understanding of expanding the use of non-selective beta-blocker (NSBB) treatment, and lay the groundwork for investigations into the onset of hepatocellular carcinoma (HCC) in non-cirrhotic patients with MASLD. Collectively, these advancements will deepen our understanding of liver diseases and propel progress in the field of MASLD.

This doctoral thesis not only marks the achievement of my research efforts, but also reflects the collaborative spirit that drives scientific discovery. I am deeply grateful to my mentors, colleagues, and loved ones, whose support and encouragement inspired me to persevere through challenges. This work stands as a testament to our shared commitment to understanding and addressing MASLD, with the hope that our findings will contribute to improved patient care and outcomes.

THE CURRENT STATE OF KNOWLEDGE

1. Metabolic dysfunction-associated steatotic liver disease (MASLD)

Metabolic dysfunction-associated steatotic liver disease (MASLD), previously known as non-alcoholic fatty liver disease (NAFLD) (1), is currently a significant challenge for the healthcare system. Its prevalence is rapidly increasing, leading to a substantial global burden (2, 3).

A recent meta-analysis revealed that the prevalence of MASLD has risen significantly over time, increasing from 25.5% in 2005 to an alarming 37.8% in 2016 and beyond (2). This follows a similar upward trend previously reported, with prevalence rising from 20.1% to 26.8% between 2000 and 2015 (4).

Within three years, 25% of MASLD cases progress to metabolic dysfunction-associated steatohepatitis (MASH). MASH is responsible for 12% of all liver transplants in Europe (5). Unlike hepatitis C and other liver-specific conditions, which are typically caused by a single etiological factor, MASLD is a multifactorial and complex metabolic disorder that is part of a broader systemic disease. This complexity makes managing and monitoring the disease more challenging (6). Throughout its history and progression, MASLD is associated with liver injury, which can result in fibrosis progression, clinically significant portal hypertension (CSPH), cirrhosis, hepatocellular carcinoma, and both initial and further decompensation (7). Patients with compensated MASLD-related cirrhosis remain in this state for an average of four years, with a 10% annual risk of progressing to decompensation or death. Once they experience their first decompensation event, their risk of further progression triples (8).

Traditionally, the diagnosis of MASLD has relied on histopathological changes in the liver, typically assessed through a liver biopsy (LB). The condition is formally identified by the accumulation of triglycerides in more than 5% of hepatocytes (9). The progressive form of MASLD, known as MASH, has traditionally required histological assessment for a standard diagnosis, typically conducted when steatotic liver disease is suspected. MASH is generally characterized by the presence of steatosis, lobular inflammation, and ballooning, with or without fibrosis (10). However, LB is indicated with caution, as it holds the potential for adverse effects, sampling errors, inter and intra-observer variability (11). The procedure is prone to interpretation errors due to the uneven distribution of liver fibrosis. When two samples are taken from the right and left hepatic lobes of the same MASH patient, the fibrosis stage was consistent in only 47% of patients. Discrepancies of at least one stage were found in 41% of cases, while differences of two stages occurred in 12% of cases (12).

As highlighted in most retrospective studies on MASLD, the risk of liver-related events (LREs) significantly rises at fibrosis stage two (F2—significant fibrosis) and increases exponentially as patients move into advanced fibrosis stages (F3—advanced fibrosis; F4—cirrhosis) (13, 14). Higher mortality rates are registered for F4 (1.76 deaths per 100 person years), and among those at stage F3 (0.89 deaths per 100 person years) (15).

In summary, the risk of all-cause mortality and liver-related mortality increases substantially with the fibrosis stage, as reported in a recently published meta-analysis (16). Consequently, the fibrosis stage is a crucial predictor of long-term liver-related outcomes and overall mortality in MASLD. Identifying advanced stages (≥F3, F4) in patients with MASLD and MASH is essential (17).

In this context, new insights from non-invasive tests (NIT) for assessing liver fibrosis, such as ultrasound elastography, assist clinicians in making early and accurate diagnoses and prognoses. These methods help minimize the need for liver biopsies and support more cost-effective surveillance strategies.

2. Liver ultrasound elastography

All liver diseases, whether focal or diffuse, lead to changes in tissue structure that alter the liver's biomechanical properties. These changes can be measured and quantified using tissue elastography

The elastography techniques can be divided into two main categories, magnetic resonance imaging (MRI)-based elastography techniques and ultrasound (US)-based elastography techniques.

The MRI-based elastography techniques proposed for staging liver fibrosis include magnetic resonance elastography (MRE) and MRI index tests such as LiverMultiScan™ (LMS), which measures iron-corrected T1 (cT1), diffusion-weighted imaging (DWI), and specialized techniques for detecting metabolic and liver injury (deMILI). MRE provides a quantitative three-dimensional elasticity map of the entire liver, is less dependent on operator skill, and is not influenced by the presence of air or bones. Although MRE demonstrates strong performance in detecting significant fibrosis (≥F2) with an sAUC of 0.91 (95% CI 0.80–0.97), advanced fibrosis (≥F3) with an sAUC of 0.92 (95% CI 0.88–0.95), and cirrhosis (F4) with an sAUC of 0.90 (95% CI 0.81–0.95) in biopsy-proven MASLD, its utility is somewhat limited compared to ultrasound-based elastography techniques due to higher costs and more restricted availability (18).

The ultrasound elastography techniques can be divided into quantitative ("shear wave elastography", (SWE) and qualitative ("Strain Elastography") (19).

Quantitative techniques such as vibration-controlled transient elastography (VCTE), two-dimensional shear wave elastography (2D-SWE), and point shear wave elastography (pSWE) are commonly used for assessing diffuse liver diseases. In contrast, strain elastography techniques generally have lower applicability for this purpose (20).

2. 1. Vibration-controlled transient elastography (VCTE)

In the 2000s, vibration-controlled transient elastography (VCTE) was the pioneering method for measuring and studying liver stiffness (LS). It remains the only quantitative elastography technique not incorporated into a standard ultrasound system and is conducted using the FibroScan® device (Echosens, Paris, France (21), as shown in **Figure 1**. VCTE is also the modality with the most extensive data for assessing liver fibrosis in MASLD, as evidenced by its inclusion in 53 studies in a recent meta-analysis (18).

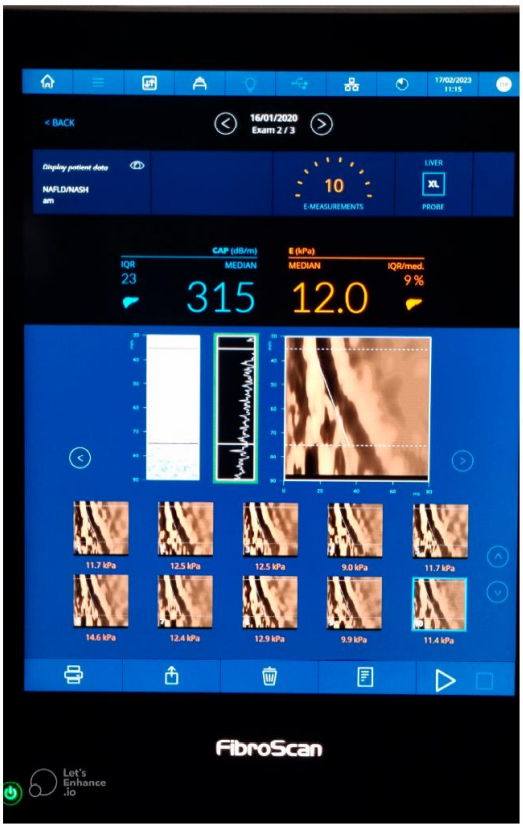

Figure 1. Vibration-controlled transient elastography (VCTE)
Image obtained from Medical Clinic 3, Cluj-Napoca, Romania

To conduct the examination, the patient is positioned supine with the right arm fully abducted to optimize exposure of the right quadrant. The transducer is placed perpendicular to the intercostal space in direct contact with the skin, at a site of maximal hepatic dullness (at least 6 cm thick), and away from any large vascular structures (22). There are two types of transducers that are mainly utilized in the adult population, the M (3.5 MHz) and XL (2.5 MHz) probes. Regarding the XL probe, the machine usually recommends its utilization (23, 24).

Pressing the transducer button generates a painless mechanical vibration that creates a series of elastic waves (50 Hz). These waves travel through the skin and subcutaneous tissue, reaching the liver parenchyma (25). The shear wave is monitored through multiple acquisitions, requiring at least 10 valid measurements. The results include a reported interquartile range (IQR) and an interquartile range/median ratio (IQR/M) based on these 10 conclusive measurements (26). The time taken for the waves to travel through the area of interest and the velocity of their propagation are recorded. From these measurements, the Young's modulus (E) is calculated in

kilopascals (kPa), which clinically corresponds to liver stiffness (LS), with values ranging from 1.5 to 75 kPa (27). For an accurate liver stiffness measurement (LSM), the interquartile range (IQR) should be less than 30% of the median, regardless of the success rate (SR), provided that 10 valid measurements are obtained (19) (**Figure 1**).

The equipment measures liver stiffness (for assessing fibrosis) and the controlled attenuation parameter (CAP) (for evaluating steatosis). Higher values of liver stiffness (LS) indicate stiffer tissue, while lower values suggest a more elastic liver. In a healthy population, LS values are typically reported to be around 4.5–5.5 kPa (19). Using this technique, liver stiffness (LS) is measured in a cylindrical volume of parenchyma with a 1 cm diameter and 4 cm height, which represents approximately 1/500 of the total liver volume (28). Measurements can be conducted by a technician after undergoing a training period of approximately 100 cases. However, the clinical interpretation of the results should always be carried out by an expert who takes into account the patient's demographic data, disease etiology, and biochemical profile at the time of the examination (29). For accurate assessment, the examination must be conducted after an overnight fast or at least 3 hours of fasting following a meal. A postprandial examination can lead to increased stiffness values due to heightened hepatic blood flow (19).

When using the M probe to measure liver stiffness (LS), lower success rates were observed in obese individuals (30). To address this limitation, the XL probe was introduced. The primary constraints for using the XL probe include a skin-to-liver capsule distance greater than 3.4 cm and extreme obesity (BMI > 40 kg/m^2) (26, 31). Values obtained with the XL probe are generally lower compared to those from the M probe, but the current guidelines do not provide specific recommendations for cut-off values using the XL probe (19).

Liver tissue abnormalities such as edema, inflammation (cytolysis), cholestasis, congestion (heart failure), and infiltrative diseases may interfere with LSM independently of fibrosis stage, so these factors should be considered when one is interpreting the values of the hepatic rigidity (32-36). The influence of steatosis on LS is still rather controversial; some studies indicate that steatosis may lead to higher LS values (37-39), independently of the fibrosis stage, whereas others did not report the same effect (40).

2.1.1. Performance of VCTE for liver fibrosis evaluation in MASLD

In a recent meta-analysis (18), assessing the diagnostic accuracy of five elastography and imaging modalities for non-invasive fibrosis detection in patients with biopsy-proven or suspected MASLD, the authors reported the following sAUC values for VCTE: 0.82 (95% CI 0.78–0.85, sensitivity 78%, specificity 72%) for detecting mild fibrosis (≥F1), 0.83 (95% CI 0.80–0.87, sensitivity 80%, specificity 73%)

for significant fibrosis (≥F2), 0.85 (95% CI 0.83–0.87, sensitivity 80%, specificity 77%) for advanced fibrosis (≥F3), and 0.89 (95% CI 0.84–0.93, sensitivity 76%, specificity 88%) for cirrhosis. When performing a multiple-threshold meta-analysis that included studies reporting more than two cut-off values for VCTE, the sAUC for diagnosing advanced fibrosis (≥F3) was 0.85 (sensitivity 80%, specificity 75%), with the Youden index optimized at an 8.7 kPa cut-off. A cut-off of 8.9 kPa yielded 80% sensitivity and 77% specificity, while a 9.5 kPa cut-off resulted in 76% sensitivity and 80% specificity for diagnosing ≥F3. These findings should be interpreted with caution, as some studies may not have used the XL probe or may not have followed the manufacturer's guidelines. Additionally, recent advancements in VCTE, such as the continuous CAP algorithm and its application in patients with morbid obesity, were not included in this analysis.

The recently published Baveno VII guidelines (41), which are also relevant for MASLD and MASH, provide key recommendations for using LSM-VCTE. According to these guidelines, liver stiffness (LS) values of less than 10 kPa, in the absence of other clinical or imaging signs, rule out compensated advanced chronic liver disease (cACLD). LS values between 10 and 15 kPa suggest cACLD, while values greater than 15 kPa are highly indicative of cACLD. However, patients with LS values between 7 and 10 kPa who have ongoing liver injury should be monitored individually for signs of progression to cACLD(41). The guidelines also introduce "the rule of five" (10–15–20–25 kPa) to represent progressively higher relative risks of decompensation and liver-related mortality, regardless of the chronic liver disease etiology.

Currently, there is considerable variability in the cut-off values used in clinical practice for non-invasive tests (NIT) for MASLD risk stratification. A recent report highlighted this inconsistency, particularly with VCTE. Among 28 respondents using FibroScan®, 6 (21%) employed a single cut-off value, with only 3 (50%) specifying 8 kPa. The remaining values used were 7.2 kPa, 7.8 kPa, and 8.7 kPa. For those 63% of respondents who utilized both lower and upper LS cut-offs, the most frequently reported lower cut-off was <8.0 kPa, noted by 7 respondents (32%), while the most common higher cut-off was >15 kPa, reported by 5 respondents (23%) (42).

2.1.2. Assessing liver steatosis through the controlled attenuation parameter (CAP)

In summary, the controlled attenuation parameter (CAP) measures total ultrasonic attenuation and is a feature of the FibroScan® device used to assess liver steatosis. CAP values are expressed in decibels per meter (dB/m), ranging from 100 to 400 dB/m, with normal values being below 247 dB/m (43). Optimal cut-off values were established in a meta-analysis that included 2735 patients (of which 20% were diagnosed with MASLD/MASH) for the prediction of mild (S1), moderate (S2), and severe steatosis (S3). The cut-off values were established at 248 dB/m, (AUC 0.823, Se 68.8%, Sp 82.2%), 268 dB/m, (AUC 0.865, Se 77.3%, Sp 81.2%), and 280 dB/m (AUC

0.882, Se 88.2%, Sp 77.6%) for detecting mild steatosis (≥S1), moderate steatosis (≥S2), and severe steatosis (S3), respectively. Steatosis was graded on histology according to the number of affected hepatocytes as: absence of steatosis (S0) (<5 or <10% depending on the trial), S1 (between 5 and 10–33%), S2 (34–66%), and S3 (>66%) (44). The authors recommended adjusting the CAP cut-offs based on specific factors, as they are influenced by various covariates. For patients with MAFLD/MASH, a deduction of 10 dB/m from the CAP value is suggested. Similarly, a 10 dB/m deduction is recommended for diabetes patients. Additionally, for each unit of BMI above or below 25 kg/m^2 within the 20–30 kg/m^2 range, an adjustment of ±4.4 dB/m should be applied.

2. 2. Two-dimensional shear wave elastography (2D-SWE)

The use of two-dimensional shear wave elastography (2D-SWE) for non-invasive liver fibrosis assessment has rapidly increased. In liver stiffness measurement (LSM), 2D-SWE applies dynamic stress across multiple focal zones using the acoustic radiation force impulse (ARFI) technique, producing a quantitative elastographic measurement expressed in kilopascals (kPa) or meters per second (m/s) (19).

Briefly, radiation force is applied to tissues using focused ultrasonic beams at a high frame rate, allowing real-time capture of the transient propagation of the resulting shear waves (45) (**Figure 2**). This imaging modality is conducted with a conventional ultrasound probe during a standard intercostal ultrasonographic examination. The Doppler-like acquisition estimates shear wave speed within a region of interest (ROI). A color-coded ROI map is generated and overlaid on the B-mode image, offering information on tissue stiffness (46). The Young's modulus (E) is determined by the equation E = 3pc2, where p is the tissue density (constant), and c is the shear wave speed. Values between 4.5 - 5.5 kPa using the SuperSonic Imagine (SSI) equipment were reported in the healthy population. At present, SSI is the most validated 2D-SWE technique (19).

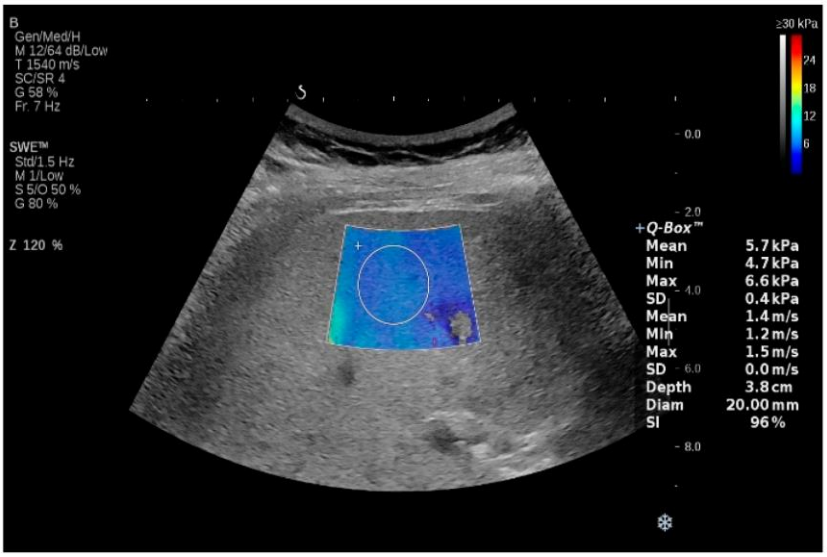

Figure 2. Two-dimensional shear wave elastography (2D-SWE) using SuperSonic Imagine equipment Image obtained from Medical Clinic 3, Cluj-Napoca, Romania

Liver stiffness of less than or equal to 5 kPa (1.3 m/sec) has a high probability of being normal (47). For 2D-SWE, current guidelines recommend performing a minimum of three measurements. The results should be reported as the median along with the interquartile range (IQR) (19, 48). The variability between consecutive liver stiffness measurements, evaluated using the interquartile range-to-median ratio, is a crucial quality criterion. If this ratio exceeds 30% for measurements in kilopascals or 15% for measurements in meters per second, the accuracy of the technique is considered to be reduced (19, 47, 48).

Narrow intercostal spaces, a high body mass index (BMI), and a thoracic wall thickness greater than 25 mm are associated with a higher rate of invalid measurements (49). The main factors that can confound elevated liver stiffness measurements are similar across various elastographic ultrasound techniques. These include necroinflammation, congestion, mechanical cholestasis, food intake, and alcohol consumption. Additionally, conditions such as amyloidosis, lymphomas, and extramedullary hematopoiesis can independently increase liver stiffness (50).

2.2.1. Effectiveness of 2D-SWE in Predicting Liver Stiffness in MASLD

Today, nearly all ultrasound manufacturers have integrated liver stiffness (LS) modules into their latest ultrasound scanners. However, it's important to note that elastography techniques from different manufacturers do not have standardized cut-off values, which presents a significant challenge in clinical practice. Ideally, consistent criteria should apply across all ultrasound devices equipped with 2D-SWE. Despite

this, variability in liver stiffness measurements among different systems has been reduced thanks to ongoing efforts by the Quantitative Imaging Biomarkers Alliance (QIBA) (50).

A recent study compared the performance of 2D-SWE liver stiffness measurement (LSM) across different ultrasound machines, including General Electric Healthcare (2D-SWE-GE—Logiq E10), Canon Medical Systems (2D-SWE-Canon—Aplio i800), and SuperSonic Imagine (2D-SWE-SSI—Mach30 Aixplorer), with vibration-controlled transient elastography (VCTE) using FibroScan with M and XL probes for patients with a BMI > 30 kg/m^2 (51). In the study, 1,437 patients with alcohol-related or MASLD as the primary etiology were included. A single operator measured liver stiffness using 2D-SWE-SSI (SuperSonic Imagine) along with one of the following devices: 2D-SWE-GE (n = 314), 2D-SWE-Canon (n = 311), and VCTE-M probe (n = 812). The authors found that VCTE-M and 2D-SWE-SSI (Mach30 Aixplorer) exhibited the highest correlation and concordance coefficients (0.933 and 0.920, respectively). While all four devices performed similarly in excluding advanced chronic liver diseases (ACLD) in a general population-based scenario, discrepancies were noted in the higher percentile values.

In 2020, a study evaluated the performance of 2D-SWE in identifying compensated advanced chronic liver disease (cACLD) based on Baveno VI criteria using VCTE cut-off values. This assessment was conducted on a cohort of 1,219 consecutive patients, including 345 with MASLD, who underwent both VCTE and 2D-SWE examinations on the same day (52). According to the authors, 2D-SWE (performed using Aixplorer™ ultrasound device—SuperSonic Imagine, Aix-en-Provence, France) accurately identified cACLD (Pearson's correlation coefficient, 0.882; $p < 0.0001$; Lin concordance coefficient, 0.846; $p < 0.0001$). A 10 kPa (Se 92%, Sp 87%) 2D-SWE cut-off value was used to rule out cACLD.

2.2.2. Evaluation of hepatic steatosis in MASLD using 2D-SWE techniques

Attenuation Imaging (ATI), a recent advancement by Canon Medical Systems, quantifies ultrasound attenuation in tissue using a large sample measurement and real-time color mapping. This technique aims to evaluate hepatic steatosis in a quantitative and non-invasive manner (53, 54). With this technique, the attenuation coefficient can be calculated in decibels per centimeter per megahertz (dB/cm/MHz).

To ensure accurate examination, the patient should fast for at least 6 hours. Measurements should be taken from the right lobe of the liver through the intercostal spaces, with the patient in a supine position, similar to the procedure for liver fibrosis assessment using 2D-SWE. Reliable measurements are typically defined as the median value of five measurements conducted in a homogeneous area of liver parenchyma,

with an interquartile range-to-median ratio (IQR/M) of less than 30% and an R^2 value greater than 0.90 (R^2 is a quality parameter recommended by the manufacturer) (55).

In a recently published study involving 132 patients with biopsy-proven MASLD who underwent ATI evaluation, the AUROCs for diagnosing various grades of steatosis were as follows: 0.94 (sensitivity 85%, specificity 97%) for ≥S1 (≥5% steatosis), 0.94 (sensitivity 95%, specificity 80%) for ≥S2 (≥34% steatosis), and 0.94 (sensitivity 100%, specificity 83%) for ≥S3 (≥67% steatosis) (56). For patients with ascites, shear waves can be effectively generated using focused ultrasound through the fluid, unlike the mechanical vibration used in CAP. The authors concluded that ATI is a highly feasible method for quantifying liver steatosis (56).

The Ultrasound-Guided Attenuation Parameter (UGAP), developed by General Electric Healthcare, is also employed for assessing hepatic steatosis. UGAP measures the attenuation coefficient (AC) in decibels per centimeter per megahertz (dB/cm/MHz) of the B-mode ultrasonic signal (57). Measurements should be taken from the right liver lobe using an intercostal approach during brief breath holds. The patient should be fasting for at least 4 hours and positioned supine (58). In a recent published study, 84 patients with biopsy-proven MASLD underwent UGAP evaluations (59). UGAP presented a good diagnostic performance of AC values for ≥S1, ≥S2, and S3, with AUROCs of 0.94, 0.95, and 0.88, respectively. The authors concluded that AC values obtained using UGAP could be a useful new method for quantifying steatosis in MASLD.

2.2.3. Evaluation of hepatic inflammation in MASLD using 2D-SWE techniques

Shear Wave Dispersion Imaging (Dispersion Slope, DS) is a newly developed ultrasound technology that analyzes the frequency dispersion properties of tissue. It offers new insights into tissue viscosity and has recently been applied to the assessment of diffuse liver diseases (60). Preliminary data are now available regarding the clinical use of Shear Wave Dispersion Imaging for characterizing chronic liver diseases and detecting allograft damage following liver transplantation (61, 62). In a recently published study evaluating the lobular inflammatory activity in 132 participants with biopsy-proven MASLD, the AUROCs for detecting mild inflammation (≥I1), moderate inflammation (≥I2), and severe inflammation (I3) were 0.86 (Se=82%, Sp=82%), 0.86 (Se=90%, Sp=77%), and 0.79 (Se=100%, Sp=61%), respectively (56).

3. Ultrasound elastography-based scores with applicability in MASLD

3. 1. Agile 3+ and Agile 4 Scores for the identification of advanced fibrosis and cirrhosis in suspected MASLD

Recently developed and validated FibroScan-based scores, Agile 4 and Agile 3+, are designed to identify cirrhosis (F4) and advanced fibrosis (≥F3), respectively, in patients with MASLD, particularly within specialized liver clinics (63). Each score integrates liver stiffness measurement (LSM-VCTE) with clinical and laboratory parameters: the Agile 3+ score includes the AST/ALT ratio, platelets, gender, diabetes status, and age, while the Agile 4 score focuses on cirrhosis detection.

For Agile 4, two cut-off values were established: 0.251 for ruling out and 0.565 for ruling in cirrhosis (F4). The rule-out cut-off achieved a sensitivity of ≥85%, while the rule-in cut-off reached a specificity of ≥95% for diagnosing cirrhosis. For Agile 3+, cut-off values of 0.451 and 0.679 were set to rule out and rule in advanced fibrosis (≥F3), respectively. The rule-out cut-off had a sensitivity of ≥85%, and the rule-in cut-off had a specificity of ≥90% for detecting advanced fibrosis.

The authors concluded that combining these simple clinical parameters with routine laboratory biomarkers and LSM-VCTE can reduce the number of indeterminate results compared to using VCTE alone. These scores, designed for secondary and tertiary care settings, have the potential to aid in predicting clinical outcomes and monitoring disease progression (63, 64).

3. 2. The Fibroscan-AST (FAST) Score for the identification of at-risk MASH

The FibroScan-AST (FAST) score, which combines CAP, LS, and AST, was developed and validated in 2020 for the non-invasive identification of patients with MASH who have significant activity and fibrosis (65). The FAST score was designed to non-invasively identify "at-risk MASH" patients, characterized by MASH with a MAFLD activity score (NAS) of ≥4 and significant fibrosis (F ≥ 2). Two cut-off values were proposed: ≤0.35 to rule out and ≥0.67 to rule in at-risk MASH. The score demonstrated an AUC of 0.95 for ruling out (sensitivity 90%, specificity 53%) and an AUC of 0.95 for ruling in (sensitivity 48%, specificity 90%) at-risk MASH. This score aims to provide a non-invasive method for identifying patients with MASH who might be suitable for clinical trials or treatment interventions (65). When applied to the general population, a score that stratifies patients into low-risk and high-risk MASH categories could help reduce the number of specialist referrals and minimize unnecessary biopsies in individuals with a low likelihood of significant fibrosis (66).

4. Disease progression to MASLD-related hepatocellular carcinoma (HCC). Possibilities for optimizing screening strategies using ultrasound elastography

The presence of liver cirrhosis increases the risk of HCC in patients with MASLD, as it does in other types of liver disease (67). However, patients with MASLD who do not have cirrhosis, but are at risk of developing hepatocellular carcinoma (HCC) often exhibit distinct characteristics, including diabetes or insulin resistance, obesity, or advanced age (68-71).

A notable and critical clinical feature of MASLD and MASH-related hepatocellular carcinoma (HCC) is the tendency for tumors to develop even before cirrhosis is established (72-74). Recent findings have highlighted that the incidence of hepatocellular carcinoma (HCC) increases with the progression of MAFLD. Specifically, the rate of HCC incidence is 0.8 per 1,000 person-years in cases of simple steatosis, 2.3 per 1,000 person-years in non-cirrhotic fibrosis, and 6.2 per 1,000 person-years in MAFLD-related cirrhosis (75).

On the other hand, MAFLD presents an incidence that is increasing in parallel to the rise of obesity, diabetes, and metabolic syndrome (2, 76). The presence of these comorbid conditions contributes to an altered lipid metabolism and chronic inflammation, favoring a pro-carcinogenic environment and setting the ground for liver cancer development (77, 78). In this context, MAFLD has emerged as the primary cause of HCC in individuals without cirrhosis. About 30% of HCC cases associated with MAFLD occur in livers without cirrhosis, whereas only about 10% of HCC cases in other liver conditions occur in non-cirrhotic livers (72, 73, 79).

The MAFLD-related HCC trends are definitely concerning: MAFLD-related HCC has increased in both incidence and mortality (80); MASH is the fastest growing cause of HCC in liver transplant (LT) candidates (81); despite the older age of patients with MAFLD-HCC and the presence of comorbidities, HCC has become more common in patients transplanted for MAFLD compared with other etiologies (82). There is growing apprehension that these trends may lead to a significantly increased incidence of MAFLD-related HCC in the future.

In recent years, liver fibrosis has consistently been identified as the most critical histological marker for predicting clinical outcomes in the context of MAFLD and MASH (15). Even though the build-up of hepatic fibrosis takes at least 20 years, or even longer in the setting of MAFLD (83), as the prevalence of overweight and obesity are increasing in younger age groups (84, 85), and considering the fact that modern treatments for cardiovascular diseases have improved life expectancy (86), there is

also more time for the MAFLD population to develop MASH, advanced fibrosis (≥F3), cirrhosis (F4), and cirrhosis related complications, including HCC.

Since a substantial portion of HCC arises in non-cirrhotic MAFLD patients, new clinical challenges emerge because these individuals are often excluded from HCC surveillance programs (87). Identifying the most effective screening methods to guide risk assessment and monitoring frequency for MAFLD-related HCC is a key area of interest within the scientific community (88, 89). Enhancing the detection of HCC associated with non-cirrhotic MAFLD could be achieved by assessing specific risk factors and gaining a more thorough understanding of the underlying liver disease through noninvasive techniques.

The degree of liver fibrosis is the main factor influencing the risk of HCC development in patients with non-cirrhotic MAFLD (75, 90). Risk stratification in HCC is significantly influenced by hepatic fibrosis (91), as cirrhosis is present in over 80% of patients with HCC (92). In a recently published study, the likelihood of developing HCC surpassed the accepted thresholds for HCC surveillance (0.02/1000 person-years; hazard ratio 7.62; 95% confidence interval, 5.76–10.09) (93). In a comparable manner, HCC incidence increased along with the progression of MAFLD, from simple steatosis (0.8 per 1000 person-years) to non-cirrhotic fibrosis (2.3 per 1000 person-years) and MAFLD-related cirrhosis (6.2 per 1000 person-years), respectively (75).

Patients with cirrhosis and likely advanced fibrosis (≥F3) remain at a persistent risk for HCC. As discussed earlier, liver fibrosis can be evaluated through histology or non-invasive methods, such as liver stiffness measurement (LSM)(94).

A recent study that tracked individuals with T2DM and MAFLD, who underwent VCTE-LSM at baseline and were followed for an average of 50 months, found notable results regarding baseline liver stiffness (LS) and liver-related events (LREs). Among 35 patients with baseline LS greater than 13 kPa, 6 (17.1%) experienced decompensation or primary liver cancer, with an annual HCC development rate of 2.1% in this group. After adjusting for age and pre-existing cirrhosis, those with LS greater than 13 kPa had a 27.4-fold increased risk of experiencing an LRE compared to patients with LS less than 13 kPa (95% CI: 7.86–95.50; $p < 0.001$)(95).

A recent study found that the change in liver stiffness measurement (LSM) by VCTE—specifically, the difference between follow-up and baseline LSM (D-LSM)—was independently linked to several outcomes: hepatic decompensation (hazard ratio 1.56; 95% confidence interval, 1.05–2.51; $p = 0.04$), HCC development (hazard ratio 1.72; 95% confidence interval, 1.01–3.02; $p = 0.04$), overall mortality (hazard ratio 1.73; 95% confidence interval, 1.11–2.69; $p = 0.01$), and liver-related mortality (hazard ratio 1.96; 95% confidence interval, 1.10–3.38; $p = 0.02$). The authors concluded that a D-LSM greater than 20% could be a useful predictor for elevated risks of HCC, liver decompensation, liver-related mortality, and overall mortality in patients with compensated advanced chronic liver disease (cACLD) (96).

In a study of 1,057 patients with MAFLD, both FIB-4 and VCTE demonstrated strong accuracy in predicting liver-related events (LREs), including HCC, with Harrell's C-indexes exceeding 0.80 (0.817 [0.768–0.866] for FIB-4 and 0.878 [0.835–0.921] for VCTE, p = 0.059). Although VCTE showed a higher Harrell's C-index compared to FIB-4, the difference was not statistically significant (0.878 [0.835–0.921] vs. 0.817 [0.768–0.866], p = 0.059). Furthermore, a FIB-4 cut-off value greater than 3.25 was linked to a 30-fold increased risk of LREs (adjusted hazard ratio 29.5; 95% confidence interval 10.6–82.3), while VCTE values above 12.0 kPa were associated with a 21-fold increased risk of LREs (adjusted hazard ratio 20.5; 95% confidence interval 4.9–86.5) (97).

Patients with MASLD, particularly those with advanced fibrosis (≥F3) and/or additional risk factors for HCC development, might be candidates for future HCC screening. Thresholds established in the literature, such as those currently used for FIB-4 and VCTE, or newly validated thresholds, could be applied to more accurately stratify HCC risk in MASLD. To reduce the risk of misclassification, combining multiple non-invasive tests (NITs) from different categories, such as blood-based and imaging-based tests, and evaluating their concordance could be valuable. NITs could support the creation of risk-stratification algorithms, clinical care pathways, and surveillance protocols for MASLD-related HCC, as outlined in recent studies **Figure 3**.

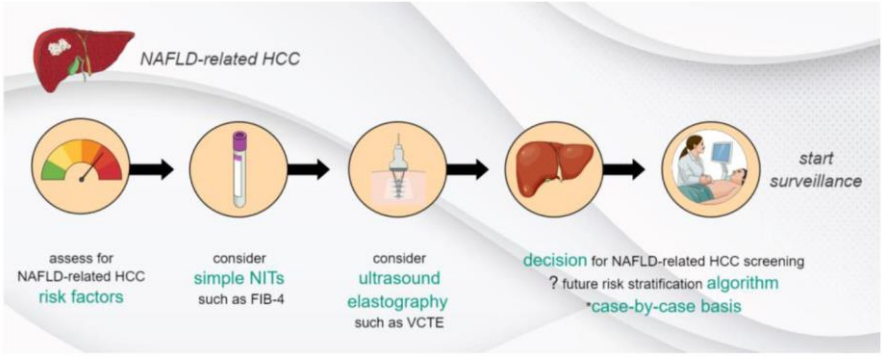

Figure 3. Outlook on developing risk stratification algorithms for MASLD (NAFLD)-related HCC
*Legend: NAFLD – non-alcoholic fatty liver disease, HCC – hepatocellular carcinoma, NITs – non-invasive tests, FIB-4 – fibrosis 4 index, VCTE – vibration-controlled transient elastography, ? – possible perspective, * - to be considered. (Image obtained from Taru MG, Lupsor-Platon M. Exploring Opportunities to Enhance the Screening and Surveillance of Hepatocellular Carcinoma in Non-Alcoholic Fatty Liver Disease (NAFLD) through Risk Stratification Algorithms Incorporating Ultrasound Elastography. Cancers. 2023 Aug 14;15(16):4097. DOI:10.3390/cancers15164097)*

Hipotethically, patients that are moderately elder (60-75 years old), but without comorbidities severe enough to prevent any HCC treatment, with advanced fibrosis (possibly > 8 kPa), with diabetes and with good ultrasound explorability and strong

motivation to adhere to surveillance, could benefit from a particularized HCC screening programme, as that one presented in Figure 3. Yet, this needs to be further tested and validated.

5. Disease progression to clinically significant portal hypertension (CSPH). Prevention of first decompensation event

Clinically significant portal hypertension (CSPH), a primary factor in cirrhosis decompensation, is characterized by a hepatic venous pressure gradient (HVPG) of 10 mmHg or higher (98). Mild or subclinical portal hypertension is a hemodynamic condition defined by a hepatic venous pressure gradient (HVPG) ranging from 6 to 9 mmHg (41). An HVPG value ≥10 mmHg identifies patients with compensated advanced chronic liver disease (cACLD) at elevated risk of decompensation, this being of outmost importance for disease management and prognosis. In patients with CSPH, decompensation can be prevented by using non-selective beta blockers (NSBBs), preferably carvedilol (99). The invasive nature of HVPG measurement has led researchers to focus on non-invasive markers that can predict clinically significant portal hypertension (CSPH). In this context, liver stiffness measurement (LSM) by VCTE has shown promise. Currently, an LSM of 10 kPa or higher is considered indicative of compensated advanced chronic liver disease (cACLD), while an LSM of 15 kPa or greater is highly suggestive of cACLD (41).

According to the guidelines (41), An LS measurement by VCTE of 15 kPa or less, combined with a platelet count of 150 × 10^9/L or higher, effectively rules out clinically significant portal hypertension (CSPH) in patients with compensated advanced chronic liver disease (cACLD), with a sensitivity and negative predictive value exceeding 90%. Conversely, in patients with virus- and/or alcohol-related cACLD, as well as non-obese (BMI <30 kg/m^2) MASH-related cACLD, an LS value of 25 kPa or greater is sufficient to confirm CSPH, demonstrating specificity and positive predictive value above 90%. This identifies individuals at higher risk for endoscopic signs of portal hypertension and greater likelihood of liver decompensation (41). The newly proposed ANTICIPATE-NASH model, which includes BMI along with liver stiffness measurement (LSM) by VCTE and platelet count, seeks to improve the prediction of clinically significant portal hypertension (CSPH) in obese MASLD patients (100). The authors found that portal hypertension is present in over 90% of cases with compensated advanced chronic liver disease (cACLD) due to alcohol (ALD), hepatitis C virus (HCV), or hepatitis B virus (HBV). In contrast, the prevalence of portal hypertension is significantly lower in patients with MASH, especially those who are obese. While an LSM of 25 kPa or greater was not sufficiently specific to confirm CSPH in obese MASH patients, an LSM of 15 kPa or less combined with a platelet count of

150 × 10^9/L or higher effectively ruled out CSPH across most chronic liver disease etiologies.

Applying the current Baveno VII criteria to determine clinically significant portal hypertension (CSPH) leaves approximately 40% of patients in an "unclassified" "grey zone," which limits the potential to identify those who could benefit from non-selective beta-blocker (NSBB) treatment without undergoing invasive procedures like hepatic venous pressure gradient (HVPG) measurement. In response, Jachs et al. recently proposed a new stratification algorithm that combines liver stiffness (LS), platelet count (PLT), and the von Willebrand antigen to PLT ratio (VITRO) for a more refined diagnosis of CSPH. In their monocentric, retrospective study of 302 patients with compensated advanced chronic liver disease (cACLD), including 13.2% with MASH etiology, CSPH prevalence was 62.3% in the derivation cohort, with 45.7% classified as 'unclassified' by the Baveno VII criteria. The sequential use of Baveno VII criteria and the new VITRO score reduced the number of previously unclassified patients by nearly 70%. A VITRO score of ≤1.5 and ≥2.5 effectively ruled out (sensitivity 97.7%; negative predictive value 97.5%) and ruled in (specificity 94.7%; positive predictive value 91.2%) CSPH, respectively, for patients who were previously unclassified by the Baveno VII criteria (101).

Spleen stiffness measurement (SSM) provides an estimate of portal hypertension in patients with advanced chronic liver disease (CLD). Recently, the incorporation of SSM by VCTE has been proposed as a method to decrease the number of patients left unclassified in the "grey zone" after applying the Baveno VII criteria (102). The Combined Baveno VII—SSM model for assessing clinically significant portal hypertension (CSPH) requires at least two of the following criteria to rule out CSPH: LSM ≤ 15 kPa, PLT ≥ 150 × 10^9/L, or SSM ≤ 40 kPa. To rule in CSPH, at least two of the following criteria are needed: LSM ≥ 25 kPa, PLT < 150 × 10^9/L, or SSM > 40 kPa. The authors found that incorporating SSM into the model significantly reduced the proportion of patients in the "grey zone" to 7%–15%, while still maintaining high negative and positive predictive values (NPV and PPV, both ≥ 90%) (102).

Recent observations suggest that patients with advanced MAFLD may face a higher prevalence of portal hypertension-related decompensation events at any given hepatic venous pressure gradient (HVPG) compared to patients with advanced HCV (103). Moreover, decompensation in advanced MAFLD may occur at lower HVPG levels compared to patients with other liver disease etiologies (104).

The adaptation of this knowledge for advanced MASLD and MASH is currently an active area of research.

PERSONAL CONTRIBUTION

1. Working hypothesis/objectives

Metabolic dysfunction-associated steatotic liver disease (MASLD) poses a significant public health challenge. Progression of the disease to more severe stages, such as advanced fibrosis (F3) and cirrhosis (F4), is linked to several adverse long-term outcomes. These include clinically significant portal hypertension (CSPH), initial and subsequent decompensation events, increased liver-related mortality, the development of hepatocellular carcinoma (even in the absence of cirrhosis), and a heightened risk of major cardiovascular events.

Risk factors, such as diabetes—which is frequently observed in patients diagnosed with MASLD—also play an independent role in the progression of liver disease, regardless of its etiology. While liver biopsy remains the gold standard for assessing fibrosis, the rising incidence and prevalence of MASLD have prompted the research community to focus on developing alternative, non-invasive methods for fibrosis prediction. These methods aim to improve the stratification and identification of MASLD patients at risk for disease progression and associated complications.

Key steps include stratifying the MASLD patient population to identify those at risk for advanced fibrosis and cirrhosis, as well as those susceptible to liver-related events like the development of decompensation and the onset of hepatocellular carcinoma. Additionally, understanding how to better select these patients and prevent the onset of these significant complications is crucial.

In this respect, the thesis has set the following objectives:

- To evaluate the effectiveness of Agile 3+, Agile 4, and FAST scores in distinguishing advanced fibrosis (≥F3), cirrhosis (F4), and fibrotic MASH (MASH + NAS ≥4 + F ≥2) within a cohort of biopsy-proven MASLD patients from a tertiary medical center in Cluj-Napoca, Romania. We hypothesized that these novel scoring systems would offer superior diagnostic accuracy compared to traditional non-invasive tests (NITs) such as LSM-VCTE, FIB-4, and APRI. Our specific objectives were to assess the performance of Agile 3+ in predicting advanced fibrosis (≥F3), Agile 4 in predicting cirrhosis (F4), and the FAST score in identifying fibrotic MASH, and to determine whether these scores provide better diagnostic accuracy than the existing NITs in these scenarios.
- To conduct a systematic review and meta-analysis using a multi-level random effects model to assess the diagnostic accuracy of 2D-SWE in patients with biopsy-proven MASLD. We aimed to establish reliable cut-off values for different stages of liver fibrosis that could be effectively applied in clinical practice. Our

hypothesis was that 2D-SWE provides a robust and non-invasive alternative for staging liver fibrosis, and that a meta-analytic approach would yield precise cut-off values enhancing its clinical utility

- To evaluate the impact of non-selective beta-blockers (NSBB) on the first occurrence of decompensation in patients with cirrhosis and clinical evidence of persistent clinically significant portal hypertension (CSPH) two years post-etiological treatment. We hypothesized that NSBB use could delay or prevent the first decompensation event. Additionally, we sought to identify independent risk factors contributing to the initial decompensation event in different etiologies, including MASLD, thus providing a clearer understanding of disease progression and potential intervention points.

2. General methodology

2.1. Patients

A cohort of 246 patients with biopsy-proven metabolic dysfunction-associated steatotic liver disease (MASLD) from the Medical 3 Clinic in Cluj-Napoca, Romania, was retrospectively followed during the period from January 2007 to July 2023. They were selected for the first study, specifically for the validation of the Agile 3+, Agile 4, and FAST scores in a population with predominantly Caucasian origins. All patients included in the study underwent a liver biopsy (either percutaneous or transjugular) for diagnostic purposes and had reliable vibration-controlled transient elastography (VCTE) measurements taken within three weeks prior to the biopsy.

We excluded patients with missing data for calculating Agile 3+, Agile 4, and FAST scores, missing fibrosis stage on liver biopsy, history of chronic liver disease other than MASLD (NAFLD) (e.g., viral, cholestatic, immune diseases), high alcohol consumption (>21 drinks/week for men, >14 drinks/week for women), elevated ALT and AST levels (>5 times the upper normal limit). At baseline, the following parameters were recorded for all patients: age, gender, body mass index (BMI), fasting glucose, history of diabetes, complete blood count, coagulation parameters, liver function profile, renal function, lipid profile, and serum electrolytes.

Another cohort of 406 patients with compensated liver cirrhosis from the Sant'Orsola Polyclinic in Bologna, Italy, was retrospectively followed during the period from 2017 to 2020. They were selected for the third study, which aimed to investigate the effect of non-selective beta-blocker treatment in preventing the first decompensation event and to study the independent risk factors influencing the development of the first decompensation episode. We included consecutive patients with compensated cirrhosis and persistent clinical evidence of clinically significant portal hypertension (CSPH) after two years of etiological treatment. Inclusion criteria were based on clinical, biochemical, imaging, and histological evidence of cirrhosis and CSPH. Patients with cirrhosis of various etiologies were included. Patients were excluded from the study if they did not fall within the age range of 18 to 80 years, lacked evidence of clinically significant portal hypertension (CSPH), had portal vein thrombosis, a history of shunt surgeries, prior hepatic decompensation, active or advanced hepatocellular carcinoma, vascular liver diseases, significant comorbid conditions, or if they had missing crucial data.

Baseline and follow-up data included the etiology of cirrhosis, comorbidities, pharmacological treatment, routine laboratory tests, and imaging studies. Hepatocellular carcinoma (HCC) surveillance was performed biannually. Endoscopy was used to assess gastroesophageal varices (GEV), and non-selective beta-blockers (NSBB) were administered based on clinical judgment.

The primary endpoint of the study was the incidence of hepatic decompensation, defined as the occurrence of variceal bleeding, ascites, or overt hepatic encephalopathy. Follow-up extended until June 2023, with hepatic decompensation or the development of hepatocellular carcinoma (HCC) and portal vein thrombosis (PVT) treated as competing risk events.

The characteristics of each analyzed cohort, as well as the extended inclusion and exclusion criteria, are presented in the following chapters, according to the objectives pursued in the respective studies.

2.2. Strategy and electronic search for meta-analysis

The meta-analysis adhered to the PRISMA guidelines and was registered on the Open Science Framework (OSF) (https://doi.org/10.17605/OSF.IO/9WV8F).

Comprehensive searches were conducted in PubMed/MEDLINE, Embase, Scopus, Web of Science, LILACS, and the Cochrane Library for articles from inception to February 1, 2023, and updated until February 26, 2024. Keywords included terms related to two-dimensional shear wave elastography (2D-SWE) and metabolic dysfunction-associated steatotic liver disease (MASLD/NAFLD). Only human studies were included, with no restrictions on gender, race, ethnicity, or language, and only full-text publications were considered.

Selection Criteria. Studies were included if they met these criteria:

- Population: Biopsy-proven NAFLD/NASH or MASLD/MASH
- Index Test: Liver stiffness measurement by 2D-SWE
- Reference Standard: Liver biopsy
- Studies were excluded if they were non-original works, lacked sufficient diagnostic performance data, or involved pediatric populations.

Data extraction involved three authors independently reviewing studies for relevant details such as demographics, diagnostic performance metrics, and technical parameters. The methodological quality was assessed using the QUADAS-2 tool, with disagreements resolved by a third author.

The primary outcome was the diagnostic accuracy of 2D-SWE for different stages of liver fibrosis in MASLD patients. Subgroup analyses considered ultrasound manufacturer, patient demographics, and comorbidities. A bivariate logit-normal random effects model was used to estimate pooled sensitivity, specificity, and AUROC. A multiple threshold model facilitated the analysis of studies reporting more than one cut-off, while enabling the calculation of positive and negative predictive values for different pre-test probabilities.

2.3. Laboratory analysis

To exclude possible laboratory variations, all biochemical, hematological, and virological determinations were performed in a single laboratory in Romania (Medical Clinic III Cluj) and in a single laboratory in Italy (Sant'Orsola Polyclinic, Bologna).

2.4. Vibration-controlled transient elastography and VCTE-based non-invasive tests

VCTE was performed using FibroScan (Echosens, Paris, France) with M and XL probes, adhering to EASL-ALEH recommendations. Measurements were considered reliable if they included 10 valid readings with an IQR/M <30%. Controlled attenuation parameter (CAP) was measured simultaneously with liver stiffness and expressed in dB/m, following similar reliability criteria.

Agile 3+, Agile 4, and FAST Scores Calculation. Scores were calculated using baseline characteristics, including diabetes status and gender:

- Agile 3+ and Agile 4 were computed using specific logistic regression models based on liver stiffness measurements, platelet count, AST to ALT ratio, diabetes status, gender, and age.
- FAST score was derived from liver stiffness, CAP, and AST levels.

2.5. Liver histology

Liver biopsies were formalin-fixed, paraffin-embedded, and subsequently analyzed by a liver disease specialist who was blinded to the results of the non-invasive tests. Fibrosis staging was performed using the NASH Clinical Research Network (CRN) scoring system, with stages ranging from F0 (no fibrosis) to F4 (cirrhosis). The NAFLD Activity Score (NAS) was computed as the sum of the grades for steatosis, ballooning, and lobular inflammation, with a total score ranging from 0 to 8. Metabolic dysfunction-associated steatohepatitis (MASH) was diagnosed based on the presence of steatosis, hepatocyte ballooning, and lobular inflammation, with at least one point in each category.

2.6. Statistical analysis for the studies that involved a retrospective enrollment of patients

Continuous variables were evaluated for normal distribution using the Kolmogorov-Smirnov test and were reported as either median with interquartile range or mean with standard deviation, depending on their distribution. Categorical variables were presented as frequencies and percentages. The one-way ANOVA test was used to compare different fibrosis stages. The diagnostic performance of Agile 3+,

Agile 4, and FAST scores was assessed through AUROC curves, and the DeLong test was employed to compare the diagnostic performance of these indices. Concordance between "grey zones" was examined using McNemar's test, with statistical significance set at $p < 0.05$. Statistical analyses also involved Levene's tests to assess homogeneity of variances, Student's t-tests for continuous variables, and Chi-square tests for categorical variables. Cumulative incidence curves were compared using Gray's test. Multivariable Cox regression analyses were conducted to identify predictors of decompensation and bacterial infections, with hazard ratios and 95% confidence intervals reported. ROC curve analysis was used to evaluate the performance of continuous parameters, with statistical significance set at $p < 0.05$. Statistical analysis was conducted using IBM SPSS (version 29), and R software.

2.7. Methodology and statistical analysis for the meta-analysis

The primary outcome was the diagnostic accuracy of 2D-SWE for different stages of liver fibrosis in MASLD patients. Subgroup analyses considered ultrasound manufacturer, patient demographics, and comorbidities. A bivariate logit-normal random effects model was used to estimate pooled sensitivity, specificity, and AUROC. A multiple threshold model facilitated the analysis of studies reporting more than one cut-off, while enabling the calculation of positive and negative predictive values for different pre-test probabilities.

2.8. Ethical considerations

The studies were conducted in accordance with the principles of the Helsinki Declaration and relevant local and national regulations. The study conducted in Cluj-Napoca, Romania, received approval from the Ethics Committee of the "Iuliu Haţieganu" University of Medicine and Pharmacy (approval number AVZ259/14.09.2022). Informed consent was obtained from all participants at the time of enrollment. Data accessed for research purposes on September 20, 2023, were anonymized to ensure patient confidentiality. The study conducted in Bologna, Italy was approved institutional review boards (MITIGO study - 405/2023). Informed consent was obtained from all participants where applicable.

2.8. Funding

Some of the results presented in this doctoral thesis were funded through the project PN-III-P4-PCE-2021-1140, offered by UEFISCDI, the Romanian Executive Agency for Higher Education, Research, Development, and Innovation Funding, under the direction of Prof. Dr. Monica Lupsor-Platon.

Additionally, for conducting my doctoral studies in Bologna, Italy, I received funding from The Study Loans and Scholarships Agency, Ministry of Education, Romania.

3. Study 1 - FAST and Agile–the MASLD drift: Validation of Agile 3+, Agile 4 and FAST scores in 246 biopsy-proven NAFLD patients meeting MASLD criteria of prevalent Caucasian origin

3.1. Introduction

Non-alcoholic fatty liver disease (NAFLD), also known as metabolic dysfunction-associated steatotic liver disease (MASLD) (1) is the most common chronic liver condition globally, with an estimated prevalence of up to 38% of the population (76). Liver fibrosis is a key factor influencing prognosis in patients with MASLD, significantly impacting overall mortality and elevating the risk of liver-related events (LREs). This risk is particularly pronounced in individuals with advanced fibrosis (≥F3) or cirrhosis (F4) (105).

Liver biopsy (LB) is currently the gold standard for assessing liver fibrosis. However, it is limited by its invasive nature, potential for intra- and inter-observer variability, and the risk of sampling errors (10, 12, 106). Given these limitations, the most practical approach for identifying MASLD patients with suspected advanced chronic liver disease (ACLD) is to use non-invasive tests (NITs) while also aiming for cost-efficiency (107). The use of non-invasive tests (NITs), which can be readily repeated and allow for the comparison of successive measurements, has the potential to enhance the overall management of patients with chronic liver disease (CLD), particularly those with MASLD (108).

Agile 3+ and Agile 4 are scoring systems that integrate clinical and laboratory factors, such as the AST/ALT ratio, platelet count, gender, diabetes status, and age (for Agile 3+), with liver stiffness measurement (LSM) obtained through vibration-controlled transient elastography (VCTE) (63). These scores have been developed to predict advanced fibrosis (≥F3) and cirrhosis (F4), respectively, in patients with MASLD (63). As established non-invasive tests (NITs), LSM-VCTE, and FIB-4 were demonstrated to have good performance in ruling-out advanced fibrosis in MASLD (109). The newly developed Agile 3+ and Agile 4 scores were meant to provide higher positive predictive values (PPVs) for ruling-in ≥F3 and F4, and to reduce the number of indeterminate results (63). These scores correlate well with the severity of liver fibrosis, decrease the number of patients left in the so-called “grey zone”, and increase the PPV for ruling-in ≥F3 and F4, respectively (63).

The FibroScan-AST (FAST) score, introduced in 2020, is designed for the non-invasive identification of patients with metabolic dysfunction-associated steatohepatitis (MASH) who also exhibit significant activity (NAS ≥4) and significant fibrosis (F ≥2) according to liver biopsy results (65).

3.2. Working hypothesis/objectives

In this study, we aimed to evaluate the effectiveness of Agile 3+, Agile 4, and FAST scores in distinguishing advanced fibrosis, cirrhosis, and fibrotic MASH in a cohort of biopsy-proven NAFLD patients who met MASLD criteria from a tertiary medical center in Cluj-Napoca, Romania. A secondary objective was to assess whether these scores provide superior predictive performance compared to commonly used non-invasive tests (NITs) such as LSM-VCTE, FIB-4, and APRI, specifically for predicting advanced fibrosis (≥F3), cirrhosis (F4), and fibrotic MASH.

3.3. Material and methods

Patients. This retrospective analysis included 246 consecutive adult patients (18-80 years old), evaluated for suspected MASLD, from our tertiary care center in Cluj-Napoca, Romania. The recruitment period started on the 1st of January 2007 and ended on the 18th of July 2023. All included patients had undergone liver biopsy (percutaneous or transjugular) for diagnostic purposes and presented baseline reliable VCTE measurements within a maximum three weeks prior to the liver biopsy. We excluded patients with missing data necessary for calculating the Agile 3+, Agile 4 and FAST scores, missing fibrosis stage on liver biopsy, history of chronic liver disease other than MASLD (such as viral, cholestatic, immune etc.), high alcohol consumption (defined by >21 drinks, on average, per week in men and >14 drinks, on average, per week in women (110)), and ALT and AST >5 times the upper normal limit.

All patients had the following parameters collected at baseline: age, gender, body mass index (BMI), fasting glucose and history of diabetes, complete blood count, coagulation parameters, liver function profile, renal function, lipidic profile, and serum electrolytes.

This retrospective study of consecutively enrolled patients was conducted in accordance with the Helsinki Declaration and relevant local and national regulations. The study protocol was approved by the Ethics Committee of "Iuliu Haţieganu" University of Medicine and Pharmacy, Cluj-Napoca, Romania (approval number AVZ259/14.09.2022, study reference PN-III-P4-PCE-2021-1474). Informed consent was obtained from all participants at the time of enrollment. Data were accessed for research purposes on September 20, 2023. During and after data collection, the authors did not have access to any information that could identify individual participants.

Liver biopsy. Liver biopsies were fixed in formalin and embedded in paraffin. Histopathological staging for liver fibrosis was performed according to the NASH Clinical Research Network (CRN) scoring system and served as the reference standard (10). Steatosis (0-3), ballooning (0-2) and inflammation (0-3) were also scored using the NASH CRN scoring system (10). One pathologist specialized in liver diseases, blinded to the NITs results, staged fibrosis on the biopsy specimens, as: stage 0 -

absence of fibrosis (F0), stage 1 - perisinusoidal or portal (F1), stage 2 - perisinusoidal and portal/periportal (F2), stage 3 - septal or bridging fibrosis (F3), stage 4 - cirrhosis (F4). The NAFLD activity score (NAS) was calculated as the sum of steatosis, ballooning, and lobular inflammation grades and ranged from 0 to 8 (10). MASH was defined on LB as the presence of steatosis, hepatocyte ballooning, and lobular inflammation with at least 1 point for each category (FLIP-NASH) (111), following the seminal study on FAST score (65). Every biopsy specimen included in the analysis was taken from the right lobe (percutaneous or transjugular) and had a minimum of 6 portal tracts.

Fibrosis prediction formulas

The Fibrosis-4 index (FIB-4) was calculated as follows:

$$FIB4 = \frac{Age\ (years) x\ AST\ (U/L)}{PLT\ (10^9/l) x \sqrt{ALT\ (U/L)}}$$ (112);

The AST to platelet ratio index (APRI) was calculated as follows:

$$APRI = \frac{AST\ level(/ULN)}{PLT\ (10^9/L)}\ x\ 100$$ (113);

Liver stiffness measurement by vibration controlled transient elastography for staging fibrosis. VCTE (FibroScan, Echosens, Paris, France) was performed by two experienced operators, blinded to the biopsy results, with both M (3.5 Hz frequency), and XL (2.5 Hz frequency) probes, according to the EASL-ALEH recommendations (109, 114) and considering the integrated automatic probe selection software. Measurements were performed in a fasting state (6 hours). We considered reliable results as being those representing the median of 10 valid measurements with an IQR/M below 30%.

Controlled attenuation parameter by vibration controlled transient elastography for grading steatosis. CAP measurements (available in our clinic since 2012) were performed by FibroScan (Echosens, Paris, France) by two experienced operators, blinded to the biopsy results, simultaneously with LSM and by respecting the principles of CAP measurement (43). CAP was computed only when the corresponding LSM was valid, utilizing the same signals used to measure liver stiffness. Consequently, both stiffness and CAP were obtained during the same examination and from the same liver parenchyma volume. Reliable results were defined as the mean of 10 valid measurements with an interquartile range to median (IQR/M) ratio below 30%. The final CAP value was reported in dB/m.

Agile 3+, Agile 4 and FAST scores

We calculated the Agile 3+, Agile 4 and FAST scores based on the baseline characteristics for each patient, considering diabetes status: yes=1, no=0 and gender: male=1, female=0, by using the following formulas (63, 65):

For Agile 3+:

$$Agile\ 3+= \frac{e^{logit(p_{F\geq F3})}}{1+\ e^{logit(p_{F\geq F3})}}$$

where

$$logit\ (p_{F\geq F3}) = -3.92368 + 2.29714 \times ln(LSM) - 0.00902 \times PLT - 0.98633\ x\ AAR^{-1} + 1.08636 \times Diabetes\ status - 0.38581 \times Sex + 0.03018 \times Age$$

For Agile 4:

$$Agile\ 4 = \frac{e^{logit(p_{F=4})}}{1+e^{logit(p_{F=4})}},$$

where

$$logit(p_{F=4}) = 7.50139 - 15.42498\ x\ \frac{1}{\sqrt{LSM}} - 0.01378 \times PLT - 1.41149 \times AAR^{-1} - 0.53281;$$

For FAST score:

$$FAST = \frac{e^{-1.65\ +1.07\ x\ \ln(LSM)\ +\ 2.66\ *\ 10^{-8}\ x\ CAP^3 - 63.3\ x\ AST^{-1}}}{1+e^{-1.65\ +1.07\ x\ \ln(LSM)\ +\ 2.66\ *\ 10^{-8}\ x\ CAP^3 - 63.3\ x\ AST^{-1}}};$$

Statistical analysis. Continuous variables were assessed for normal distribution using the Kolmogorov-Smirnov test and were expressed as either median with interquartile range (Q1-Q3), mean with standard deviation (SD), or mean with standard error of the mean (SEM). Categorical variables were reported as frequencies and percentages. Descriptive statistics were provided for the entire cohort (n=246) and for the subset of patients for whom the FAST score was calculated (n=136). Intergroup comparisons of fibrosis stages with LSM-VCTE, Agile 3+, and Agile 4 were performed using one-way ANOVA. The diagnostic performance of Agile 3+, Agile 4, and FAST scores was evaluated using receiver operating characteristic (AUROC) curves, with AUROCs and 95% confidence intervals (CI) calculated for detecting histologically confirmed advanced fibrosis (≥F3), cirrhosis (F4), and fibrotic MASH (MASH + NAS ≥4 + F≥2). The DeLong test was employed to compare the diagnostic performance of Agile scores with LSM alone, FIB-4, and APRI. For Agile 3+, Agile 4, and FAST scores, the number of patients remaining in the grey zone was determined, and concordance between grey zones was assessed using the exact McNemar's test. Statistical significance was defined as $p < 0.05$ for all tests. Analyses were conducted using IBM Statistical Package for Social Sciences (SPSS, version 29, IBM Corp., Armonk, NY, USA).

3.4. Results

246 biopsy-proven MASLD patients were included in the final analysis. The mean number of portal tracts on biopsy was 12 ±8. Of those, 136 presented reliable CAP measurements. Out of 256 patients with reliable VCTE measurements, 4 (1.6%) of them did not meet the MASLD criteria and were not included in the analysis (were considered as lean NAFLD). **Figure 1** displays a comprehensive overview of the patient selection process.

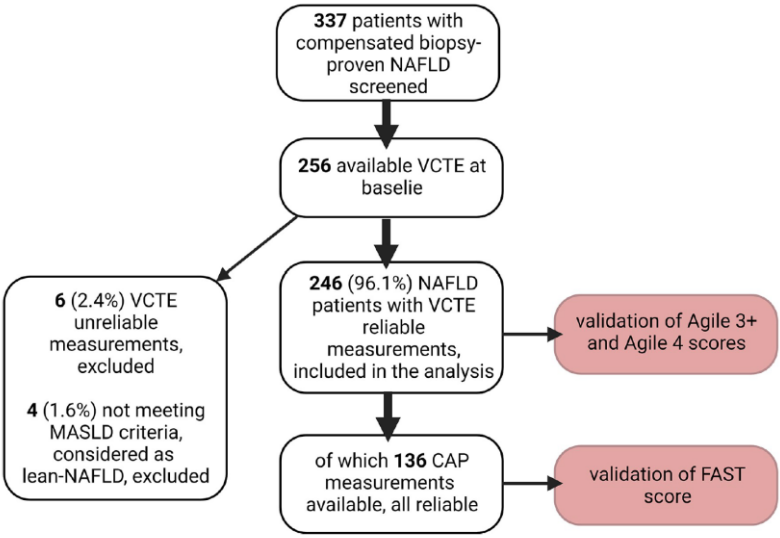

Fig 1. Flow diagram of patient selection. NAFLD- nonalcoholic fatty liver disease, VCTE- vibration controlled transient elastography, CAP- controlled attenuation parameter, FAST- FibroScan-AST score.

Figure 2 was obtained from Taru MG, Tefas C, Neamti L, Minciuna I, Taru V, Maniu A, Rusu I, Petrushev B, Procopciuc LM, Leucuta DC, Procopet B, Ferri S, Lupsor-Platon M, Stefanescu H. FAST and Agile–the MASLD drift: Validation of Agile 3+, Agile 4 and FAST scores in 246 biopsy-proven NAFLD patients meeting MASLD criteria of prevalent caucasian origin. PloS one. 2024 May 23;19(5): e0303971. DOI:10.1371/journal.pone.0303971

The median age at baseline was 52 years (IQR, 20) and median BMI was 29.0 kg/m2 (IQR, 5.1). 113 (45.9%) patients were female and 75 (30.5%) presented diabetes at baseline. **Table I** provides a comprehensive overview of the baseline characteristics for the included patients.

Table I. Baseline characteristics of the patients included in the study

		Validation of Agile 3+ and Agile 4 scores n=246	**Validation of FAST score n=136**
Variable		**Count (%) or Median (Q1-Q3)**	**Count (%) or Median (Q1-Q3)**
Age (years)		52 (41 - 61)	55 (47 - 63)
Gender	Female	113 (45.9)	74 (54.4)
BMI (kg/m^2)		29.0 (27.1 - 32.2)	29.0 (27.0 - 32.5)
T2DM	Yes	75 (30.5)	49 (36.0)
Fibrosis (NASH CRN)	F0	25 (10.2)	4 (2.9)
	F1	70 (28.4)	30 (22.1)
	F2	78 (31.7)	53 (39.0)
	F3	44 (17.9)	29 (21.3)
	F4	29 (11.8)	20 (14.7)
0Steatosis (NASH CRN)	S1	82 (33.3)	43 (31.6)
	S2	85 (34.6)	50 (36.8)
	S3	79 (32.1)	43 (31.6)
MASH/NASH		222 (90.2)	114 (83.8)
Hb (mg/dl)		14.9 (13.6 - 16.0)	14.3 (13.1 - 15.7)
Platelets (x10^9/l)		230 (187 - 268)	224 (174 - 272)
INR		1.02 (0.94 - 1.12)	1.05 (0.96 - 1.15)
TB (mg/dl)		0.70 (0.50 - 1.00)	0.70 (0.50 - 1.00)
AST (IU/l)		43 (29 - 67)	45 (28 - 63)
ALT (IU/l)		56 (35 - 101)	48 (30 - 81)
GGT (IU/l)		66 (39 - 106)	67 (39 - 116)
ALP (IU/l)		198 (148 - 283)	196 (118 - 282)
Alb (IU/l)		4.3 (4.0 - 4.8)	4.3 (4.0 - 4.8)
Glycemia (mg/dl)		104 (93 - 126)	108 (94 - 129)
Creatinine (µmol/l)		0.84 (0.71 - 1.03)	0.78 (0.64 - 0.90)
Tot Cho (mmol/l)		202 (164 - 246)	185 (160 - 227)
LDL (mmol/l)		107 (83 - 154)	112 (85 - 154)
Tg (mmol/l)		159 (114 - 230)	143 (111 - 206)
FIB-4		1.26 (0.82 - 2.11)	1.50 (0.99 - 2.25)
APRI		0.53 (0.34 - 1.03)	0.53 (0.35 - 1.01)
LS (kPa)		8.4 (5.9 - 13.4)	9.5 (6.2 - 14.8)

Legend for Table I: n- number, FAST- FibroScan-AST score, Q1- percentile 25, Q3- percentile 75, BMI- body mass index, T2DM- type 2 diabetes mellitus, NASH- nonalcoholic steatohepatitis, CRN- clinical research network, MASH- metabolic disfunction-associated steatohepatitis, Hb- hemoglobin, INR- international normalized ratio, TB- total bilirubin, AST- aspartate-aminotransferase, ALT- alanine-aminotransferase, GGT- gamma glutamyl transpeptidase, ALP- alkaline phosphatase, Alb- albumin, Tot Cho- total cholesterol, LDL- low-density lipoprotein cholesterol, Tg- triglycerides, FIB-4- Fibrosis 4 index, APRI- AST to Platelet Ratio Index, LS- liver stiffness, kPa- kilopascals

Diagnostic performance of Agile 3+ and Agile 4 scores

The mean (±SEM) values for LSM-VCTE increased progressively with advancing fibrosis stages, starting from F0 (5.6 ± 0.5 kPa) and rising to F1 (6.8 ± 0.3 kPa), F2 (9.0 ± 0.5 kPa), F3 (15.5 ± 1.2 kPa), and F4 (30.4 ± 3.1 kPa) (Figure 2a). Agile 3+ also demonstrated a progressive increase across fibrosis stages, with values for F0 (0.073 ± 0.017), F1 (0.182 ± 0.024), F2 (0.336 ± 0.032), F3 (0.686 ± 0.042), and F4 (0.939 ± 0.016) (Figure 2b). Similarly, Agile 4 followed the same trend, with values for F0 (0.006 ± 0.002), F1 (0.024 ± 0.005), F2 (0.100 ± 0.020), F3 (0.292 ± 0.039), and F4 (0.736 ± 0.041) (Figure 2c).

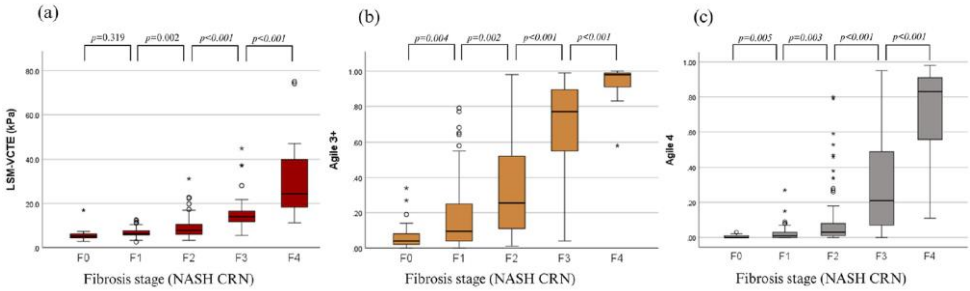

Fig 2. LSM-VCTE, Agile 3+ and Agile 4 scores among 246 patients with biopsy-proven NAFLD. Median values (lines inside boxes) for (a) LSM-VCTE, (b) Agile 3+, (c) Agile 4 are shown in the box graph, together with the 25th–75th percentiles, respectively. LSM–liver stiffness measurement, VCTE–vibration controlled transient elastography, kPa–kilopascals, NASH–nonalcoholic steatohepatitis, CRN–Clinical Research network, F0 –absence of fibrosis, F1 –mild fibrosis, F2 –significant fibrosis, F3 –advanced fibrosis, F4 –cirrhosis.

For predicting advanced fibrosis (≥F3), Agile 3+ demonstrated an AUROC of 0.909 [95% CI: 0.866–0.942], while Agile 4 showed an AUROC of 0.911 [95% CI: 0.869–0.944] (Figure 3). The performances of the two scores were slightly lower compared to the AUROC for LSM alone, which was 0.933 [95% CI: 0.894–0.961]. However, these differences were not statistically significant, with DeLong test p-values of 0.209 for Agile 3+ and 0.245 for Agile 4.

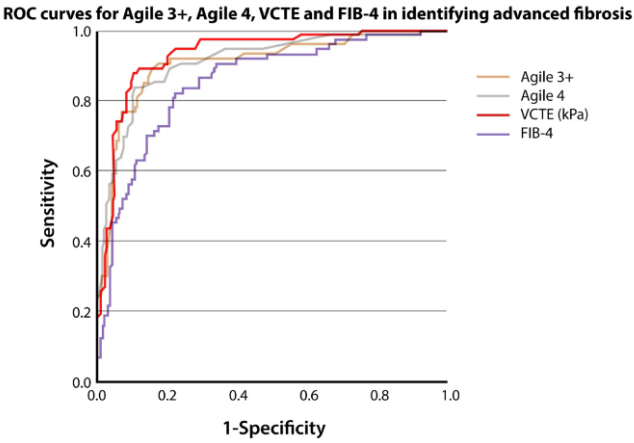

Fig 3. Diagnostic performance of Agile 3+, Agile 4, LSM-VCTE and FIB-4 in identifying advanced fibrosis (≥F3). ROC—receiver operating characteristic curve, VCTE–vibration-controlled transient elastography, FIB-4 –Fibrosis 4 Index, kPa–kilopascals.

Using a cut-off of 0.451, Agile 3+ demonstrated the following performance metrics for ruling out advanced fibrosis: sensitivity (Se) of 90.41%, specificity (Sp) of 79.77%, positive predictive value (PPV) of 65.35%, negative predictive value (NPV) of 95.17%, and accuracy (Acc) of 82.93%. For ruling in advanced fibrosis with a cut-off of 0.679, Agile 3+ showed a sensitivity of 76.71%, specificity of 91.91%, PPV of 80.00%, NPV of 90.34%, and an accuracy of 87.40%. The performance of Agile 3+ in predicting advanced fibrosis (≥F3) with the selected cut-offs for sensitivity ≥85%, ≥90%, and specificity ≥90% is detailed in Table II.

Table II. Diagnostic accuracy of Agile 3+, Agile 4, LSM-VCTE and FIB-4 in identifying advanced fibrosis (≥F3) among 246 patients with biopsy-proven MASLD

NIT	AUC [95% CI]	Aim	Cut-off	Se (%)	Sp (%)	PPV (%)	NPV (%)	Acc (%)
Agile 3+	0.909 [0.866 - 0.942]	Se ≥90 %	0.480	90.41	82.66	68.75	95.33	84.96
		Sp ≥90 %	0.680	76.71	92.49	81.17	90.40	87.81
		Se ≥85 %	0.530	86.30	85.55	71.59	93.67	85.77
			0.451*	90.41	79.77	65.35	95.17	82.93
			0.679**	76.71	91.91	80.00	90.34	87.40
Agile 4	0.911 [0.869 - 0.944]	Youden	0.090	83.56	89.60	77.22	92.81	87.81
VCTE	0.933 [0.894 - 0.961]	Youden	11.1 kPa	89.04	88.44	76.47	95.03	88.62
FIB-4	0.854 [0.803 - 0.895]	Youden	1.53	82.19	78.03	61.22	91.21	79.26

*Legend for Table II: NIT- non-invasive rest, VCTE – vibration controlled transient elastography, FIB-4 – Fibrosis 4 Index, Se – sensitivity, Sp – specificity, PPV – positive predictive value, NPV – negative predictive value, Acc-accuracy, kPa – kilopascals, *Original cut-off value to rule-out advanced fibrosis (63) ,** Original cut-off value to rule-in advanced fibrosis (63).*

For diagnosing cirrhosis (F4), Agile 3+ had an AUROC of 0.958 [95% CI: 0.925–0.980], while Agile 4 achieved an AUROC of 0.968 [95% CI: 0.937–0.986]. (Figure 4).

The performances of the two scores were slightly higher than that of LSM-VCTE alone, which had an AUROC of 0.956 [95% CI: 0.922–0.978]. However, these differences were not statistically significant, with DeLong test p-values of 0.782 for Agile 3+ and 0.312 for Agile 4.

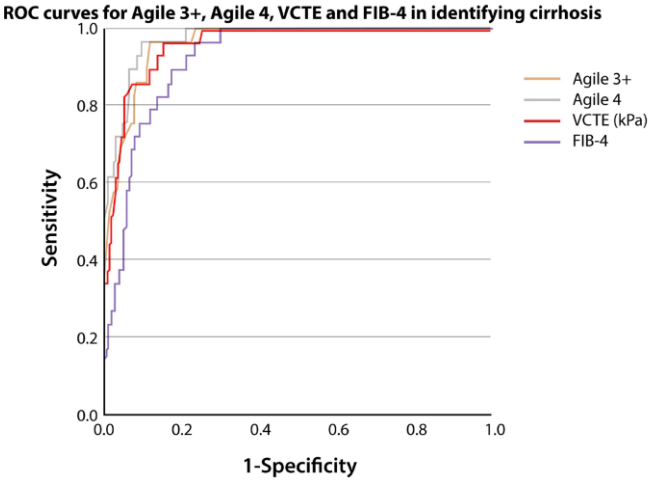

Fig 4. Diagnostic performance of Agile 3+, Agile 4, LSM-VCTE and FIB-4 in identifying cirrhosis (F4) among 246 patients with biopsy-proven NAFLD.
ROC—receiver operating characteristic curve, VCTE–vibration-controlled transient elastography, FIB-4 –Fibrosis 4 Index, kPa–kilopascals.

Using a cut-off of 0.251, Agile 4 achieved the following performance metrics for ruling out cirrhosis (F4): sensitivity (Se) of 96.55%, specificity (Sp) of 84.79%, positive predictive value (PPV) of 45.90%, negative predictive value (NPV) of 99.46%, and overall accuracy (Acc) of 86.18%. For ruling in cirrhosis, with a cut-off of 0.565, Agile 4 demonstrated a sensitivity of 72.41%, specificity of 94.47%, PPV of 63.64%, NPV of 96.24%, and an accuracy of 91.87%. The performance of Agile 4 in predicting cirrhosis using these cut-offs is detailed in Table III.

Table III. Diagnostic accuracy of Agile 3+, Agile 4, LSM-VCTE and FIB-4 in identifying cirrhosis (F4) among 246 patients with biopsy-proven MASLD

NIT	AUC [95% CI]	Aim	Cut-off	Se (%)	Sp (%)	PPV (%)	NPV (%)	Acc (%)
Agile 3+	0.958 [0.925 - 0.980]	Youden	0.820	96.55	87.56	50.91	99.48	88.62
Agile 4	0.968 [0.937 - 0.986]	Se ≥90 %	0.380	93.10	90.78	57.44	98.99	91.05
		Sp ≥90 %	0.520	75.86	94.01	62.86	96.68	91.87
		Se ≥85%	0.470	89.66	93.09	63.42	98.54	92.69
		Sp ≥95 %	0.600	72.41	96.31	72.39	96.31	93.49
			0.251*	96.55	84.79	45.90	99.46	86.18
			0.565**	72.41	94.47	63.64	96.24	91.87
VCTE	0.956 [0.922 - 0.978]	Youden	13 kPa	96.55	83.87	44.44	99.45	85.36
FIB-4	0.921 [0.880 - 0.951]	Youden	1.79	96.55	76.04	35.00	99.40	78.46

*Legend for Table III: NIT- non-invasive rest, VCTE – vibration controlled transient elastography, FIB-4 – Fibrosis 4 Index, Se – sensitivity, Sp – specificity, PPV – positive predictive value, NPV – negative predictive value, Acc – Accuracy, kPa – kilopascals, *Original cut-off value to rule-out cirrhosis (63)** Original cut-off value to rule-in cirrhosis (63).*

Comparison with other fibrosis prediction scores

A detailed comparison using DeLong protocol among different fibrosis prediction scores is presented in **Table IV**.

Table IV. Comparison between Agile 3+, Agile 4, and standard NITs in staging liver fibrosis using DeLong Protocol

Fibrosis stage	NIT	p values			
		Agile 3+	**Agile 4**	**VCTE**	**FIB-4**
≥ F3	Agile 3+	N/A	0.783	0.209	0.012
	Agile 4	0.783	N/A	0.245	0.003
	VCTE	0.209	0.245	N/A	0.006
	FIB-4	0.012	0.003	0.006	N/A
F4	Agile 3+	N/A	0.099	0.782	0.012
	Agile 4	0.099	N/A	0.312	0.001
	VCTE	0.782	0.312	N/A	0.086
	FIB-4	0.012	0.001	0.086	N/A

Legend for Table IV: F3 – advanced fibrosis, F4 – cirrhosis, NIT – non-invasive test, VCTE – vibration-controlled transient elastography, FIB-4 – Fibrosis 4 Index, N/A – not applicable

For identifying advanced fibrosis (≥F3), the AUROC for LSM-VCTE alone was 0.933 [95% CI: 0.894 - 0.961], while for the FIB-4 index, it was 0.854 [95% CI: 0.803 - 0.895]. Agile 3+ showed significantly better diagnostic performance compared to FIB-

4, with a p-value of 0.012. However, there was no statistically significant difference between Agile 3+ and LSM-VCTE, with a p-value of 0.209

In terms of identifying cirrhosis (F4), the AUROCs for LSM-VCTE alone and for FIB-4 index were 0.956 [95% CI: 0.922 - 0.978] and 0.921 [95% CI: 0.880 - 0.951], respectively (Table 3). Agile 4 had a significantly better diagnostic performance compared to FIB-4 (p=0.001), and a slightly better diagnostic performance compared to LSM-VCTE alone, but not statistically significant (p=0.312).

Proportion of patients with indeterminate results when applying Agile 3+, Agile 4 and LSM-VCTE

We next looked at the proportion of patients that remained unclassified (in the so-called "grey zone"). In our cohort of patients, by using Agile 3+ standard cut-offs for ≥F3, 0.451 and 0.679 (63), and LSM-VCTE standard cut-offs for ≥F3, 8 kPa and 12 kPa, (109), the proportion of patients that were left unclassified were 12.6% and 21.9%, respectively (McNemar's exact test p=0.003). By using Agile 4 standard-cutoffs for F4, namely 0.251 and 0.565 (63), and the LSM-VCTE cut-offs of 8 kPa and 20 kPa, then 10 kPa and 20 kPa (115), the proportion of patients that were left unclassified were 11.4%, 39.4% and 26.8%, respectively (McNemar's exact test p<0.0001 for both scenarios), as depicted in Table V.

Table V. Distribution of patients with biopsy-proven MASLD according to the individual risk

	NIT	Rule-out cutoff	Patients below the low cut-off value n (%)	Patients remained in grey zone n (%)	Rule-in cutoff	Patients above the high cut-off value n (%)
AF (≥F3)	**Agile 3+**	0.451	145 (58.9)	31 (12.6)	0.679	70 (28.5)
	LSM-VCTE	8 kPa	120 (48.8)	54 (21.9)	12 kPa	72 (29.3)
Cirrhosis (F4)	**Agile 4**	0.251	185 (75.2)	28 (11.4)	0.565	33 (13.4)
	LSM-VCTE	8 kPa	120 (48.8)	97 (39.4)	20 kPa	29 (11.8)
	LSM-VCTE	10 kPa	151 (61.4)	66 (26.8)	20 kPa	29 (11.8)

Legend for Table V: NIT – non-invasive test, AF – advanced fibrosis, F3 – advanced fibrosis. LSM – liver stiffness measurement, VCTE – vibration-controlled transient elastography, n – number, % - percentage

Diagnostic performance of FAST score in identifying fibrotic NASH

The AUROCs for identifying fibrotic NASH (NASH + NAS ≥4 + F ≥2) were as follows: FAST Score achieved 0.679 [95% CI: 0.594 - 0.757], LSM-VCTE alone was 0.591 [95% CI: 0.503 - 0.674], FIB-4 index was 0.519 [95% CI: 0.432 - 0.606], and APRI score was 0.578 [95% CI: 0.490 - 0.662] (Figure 5). In the subgroup analysis for

FAST Score, the AUROCs were 0.70 [95% CI: 0.59 - 0.80] for ALT ≥35 UI/L and 0.60 [95% CI: 0.42 - 0.77] for ALT <35 UI/L, respectively.

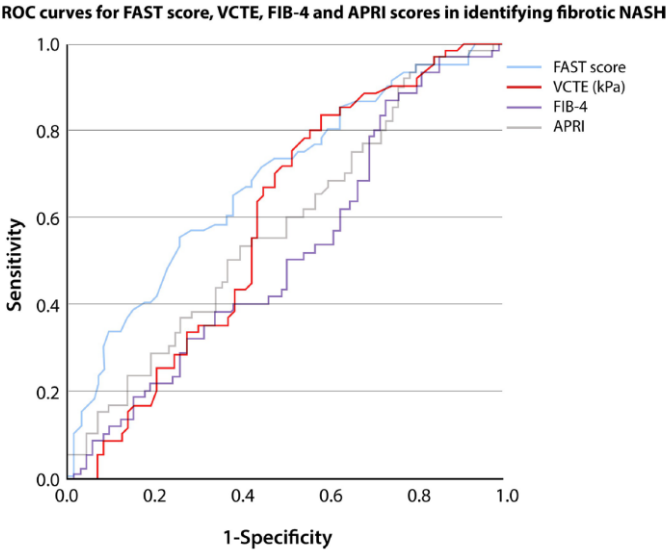

Fig 5. Diagnostic performance of FAST score and other NITs in predicting fibrotic NASH. ROC—receiver operating characteristic curve, FAST-FibroScan-AST score, VCTE–vibration-controlled transient elastography, FIB-4 –Fibrosis 4 Index, APRI—aspartate aminotransferase to platelet ratio index.

The AUROC for FAST score was significantly higher than the AUROCs for LSM-VCTE alone (p=0.02), FIB-4 (p=0.001) and APRI (p=0.002) scores.

The Se, Sp, PPV, NPV, and Acc for FAST score using the cut-off of 0.35 to rule-out fibrotic NASH and the cut-off of 0.67 to rule in the condition (109), along with our best selected cut-off values for Se ≥90% and Sp ≥90% are presented in **Table VI**.

Table VI. Diagnostic accuracy of FAST score in predicting fibrotic MASH (MASH + NAS≥4 + F≥2)

NIT	AUC (95% CI)	Aim	Cut-off	Se (%)	Sp (%)	NPV (%)	PPV (%)	Acc (%)
FAST score	0.679 (0.594, 0.757)	Se ≥90%	0.17	91.80	25.33	79.16	50.00	55.14
		Sp ≥90%	0.75	31.15	90.67	61.82	73.09	63.97
			0.35*	21.31	58.67	47.83	41.94	41.91
			0.67**	49.18	76.00	64.77	62.50	63.97

*Legend for Table VI: NIT – noninvasive test, AUC-area under the ROC curve, CI- confidence interval, %-percentage, Se- sensitivity, Sp-specificity, NPV- negative predictive value, PPV-positive predictive value, Acc-accuracy, *original cut-off value to rule-out fibrotic NASH (65), **original cut-off value to rule-in fibrotic NASH (65).*

In our cohort of patients, when applying the FAST score with its standard cut-off values (65), 44 (32.4%) patients remained below the inferior cut-off, 44 (32.4%) in the grey zone and 48 (35.2%) patients were above the superior cut-off.

3.5. Discussions

The purpose of this study was to validate three new non-invasive scoring systems—Agile 3+, Agile 4, and the FAST score—in a cohort of 246 patients with biopsy-confirmed NAFLD meeting MASLD criteria. We aimed to assess their effectiveness in distinguishing between advanced fibrosis, cirrhosis, and fibrotic MASH, and our findings successfully confirmed their utility. During the validation process, we evaluated the performance of previously published cut-offs and provided optimal cut-off values tailored to our cohort. Our goal was to achieve sensitivities of ≥85% and ≥90% for ruling out the conditions, and specificities of ≥90% and ≥95% for ruling in the conditions (63).

Agile 3+ and Agile 4 scores were specifically developed for individuals with MASLD in 2023 (63). These scoring systems aim to achieve several key objectives. They are designed to accurately identify advanced fibrosis and cirrhosis, which are critical for assessing the severity of liver disease. Additionally, they work to optimize the positive predictive value, ensuring that those who test positive for these conditions are indeed at high risk. Another important goal is to reduce the number of indeterminate results, often referred to as the "grey zone," where further invasive testing might otherwise be required, thereby improving diagnostic clarity and minimizing the need for additional procedures (63).

Agile 3+

Upon assessing its diagnostic performance, the AUROC for Agile 3+ in discriminating advanced fibrosis (≥F3) was excellent but slightly lower than that for LSM-VCTE alone (0.909 vs. 0.933), though this difference was not statistically significant (p=0.209). However, when comparing the number of patients with indeterminate results after applying dual cut-off approaches for Agile 3+ and LSM-VCTE, Agile 3+ significantly reduced the number of patients in the grey zone (p=0.003) while maintaining very good accuracy (Table V).

Agile 4

Upon assessing its diagnostic performance, the AUROC for Agile 4 in discriminating cirrhosis (F4) demonstrated excellent performance, slightly superior to that of LSM-VCTE alone (0.968 vs. 0.956), though the difference was not statistically significant. With the application of the dual cut-off approach for Agile 4, only 11.4% of patients remained in the grey zone, while maintaining excellent accuracy. Furthermore, Agile 4 significantly reduced the number of patients with indeterminate results compared to LSM-VCTE, with a p-value of <0.0001.

Agile 3+ and Agile 4 Scores

Both Agile 3+ and Agile 4 scores significantly outperformed the FIB-4 index in discriminating advanced fibrosis (≥F3) and cirrhosis (F4). These findings suggest that Agile 3+ and Agile 4 are well-optimized tools for distinguishing MASLD patients with advanced fibrosis and cirrhosis. Our results align with those of previously reported studies, reinforcing the effectiveness of these scores in clinical practice (63, 116). The seminal study by Sanyal et. all. (63), that developed the Agile scores, reported significantly greater AUROCs when compared to LSM-VCTE alone (0.86-0.90 for Agile 3+ and 0.83-0.85 for LSM-VCTE in depicting ≥F3, and 0.89-0.93 for Agile 4 and 0.85-0.88 for LSM-VCTE in discriminating F4). In our cohort, although the Agile 3+ and Agile 4 scores did not achieve significantly higher AUROCs compared to LSM-VCTE alone, their clinical utility was evident. Agile 3+ notably reduced the number of patients with indeterminate results, while Agile 4 demonstrated excellent accuracy, reaching 92%. Specifically, applying the optimal cut-off of 0.600 for Agile 4 allowed for ruling-in cirrhosis with a high accuracy of 93.5%. These results underscore the practical value of these scoring systems in managing patients with MASLD and cirrhosis.

The lack of significant superiority in AUROCs for Agile scores in our cohort compared to the seminal study may be attributed to several factors. First, our cohort had a slightly different prevalence of F3 and F4 fibrosis stages, which could influence the performance metrics. Additionally, there may be variations in clinical and laboratory data used for score computation, affecting the results. Our study included consecutive patients with a clinical suspicion of MASH, which likely mirrors the general population's distribution of fibrosis stages. Furthermore, our cohort was predominantly of Caucasian descent, who may have different risks for severe fibrosis compared to populations such as Latin-Americans or Hispanics. These differences highlight the importance of considering demographic and clinical variations when evaluating the performance of diagnostic scoring systems (76). Given these considerations, our results hold particular significance for Central and Eastern Europe, where the Caucasian population is prevalent. The observed performance of the Agile 3+ and Agile 4 scores in our cohort provides valuable insights into their applicability in this specific demographic.

In our cohort, the prevalence of advanced fibrosis (≥F3) was 29.7% and cirrhosis (F4) was 11.8%. This contrasts with the study by Sanyal et al. (63), where the prevalence of these conditions was higher: 54% for advanced fibrosis and 23% for cirrhosis in both the training and validation sets, and 37% and 13% in the external validation cohort, respectively. Additionally, Sanyal et al. reported a mean age of 55 ± 16 years for both their training and validation cohorts, with a significant proportion of patients having diabetes (50.4% in the training cohort and 51% in the validation cohort). In comparison, our study had a median age of 52 years (range 41-61) and a lower proportion of patients with diabetes, at 30.5%.

For Agile 3+, the thresholds we used—0.480 for ruling out advanced fibrosis (with a sensitivity of ≥90%) and 0.680 for ruling in advanced fibrosis (with a specificity of ≥90%)—were closely aligned with the standard thresholds of 0.451 and 0.679, respectively. Similarly, for Agile 4, our thresholds—0.380 for ruling out cirrhosis (with a sensitivity of ≥90%) and 0.520 for ruling in cirrhosis (with a specificity of ≥90%)—were consistent with the proposed thresholds in the literature of 0.251 and 0.565, respectively. The excellent diagnostic performance of these standard cut-offs in our cohort suggests that they can be reliably applied to the Caucasian population.

One notably significant element emphasized in our article is the outstanding capability of Agile 4 in distinguishing cirrhosis (accuracy of 92 %), in a population with a median BMI of 29.0 (IQR, 5.1). It was previously established that LSM-VCTE alone ≥25 kPa is adequate for confirming CSPH in non-obese individuals with NASH, but it falls short in the case of obese patients with NASH (117). In this regard, composite scores with remarkable accuracy, such as Agile 4, could offer significant improvements in depicting CSPH and improve the management of these patients.

As part of the clinical evaluation, especially for risk stratification, the patients that are left in the "grey zone" should undergo, in our opinion, additional monitoring to determine their real fibrosis status. In this scenario, the causes for false positives should be considered, and another non-invasive test could be applied (ELF™, FibroMeter™, FibroTest®) or the patient could undergo liver biopsy in case of discordant NITs (109).

Another notable accomplishment of using Agile scores in clinical practice is their ability to predict liver-related events. Recent studies have demonstrated that these scores not only effectively differentiate between stages of fibrosis and cirrhosis but also offer valuable prognostic information regarding the risk of liver-related complications. This predictive capability enhances patient management by identifying those at higher risk for adverse outcomes, thereby guiding more personalized and timely interventions (64, 118). Since these scores incorporate factors like diabetes (119), which predisposes to hepatic decompensation, and other variables related to prediction of liver-related events (including hepatocellular carcinoma), we anticipate that this field will remain highly dynamic and lively, with continued validation and exploration of the Agile scores.

FAST-score

When developed, the FAST score exhibited satisfactory performance in both deviation (C-statistic 0.80, 95% CI 0.76-0.85) and validation (C-statistic range 0.85; 95% CI 0.83-0.87) cohorts and was further validated in some populations (65). For depicting fibrotic MASH, the FAST score demonstrated satisfactory performance in a recently published meta-analysis encompassing 12 studies, achieving an AUROC of 0.79 (120). By applying the rule-out (≤0.35) and rule-in (≥0.67) cut-offs, 33% remained in the grey zone (120). In our cohort of patients, the FAST score exhibited

moderate performance in discriminating fibrotic MASH, with an AUROC of 0.679. It outperformed FIB-4 (0.679 vs. 0.519), APRI (0.679 vs. 0.578), and LSM-VCTE alone (0.679 vs. 0.591). However, it is important to note that LSM-VCTE was primarily designed for assessing fibrosis and steatosis, and the presence of inflammation can significantly influence its results.

Given that Agile 3+, Agile 4, and FAST scores are designed to identify populations with varied fibrotic and inflammatory statuses, they hold significant promise for inclusion in screening algorithms for fibrosis and fibrotic NASH (MASH). These scores can enhance the precision of non-invasive assessments and improve the management of patients by better stratifying those at risk for advanced liver conditions (121). We believe that Agile 3+, Agile 4, and FAST scores could play a pivotal role within a clinical pathway, potentially serving as a "secondary step" in evaluations conducted in specialized medical centers. It is important to recognize that these scores incorporate laboratory tests such as platelets, AST, and ALT, which are also commonly included in initial screening tools like FIB-4 or NAFLD fibrosis score. Therefore, the performance of a multistep algorithm, which integrates Agile 3+, Agile 4, or FAST scores, should be carefully evaluated and validated in future studies to determine its effectiveness and utility in clinical practice.

The limitations of our study stem primarily from its retrospective design and cross-sectional nature, which precluded an exploration of the association between the scores and clinical outcomes. Despite these limitations, the study's strengths are notable. We enrolled a relatively large cohort of patients, and this represents the first report on the use of Agile scores from Eastern Europe, specifically involving a predominantly Caucasian population. Additionally, all liver biopsy samples were assessed by a single expert pathologist, minimizing variability in pathological staging. Among the 256 patients with reliable VCTE measurements, 252 (98.4%) met the criteria for MASLD, highlighting the relevance of our findings in the context of the recent redefinition of the disease. However, the study faced some limitations due to the extended analysis period (2007-2023) and the use of two different FibroScan devices (FibroScan X1115305 and FibroScan® Expert 630 starting in 2016). Despite these challenges, the study maintained rigorous adherence to its protocol throughout.

3.6. Conclusions

In conclusion, this study successfully validated the utility of three non-invasive scoring systems—Agile 3+, Agile 4, and FAST score—in a cohort of patients with biopsy-confirmed NAFLD who met the criteria for MASLD and were of Caucasian origin. The Agile 3+ and Agile 4 scores proved effective in distinguishing between advanced fibrosis and cirrhosis, and they notably reduced the number of indeterminate results compared to the FIB-4 score. Although the AUROCs for these scores did not significantly surpass those of LSM-VCTE alone, the Agile scores enhanced overall accuracy and minimized indeterminate cases. The Agile 4 score, in particular, demonstrated excellent accuracy in differentiating cirrhosis, making it a promising tool for non-invasive assessment of CSPH in patients with obese NASH (MASH). The FAST score showed moderate performance in identifying fibrotic NASH (MASH). These findings indicate that Agile 3+, Agile 4, and FAST scores offer valuable contributions to the evaluation and management of MASLD and should be further explored in clinical practice.

Preliminary results were presented at the EASL Congress 2024, Milan, Italy - Taru MG, Tefas C, Neamti L, Minciuna I, Taru V, Maniu A et all. FAST and Agile – the MASLD Drift: validation of Agile 3+, Agile 4 and FAST scores in 246 biopsy-proven MASLD patients of prevalent caucasian origin. EASL Congress 2024. Milan, Italy. 5-8 June 2024.

The results of this study have been published in the article: Taru MG, Tefas C, Neamti L, Minciuna I, Taru V, Maniu A, Rusu I, Petrushev B, Procopciuc LM, Leucuta DC, Procopet B, Ferri S, Lupsor-Platon M, Stefanescu H. FAST and Agile—the MASLD Drift: Validation of Agile 3+, Agile 4, and FAST Scores in 246 Biopsy-Proven NAFLD Patients Meeting MASLD Criteria of Predominant Caucasian Origin. PLoS One. 2024 May 23;19(5): e0303971. DOI:10.1371/journal.pone.0303971 (ISI IF 2.9, Q1; WOS:001231237700084).

4. Diagnostic accuracy of two-dimensional shear wave elastography (2D-SWE) ultrasound for liver fibrosis assessment in metabolic dysfunction-associated steatotic liver disease (MASLD): A multi-level random effects model meta-analysis

4.1. Introduction

Non-alcoholic fatty liver disease (NAFLD), which has recently been reclassified as metabolic dysfunction-associated steatotic liver disease (MASLD) (1), presents a significant challenge to the healthcare system. Its prevalence is rising rapidly, imposing a considerable global burden. Identifying affected individuals through targeted screening is crucial given the large population at risk (2, 3). According to recently published data, the two definitions meet a high level of agreement, up to 99.3% (122). Liver fibrosis is associated with long-term outcomes in patients with MASLD (4), and fibrosis progression to advanced stages, namely advanced fibrosis (≥F3) and cirrhosis (F4), leads to an increased risk of liver-related mortality, all-cause mortality, and higher incidence of major cardiovascular events (15, 16, 123). This necessitates effective identification of liver fibrosis stages, particularly advanced ones (≥F3-4), as well as timely monitoring and appropriate interventions (124, 125). Those at risk may experience greater benefits from intensive lifestyle interventions, enrolment into clinical trials (8), or treatment (126).

Liver biopsy (LB) is still the gold standard for liver fibrosis assessment, but it is hampered by its invasive nature, sampling errors, and inter and intra-observer variability (11, 106). To address the limitations of liver biopsy, several non-invasive tests (NITs) based on blood samples or elastography have been developed. Vibration-controlled transient elastography (VCTE), known as FibroScan (Echosens, Paris), is the most validated elastography method for non-invasive liver fibrosis assessment (18, 94). However, its use is constrained by high costs, limited availability in resource-poor settings, and technical issues, such as difficulties in patients with ascites or higher failure rates in obese individuals (125), thus raising the need for other non-invasive diagnostic alternatives (127).

Two-dimensional shear-wave elastography (2D-SWE) is a promising and non-invasive method for measuring liver stiffness (LS) (128). Today, most modern ultrasound machines come with elastography modules. When validated with reliable cut-off values, 2D-Shear Wave Elastography (2D-SWE) could be highly beneficial for

measuring liver stiffness in patients with MASLD, both in primary care and specialized settings. One of the key advantages of 2D-SWE is its ability to integrate liver stiffness measurement with ultrasound-based liver structural assessment, offering a comprehensive multiparametric evaluation. Additionally, some advanced equipment can also assess liver steatosis and inflammation in a single session (129). While VCTE has been extensively validated for biopsy-confirmed MASLD, further research is required to evaluate the diagnostic performance of 2D-SWE in this patient population (18). Despite the existence of guidelines describing its application, establishing standardised and more widely applicable cut-off values remains essential for robust validation and clinical implementation (19, 130). Moreover, 2D-SWE elastography techniques of different manufacturers do obviously attain different hardware and software, leading to a risk for widely adopted cut-off values (131), although the diversity in LSM across different systems has diminished due to the ongoing endeavours of the Quantitative Imaging Biomarkers Alliance (QIBA) (47).

In clinical practice, it is essential to establish efficient and cost-effective referral pathways between primary and secondary care. This is particularly important for identifying patients with MASLD who have significant fibrosis (F2 or higher), advanced fibrosis (F3 or higher), or cirrhosis (F4) (132). Although pathways based on VCTE have been identified (121), referral pathways incorporating 2D-SWE could be promising for diagnosing, risk stratification, and managing chronic liver diseases, particularly MASLD. In fact, almost all patients at risk for MASLD undergo a US scan nowadays, but only a few receive LSM with VCTE. The rapidly expanding US equipment industry, incorporating 2D-SWE assessment, allows one to speculate that most MASLD patients in the future will receive an LSM using 2D-SWE, although not with VCTE. To facilitate the global application and utility of 2D-SWE, reliable thresholds for fibrosis assessment are urgently warranted and must be widely applied.

4.2. Working hypothesis/objectives

We aimed to conduct a systematic review and meta-analysis using a multi-level random effects model to evaluate the diagnostic accuracy of 2D-SWE in patients with biopsy-confirmed MASLD. Our goal was to identify reliable cut-off values for different stages of liver fibrosis that would be applicable in clinical practice.

4.3. Material and methods

Registration of review protocol. A systematic review and meta-analysis of the multi-level random effects model were conducted according to the Preferred Reporting Items for Systematic Reviews and Meta-Analyses (PRISMA) guidelines (133-135). The protocol was registered on OFS (https://doi.org/10.17605/OSF.IO/9WV8F).

Search strategy and selection criteria. We systematically searched PubMed/MEDLINE, Embase, Scopus, Web of Science, LILACS, and Cochrane Library

electronic databases for full-text articles published in any language from inception to the 1st of February 2023 and subsequently updated the search to the 26th of February 2024.

The search was performed using the following keywords: "two-dimensional shear wave elastography" OR "2D-SWE" OR "multiparametric ultrasound" OR "acoustic radiation force impulse" OR "elasticity imaging techniques" AND "non-alcoholic fatty liver disease" OR "NAFLD" OR "non-alcoholic steatohepatitis" OR "NASH" OR "fatty liver" OR "liver disease". The search was restricted to human studies. **Table I** presents the entire search syntax.

Table I. Electronic search strategy (up to February 26, 2024)

Source	Electronic Search Strategy	Results
PubMed/MEDLINE	("2D shear wave elastography" OR "two-dimensional shear-wave elastography" OR "2DSWE"[Title/Abstract] OR "2D-SWE"[Title/Abstract] OR "multiparametric ultrasound" OR "speed of sound" OR "acoustic radiation force impulse" OR "ARFI"[Title/Abstract] OR "Elasticity Imaging Techniques"[Mesh]) AND ("Non-alcoholic Fatty Liver Disease"[Mesh] OR "non-alcoholic fatty liver"[All Fields] OR "non alcoholic fatty liver"[All Fields] OR "nonalcoholic fatty liver"[All Fields] OR ("non-alcoholic"[All Fields] AND "fatty"[All Fields] AND "liver"[All Fields] AND "disease"[All Fields]) OR "non-alcoholic steatohepatitis"[All Fields] OR "non alcoholic steatohepatitis"[All Fields] OR "nonalcoholic steatohepatitis"[All Fields] OR "fatty liver"[MeSH Terms] OR steatohepatitis[All Fields] OR ("fatty"[All Fields] AND "liver"[All Fields]) OR NASH[Title/Abstract] OR NAFLD[Title/Abstract])	**1597** results
Embase	('2d shear wave elastography' OR 'two-dimensional shear-wave elastography' OR 2dswe OR '2d swe' OR 'multiparametric ultrasound'/exp OR 'multiparametric ultrasound' OR 'speed of sound'/exp OR 'speed of sound' OR 'acoustic radiation force impulse'/exp OR 'acoustic radiation force impulse' OR arfi OR 'elasticity imaging techniques'/exp OR 'elasticity imaging techniques') AND ('non-alcoholic fatty liver disease'/exp OR 'non-alcoholic fatty liver disease' OR 'non-alcoholic fatty liver'/exp OR 'non-alcoholic fatty liver' OR 'non alcoholic fatty liver'/exp OR 'non alcoholic fatty liver' OR 'nonalcoholic fatty liver'/exp OR 'nonalcoholic fatty liver' OR ('non-alcoholic' AND 'fatty' AND ('liver'/exp OR 'liver') AND ('disease'/exp OR 'disease')) OR 'non-alcoholic steatohepatitis'/exp OR 'non-alcoholic steatohepatitis' OR 'non alcoholic steatohepatitis'/exp OR 'non alcoholic steatohepatitis' OR 'nonalcoholic steatohepatitis'/exp OR 'nonalcoholic steatohepatitis' OR 'fatty liver'/exp OR 'fatty liver' OR 'steatohepatitis'/exp OR steatohepatitis OR ('fatty' AND ('liver'/exp OR 'liver')) OR nash OR nafld) AND ('article'/it OR 'article in press'/it) AND 'human'/de	**2193** results
SCOPUS	ALL (("2D shear wave elastography" OR "two-dimensional shear-wave elastography" OR "2DSWE" OR "2D-SWE" OR "multiparametric ultrasound" OR "speed of sound" OR "acoustic radiation force impulse" OR "ARFI" OR "Elasticity Imaging Techniques") AND ("Non-alcoholic Fatty Liver Disease" OR "non-alcoholic fatty liver" OR "non alcoholic fatty liver" OR "nonalcoholic fatty liver" OR ("non-alcoholic" AND "fatty" AND "liver" AND "disease") OR "non-alcoholic steatohepatitis" OR "non alcoholic steatohepatitis" OR "nonalcoholic steatohepatitis" OR "fatty liver" OR steatohepatitis OR ("fatty" AND "liver") OR nash OR nafld)) AND (LIMIT-TO (DOCTYPE , "ar"))	**3988** results
Web of Science	TS=(("2D shear wave elastography" OR "two-dimensional shear-wave elastography" OR "2DSWE" OR "2D-SWE" OR "multiparametric ultrasound" OR "speed of sound" OR "acoustic radiation force impulse" OR "ARFI" OR "Elasticity Imaging Techniques") AND ("Non-alcoholic Fatty Liver Disease" OR "non-alcoholic fatty liver" OR "non alcoholic fatty liver" OR "nonalcoholic fatty liver" OR ("non-alcoholic" AND "fatty" AND "liver" AND "disease") OR "non-alcoholic steatohepatitis" OR "non alcoholic steatohepatitis" OR "nonalcoholic steatohepatitis" OR "fatty liver" OR steatohepatitis OR ("fatty" AND "liver") OR NASH OR NAFLD))	**379** results
LILACS	tw:(("2D shear wave elastography" OR "two-dimensional shear-wave elastography" OR "2DSWE" OR "2D-SWE" OR "multiparametric ultrasound" OR "speed of sound" OR "acoustic radiation force impulse" OR "ARFI" OR "Elasticity Imaging Techniques") AND ("Non-alcoholic Fatty Liver Disease" OR "non-alcoholic fatty liver" OR "non alcoholic fatty liver" OR "nonalcoholic fatty liver" OR ("non-alcoholic" AND "fatty" AND "liver" AND "disease") OR "non-alcoholic steatohepatitis" OR "non alcoholic steatohepatitis" OR "nonalcoholic steatohepatitis" OR "fatty liver" OR steatohepatitis OR ("fatty" AND "liver") OR NASH OR NAFLD))	**161** results
COCHRANE Library	("2D shear wave elastography " OR " two-dimensional shear-wave elastography " OR "2DSWE" OR "2D-SWE" OR "multiparametric ultrasound" OR "speed of sound" OR "acoustic radiation force impulse" OR "ARFI" OR "Elasticity Imaging Techniques") AND ("NAFLD" OR "NASH" OR "non-alcoholic fatty liver disease" OR "steatohepatitis" OR "nonalcoholic fatty liver" OR "fatty liver")	**72** results

We imposed no restrictions based on gender, race, or ethnicity in our review. Additionally, our search strategy was not limited to publications in specific languages; only full-text articles were included. The initial selection was conducted by two authors based on titles and abstracts. They then independently carried out a thorough full-text evaluation of the potentially relevant studies. Any disagreements were resolved through discussion with a third author.

We included the studies if they met the following pre-specified criteria: i) population - biopsy-proven NAFLD/NASH (or MASLD/MASH); ii) target condition – liver fibrosis assessment via LB (as reference standard); iii) index test – LSM by 2D-SWE. We considered any ultrasound (US) machine equipped with 2D-SWE software. The exclusion criteria were as follows: i) conference abstracts, case reports or non-original works (reviews, comments, editorials and practical guidelines); ii) studies

with insufficient information on the diagnostic performance of 2D-SWE in different stages of liver fibrosis (≥F1, ≥F2, ≥F3, F4) by true positives (TP), true negatives (TN), false positives (FP), false negatives (FN) and which did not allow to extract sensitivity (Se), specificity (Sp) or obtain the area under the ROC curve (AUC); iii) studies conducted in the pediatric population (age <18 years).

Data extraction and quality assessment. Data from the studies considered eligible to be included in the meta-analysis were independently extracted by three authors.

The following items were extracted from each study: first author, year of publication, country, type of ultrasound manufacturer, type of ultrasound machine, number of participants, age, body mass index (BMI), percentage of women, presence of diabetes, number of patients diagnosed via LB with different stages of liver fibrosis - F0 (absence of fibrosis), F≥1 (mild fibrosis), F≥2 (significant fibrosis), F≥3 (advanced fibrosis), F4 (cirrhosis), 2D-SWE unit of measurement (kPa – kilopascals, or m/sec – meters per second), for each stage of liver fibrosis the reported cut-off values, sensitivity (Se), specificity (Sp), area under the ROC curve (AUC) with 95% confidence interval (CI). We additionally reported the percentage of steatosis reported on LB, information about the histology readers and ultrasound examiners, and the number of 2D-SWE reliable and unreliable measurements when available.

In the case of multiple publications, we included the one that reported the most comprehensive information for this meta-analysis. If needed, we contacted any corresponding authors of the eligible studies to obtain additional information.

We assessed potential biases in the patient selection process, blinding to histological diagnosis or the index test, description of the reference standard, and inclusion of all patients in the analysis. Two authors independently evaluated the methodological quality of the included studies using the QUADAS-2 (Quality Assessment of Diagnostic Accuracy Studies) tool (136). Any disagreements were resolved through discussion with a third author.

Data synthesis and analysis. The primary outcome of the meta-analysis was to assess the diagnostic accuracy of 2D-SWE in detecting various stages of liver fibrosis in patients with biopsy-confirmed MASLD, using liver biopsy as the gold standard. We also conducted subgroup analyses based on ultrasound manufacturer, population characteristics, and the presence of comorbidities, such as type 2 diabetes mellitus (T2DM) and obesity.

Statistical analysis. A meta-analysis was conducted for index tests and target conditions with more than three studies that provided sufficient information to create classification tables. For index tests with inadequate studies for meta-analysis, a narrative synthesis was used. When authors provided a single cut-off for a specific liver fibrosis stage or described it as "optimal," "best," or based on the "Youden index," it was labeled as the "best cut-off." A cut-off defined for sensitivity (Se) ≥90% was

considered a "rule-out" threshold, while a cut-off for specificity (Sp) ≥90% was regarded as a "rule-in" threshold. We used a bivariate logit-normal random effects model to estimate the mean sensitivity, specificity, respective variances, and covariance. Summary receiver operator characteristic curves (sAUC) were generated with 95% confidence and 95% prediction regions. The 95% confidence region is based on the confidence interval around the summary point and indicates that, based on the available data, we expect the 'real value' to be within that region 95% of the time. A linear mixed-effects model was used to model the multiple threshold data of individual studies that also reported two or more two cut-offs (18, 137, 138). The multiple thresholds model is a multi-level random effects model that enables the calculation of summary sensitivities and specificities of different cut-offs and the calculation of the PPV and NPV, given the prevalence of the target condition. Sensitivity and specificity were combined at every recommended cut-off to produce a multiple threshold sAUC. In addition, PPV and NPV were also obtained for studies prevalence's and at pre-defined 30% and 60%, and cut-offs required to achieve minimum acceptable criteria were determined. To address the anticipated high heterogeneity across the eligible studies, we conducted sensitivity analyses based on study setting (Asian vs. non-Asian cohorts) and the presence of obesity (defined as BMI ≥30 kg/m^2 or ≥25 kg/m^2 in the Asian cohort) (139-141), presence of T2DM, and type of ultrasound manufacturer. We decided against using funnel plots because they are generally considered unreliable for distinguishing between publication bias and other sources of asymmetry, such as the use of multiple thresholds, in systematic reviews of diagnostic test accuracy studies (142).

All the analyses were performed using the statistical software R with the *mada* and *diagmeta* packages (Version 4.3.2; R Foundation for Statistical Computing, Vienna, Austria) was used in all analyses.

4.4. Results

An electronic search yielded 8,390 records. After removing 2,353 duplicates, we reviewed the titles and abstracts of the remaining 6,037 publications. We then assessed 116 full-text articles for eligibility. Of these, 96 were excluded for various reasons, leaving 20 studies that met the inclusion criteria for the meta-analysis. The PRISMA Flow Diagram (**Figure 1**) visually represents the selection process.

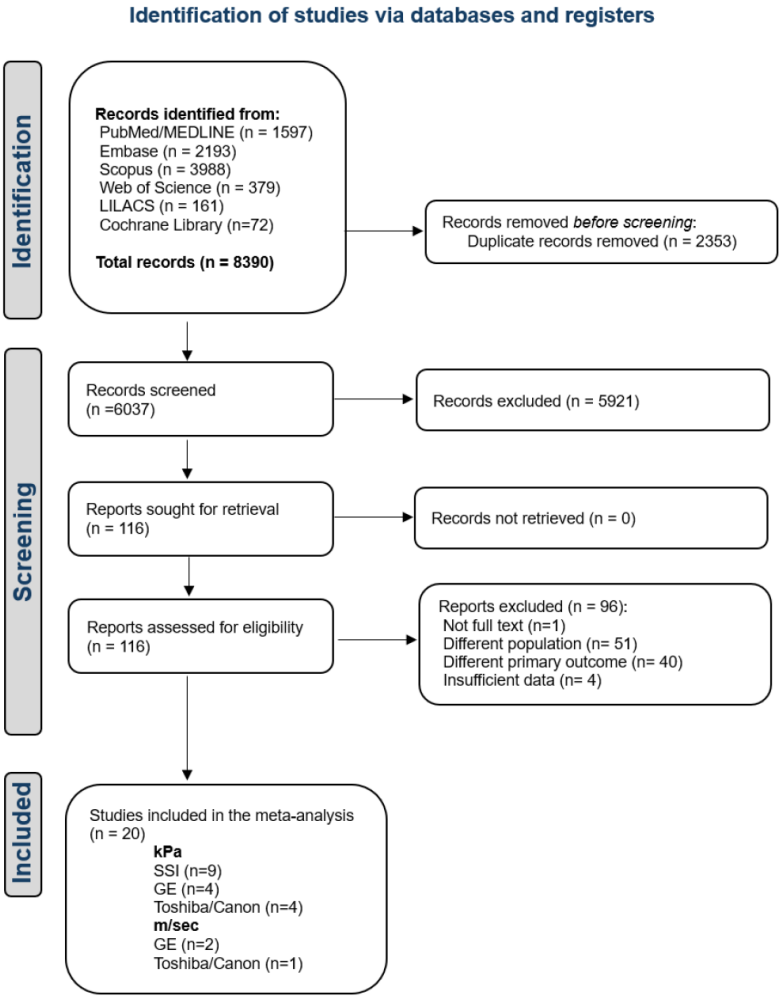

Figure 1. PRISMA Flow Diagram

Study characteristics.

The main characteristics of the included studies in the meta-analysis are presented in **Table II**.

Table II. Main characteristics of the included studies (n=20)

Measurement in kPa									
Author, Year (Ref)	**Country**	**Population** (n)	**M** (n)	**Study design, setting**	**Condition**	**Age** (years) mean ± SD	**Gender, F** n(%)	**BMI** (kg/m²) mean ± SD	**T2DM** n(%)
Supersonic Imagine (SSI)									
Cassinotto C, 2016	France	291	5	prospective multicentric cross-sectional	b-p MASLD	56.7 ± 12	119 (40.9)	32.1 ± 6	153 (52.6)
Lee MS, 2017	Korea	94	10	prospective single-centre	b-p MASLD	55.5 ± 3.87	53 (56.4)	27.13 ± 1.12	37 (39.4)
Takeuchi H, 2018	Japan	71	5	prospective single-centre	b-p MASLD	50.8 ± 15.7	25 (35.2)	29.2 ± 5.1	-
Jamialahmadi T, 2019	Iran	90	10	observational single-centre bariatric surgery	b-p MASLD	38.5 ± 11.1	72 (80)	45.46 ± 6.26	25 (27.8)
Ozturk A, 2020	USA	116	10	retrospective single-centre	b-p MASLD	50.6 ± 11.8	62 (53.4)	31.4 ± 5.1	38 (32.8)
Sharpton SR, 2021	USA	114	3 to 5	prospective cross-sectional single-centre	b-p MASLD	54.7 ± 14.27	62 (54.4)	31.5 ± 3.98	-
Chen G, 2022	China	100	-	retrospective single-centre bariatric surgery	b-p MASLD	31.55 ± 10.12	69 (69)	38 ± 14.56	37 (37)
Mendoza YP, 2022	Switzerland	88	3	prospective single-centre	b-p MASLD	53.2 ± 12.7	33 (57.5)	31.6 ± 7.1	39 (44.3)
Zhou, 2022	China	116	5	retrospective single centre	b-p MASLD	46.4 ± 16.45	61 (52.6)	-	23 (19.8)
General Electric Healthcare (GE)									
Furlan A, 2020	USA	62	3 to 12	prospective cross-sectional single-centre	b-p MASLD	50 ± 13	36 (58)	34.8 ± 7.2	22 (35)
Kuroda H, 2021	Japan	202	10	prospective cross-sectional single-centre	b-p MASLD	55.2 ± 12.9	103 (51)	29.27 ± 5.67	82 (40.6)
Imajo K, 2022	Japan	201	10	prospective single-centre	b-p MASLD	61 ± 14.93	95 (47.3)	27.17 ± 4.18	127 (61.9)
Kalaiyarasi K, 2024	Singapore	16	5	pilot, cross-sectional single-centre	b-p MASLD	49.2 ±11.9	11 (68.8)	29.6 ± 3.7	11 (68.8)
Canon Medical Systems/ Toshiba									
Lee DH, 2021	Korea	102	9	prospective single-centre	b-p MASLD	47 ± 24.82	59 (57.8)	25.6 ± 5.49	17 (16.7)
Jang JK, 2022	Korea	132	5	prospective cross-sectional multicentric	b-p MASLD	39.67 ± 20.24	69 (52.3)	24.9 ± 3.75	30 (22.7)
Laroia ST, 2021	India	50	10	prospective cross-sectional single-centre	b-p MASH	46.76 ± 10.7	19 (38)	-	-
Kim JW, 2022	Korea	60	10	retrospective single-centre	b-p MASLD b-p MASH	50.9 ± 13.4	32 (53.3)	29.9 ± 4.3	37 (61.7)
Measurement in m/sec									
Author, Year (Ref)	**Country**	**Population** (n)	**M** (n)	**Study design, setting**	**Condition**	**Age** (years) mean ± SD	**Gender, F** n(%)	**BMI** (kg/m²) mean ± SD	**T2DM** n(%)
General Electric Healthcare (GE)									
Zhang YZN, 2022	USA	100	10	prospective cross-sectional single-centre	b-p MASLD	51.8 ± 12.9	54 (54)	31.6 ± 4.7	-
Ogino, 2023	Japan	107	6	retrospective single-centre	b-p MASLD	51 ± 14	42 (39.3)	29.0 ± 4.3	-
Canon Medical Systems/ Toshiba									
Sugimoto K, 2020	Japan	111	10	prospective cross-sectional single-centre	b-p MASLD	53 ± 18	54 (48.6)	27.7 ± 4.3	-

Abbreviations: "-"not available, b-p – biopsy-proven, F – women, M – measurements, MASLD - metabolic dysfunction-associated steatotic liver disease, MASH - metabolic dysfunction-associated steatohepatitis, SD - standard deviation, T2DM – type 2 diabetes mellitus

The 20 observational studies included a total of 2,223 participants with biopsy-confirmed MASLD. The prevalence rates for the different stages of fibrosis were as follows: mild fibrosis (F1) at 30.0% (n=666), significant fibrosis (F2) at 18.5% (n=411), advanced fibrosis (F3) at 17.8% (n=397), and cirrhosis (F4) at 10.9% (n=242). Additionally, 22.8% (n=507) of the patients were classified as having no fibrosis (F0).

The mean age (±SD) of the participants ranged from 31.5 (± 10.1) to 61 (± 14.9) years, and the percentage of females ranged from 35.2% to 80%. The mean BMI

ranged from 24.9 (± 3.75) kg/m^2 to 45.46 (± 6.26) kg/m^2, with a prevalence of obesity for both non-Asian and Asian populations. 14 (70%) studies were conducted in Asia (56, 143-155), 4 (20%) in America (156-159), and 2 (10%) in Europe (160, 161). Two (10%) studies were multicentric (56, 160), and 18 (90%) were single centres. Most studies (90%, n=18) included cohorts of patients with biopsy-proven MASLD from tertiary care liver centres, whereas 2 (10%) studies included patients from bariatric surgery centres with available liver biopsy data. The studies were conducted with 50% as a retrospective cohort and 50% as a cross-sectional design. **Table III** reports the summary diagnostic performance of 2D-SWE for detecting fibrosis stages in biopsy-proven MASLD by applying a bivariate logit-normal random effects model.

Table III. Summary diagnostic performance of 2D-SWE for the detection of different stages of liver fibrosis in biopsy-proven MASLD by bivariate logit-normal random effects model

Measurement in kPa							
Fibrosis stage	**Studies** n(%)	**Patients** (n)	**Prevalence (%)**	**Cut-off range**	**sAUC** [95%CI]	**Se** [95%CI]	**Sp** [95%CI]
All US device together							
Mild fibrosis, ≥F1; F0 vs. F1-F4	9 (45)	1489	78.2	5.85 - 8.9	0.84 [0.81-0.87]	0.76 [0.69 - 0.82]	0.80 [0.69 - 0.87]
Significant fibrosis, ≥F2; F0-F1 vs. F2-F4	16 (80)	936	49.1	5.7 - 11.9	0.84 [0.80-0.87]	0.78 [0.70 - 0.84]	0.76 [0.69 - 0.82]
Advanced fibrosis, ≥F3; F0-F2 vs. F3-F4	17 (85)	556	29.2	6.75 - 13.07	0.87 [0.84-0.90]	0.81 [0.73 - 0.86]	0.80 [0.74 - 0.84]
Cirrhosis, F4; F0-F3 vs. F4	12 (60)	208	10.9	6.75 - 15.73	0.93 [0.91-0.95]	0.90 [0.84 - 0.94]	0.82 [0.77 - 0.87]
SuperSonic Imagine							
Significant fibrosis, ≥F2; F0-F1 vs. F2-F4	9 (45)	533	49.4	6.6 - 11.57	0.81 [0.77-0.84]	0.72 [0.63 - 0.81]	0.77 [0.65 - 0.86]
Advanced fibrosis, ≥F3; F0-F2 vs. F3-F4	9 (45)	294	27.2	6.75 - 13.07	0.85 [0.82-0.88]	0.79 [0.71 - 0.86]	0.77 [0.69 - 0.83]
Cirrhosis, F4; F0-F3 vs. F4	7 (35)	105	9.7	6.75 - 15.73	0.93 [0.90-0.95]	0.91 [0.80 - 0.96]	0.81 [0.74 - 0.87]

Abbreviations: % percentage, CI confidence interval, F1 mild fibrosis, F2 significant fibrosis, F3 advanced fibrosis, F4 cirrhosis, kPa kilopascals, n number, sAUC summary area under the ROC curve, Se sensitivity, Sp specificity

Study quality assessment. The methodological quality of the eligible studies was assessed with the QUADAS-2 tool (136), as summarised in **Figure 2**. Nineteen of the 20 studies (95%) showed no risk of bias or concerns regarding applicability. However, three studies (15%) were considered to have a "high risk" of bias in the patient selection domain of the QUADAS-2 tool, as they did not specify whether consecutive or random sampling was used. All studies were assessed as having a "high risk" of bias in the index test domain, as no pre-specified threshold for 2D-SWE is currently in use (19). The flow and timing domain of the QUADAS-2 tool was judged as having an "unclear risk" of bias in 19 (95%) studies, as the "intention to diagnose" (ITD) approach was specified in one study.

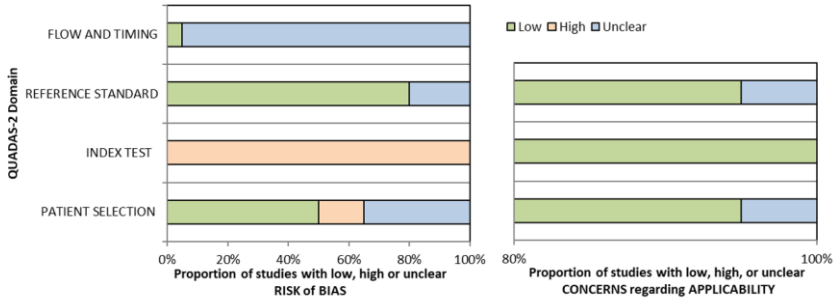

Figure 2. The proportion of studies with low, high, or unclear risk of bias and concerns regarding the applicability of the included studies (QUADAS-2)

Diagnostic performance of 2D-SWE by kPa for different stages of liver fibrosis by multiple threshold data meta-analysis

Mild fibrosis (≥F1; F0 vs. F1-F4)

The diagnostic accuracy in detecting mild fibrosis (≥F1) was investigated in 9 (45%) studies that reported the results in kPa. The sAUC [95% CI], Se [95% CI], and Sp [95% CI], when all ultrasound machines were considered together, were 0.82 [0.16-0.98], 0.76 [0.66-0.83], and 0.76 [0.60-0.86], respectively, with an optimal cut-off for depicting ≥F1 of 6.432 kPa (**Table IV, Figure 3**).

Table IV. Diagnostic performance of 2D-SWE in detecting different stages of liver fibrosis in biopsy-proven MASLD (all US devices together) by multi-level random effects model

Measurement in kPa						
All US devices together						
Fibrosis stage	**No of studies/No of cut-offs**	**Cut-off**	**Se** [95%CI]	**Sp** [95%CI]	**sAUC for Se given Sp** [95%CI]	**sAUC for Sp given Se** [95%CI]
Mild fibrosis, ≥F1; F0 vs. F1-F4	9/13	6.432	0.76 [0.66 - 0.83]	0.76 [0.60 - 0.86]	0.82 [0.16 - 0.98]	0.82 [0.14 - 0.98]
Significant fibrosis, ≥F2; F0-F1 vs. F2-F4	16/28	8.174	0.76 [0.65 - 0.84]	0.76 [0.65 - 0.84]	0.82 [0.76 - 0.88]	0.82 [0.76 - 0.87]
Advanced fibrosis, ≥F3; F0-F2 vs. F3-F4	17/29	9.418	0.79 [0.67 - 0.88]	0.79 [0.71 - 0.86]	0.86 [0.77 - 0.93]	0.86 [0.79 - 0.92]
Cirrhosis, F4; F0-F3 vs. F4	12/20	11.548	0.82 [0.66 - 0.91]	0.82 [0.75 - 0.87]	0.89 [0.80 - 0.95]	0.89 [0.83 - 0.93]
Measurement in m/sec						
All US devices together						
Fibrosis stage	**No of studies/No of cut-offs**	**Cut-off**	**Se** [95%CI]	**Sp** [95%CI]	**sAUC for Se given Sp** [95%CI]	**sAUC for Sp given Se** [95%CI]
Significant fibrosis, ≥F2; F0-F1 vs. F2-F4	3/6	1.481	0.76 [0.42 - 0.93]	0.76 [0.43 - 0.93]	0.82 [0.65 - 0.94]	0.82 [0.61 - 0.92]
Advanced fibrosis, ≥F3; F0-F2 vs. F3-F4	3/6	1.633	0.77 [0.63 - 0.87]	0.77 [0.70 - 0.83]	0.84 [0.51 - 0.95]	0.84 [0.57 - 0.94]
Cirrhosis, F4; F0-F3 vs. F4	3/6	1.748	0.82 [0.56 - 0.94]	0.82 [0.75 - 0.88]	0.89 [0.38 - 0.99]	0.89 [0.34 - 0.97]

Abbreviations: 95% CI, 95% confidence interval, F1 mild fibrosis, F2 significant fibrosis, F3 advanced fibrosis, F4 cirrhosis, kPa kilopascals, m/sec meters per second, No number, sAUC Summary Area Under ROC Curve, Se sensitivity, Sp specificity

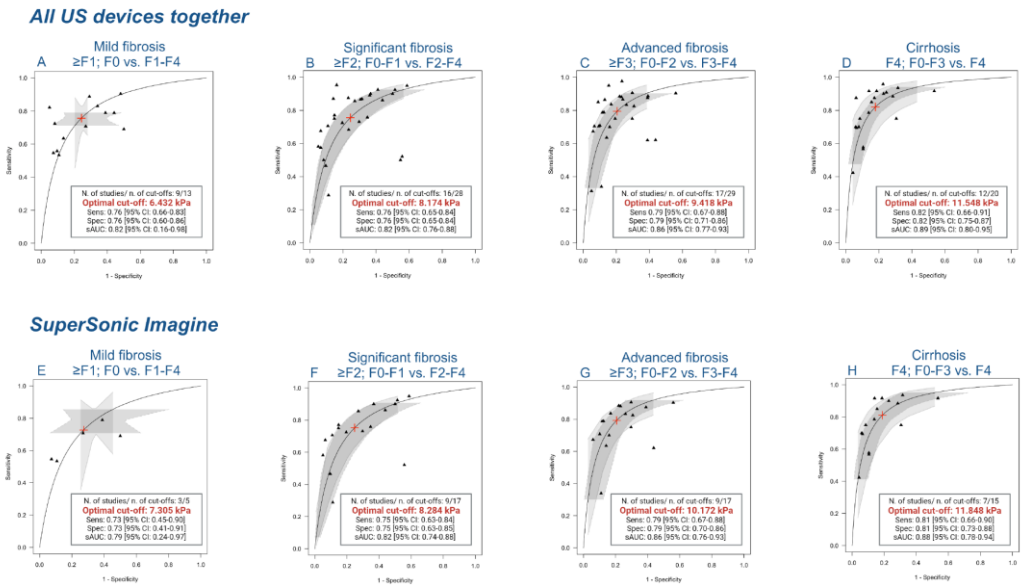

Figure 3. sAUC by multi-level random effects (CICS) model for multiple thresholds data for all US device together and SuperSonic Imagine (kPa)

Legend: 95% CI, 95% confidence interval, CICS Common random intercept and common slope, F1 mild fibrosis, F2 significant fibrosis, F3 advanced fibrosis, F4 fibrosis, kPa kilopascals, N number, sAUC Summary Area Under ROC Curve, Sens sensitivity, Spec specificity, US ultrasound

Significant fibrosis (≥F2; F0-F1 vs. F2-F4). The diagnostic accuracy in detecting significant fibrosis (≥F2) was investigated in 16 (80%) studies that reported the results in kPa. The sAUC [95% CI], Se [95% CI], and Sp [95% CI], when all ultrasound machines were considered together, were 0.82 [0.76-0.88], 0.76 [0.65-0.84] and 0.76 [0.65-0.84], respectively, with an optimal cut-off for depicting ≥F2 of 8.174 kPa (**Table IV, Figure 3**).

Advanced fibrosis (≥F3; F0-F2 vs F3-F4). The diagnostic accuracy in detecting advanced fibrosis (≥F3) was investigated in 17 (85%) studies that reported the results in kPa. The sAUC [95% CI], Se [95% CI], and Sp [95% CI], when all ultrasound machines were considered together, were 0.86 [0.77-0.93], 0.79 [0.67-0.88] and 0.79 [0.71-0.86], respectively, with an optimal cut-off for depicting ≥F3 of 9.418 kPa (**Table IV, Figure 3**).

Cirrhosis (F4; F0-F3 vs. F4). The diagnostic accuracy in detecting cirrhosis (F4) was investigated in 12 (60%) studies that reported the results in kPa. The sAUC [95% CI], Se [95% CI], and Sp [95% CI], when all ultrasound machines were considered together, were 0.89 [0.80-0.95], 0.82 [0.66-0.91] and 0.82 [0.75-0.87],

respectively, with an optimal cut-off for depicting F4 of 11.548 kPa (**Table IV, Figure 3**).

Diagnostic performance of 2D-SWE by m/sec for different stages of liver fibrosis by multiple threshold data meta-analyses

The diagnostic accuracy in detecting ≥F2, ≥F3, and F4 was investigated in 3 (15%), 3 (15%), and 3 (15%) studies that reported the results in m/sec, respectively. The sAUC [95% CI], Se [95% CI], and Sp [95% CI] were 0.82 [0.65-0.94], 0.76 [0.42-0.93], and 0.76 [0.43-0.93] for ≥F2; 0.84 [0.51-0.95], 0.77 [0.63-0.87], and 0.77 [0.70-0.83] for ≥F3; 0.89 [0.38-0.99], 0.82 [0.56-0.94], and 0.82 [0.75-0.88] for F4, respectively. The optimal cut-offs in detecting ≥F2, ≥F3, and F4 were 1.481, 1.633, and 1.748 m/sec, respectively (**Table IV, Figure 4**).

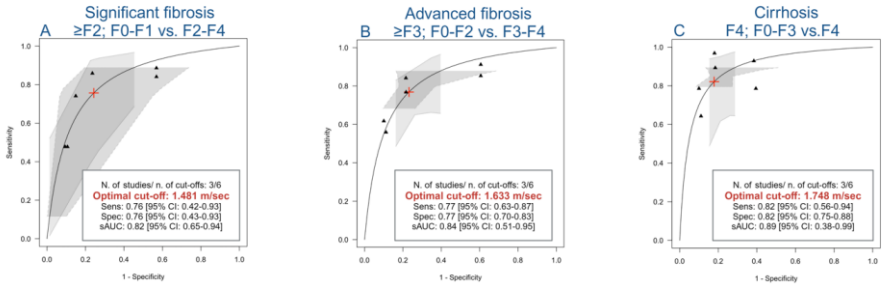

Figure 4. *sAUC by multi-level random effects (CICS) model for multiple thresholds data for all US devices together (m/sec)*

Figure 4 legend: 95% CI, 95% confidence interval, CICS Common random intercept and common slope, F2 significant fibrosis, F3 advanced fibrosis, F4 fibrosis, kPa kilopascals, N number, sAUC Summary Area Under ROC Curve, Sens sensitivity, Spec specificity

Sensitivity analysis of the diagnostic performance of 2D-SWE (kPa) for different stages of liver fibrosis

In **Table V** and **Figure 4** we explored heterogeneity across studies by performing sensitivity analyses.

Asian population. The diagnostic accuracy in detecting ≥F1, ≥F2, ≥F3, and F4 was investigated in 8 (40%), 11 (55%), 12 (60%), and 9 (45%) Asian studies that reported the results in kPa, respectively. The sAUC [95% CI], Se [95% CI], and Sp [95% CI] were 0.83 [0.73-0.90], 0.76 [0.62-0.86], and 0.76 [0.57-0.88] for ≥F1; 0.80 [0.69-0.88], 0.74 [0.60-0.84], and 0.74 [0.63-0.83] for ≥F2; 0.84 [0.43-0.96], 0.78 [0.60-0.89], and 0.78 [0.68-0.85] for ≥F3; 0.90 [0.78-0.97], and 0.83 [0.62-0.94], and 0.83 [0.75-0.89] for F4, respectively. The optimal cut-offs in detecting ≥F1, ≥F2, ≥F3, and F4 were 6.953, 8.561, 10.182, and 12.466 kPa, respectively (**Table V, Figure 5**).

Population with type 2 diabetes mellitus. The diagnostic accuracy in detecting ≥F2, ≥F3, and F4 for the population with type 2 diabetes mellitus was investigated in 9 (45%), 10 (50%), and 6 (30%) studies that reported the results in kPa, respectively. The sAUC [95% CI], Se [95% CI], and Sp [95% CI] were 0.84 [0.77-

0.90], 0.77 [0.64-0.87], and 0.77 [0.63-0.87] for ≥F2; 0.88 [0.81-0.93], 0.81 [0.68-0.90], and 0.81 [0.69-0.89] for ≥F3; 0.88 [0.81-0.93], 0.81 [0.67-0.90], and 0.81 [0.73-0.87] for F4, respectively. The optimal cut-offs in detecting ≥F2, ≥F3, and F4 were 7.961, 9.010, and 11.760 kPa, respectively (**Table V, Figure 5**).

Population with obesity. The diagnostic accuracy in detecting ≥F1, ≥F2, ≥F3, and F4 for the population with obesity was investigated in 7 (35%), 13 (65%), 14 (70%), and 9 (45%) studies that reported the results in kPa, respectively. The sAUC [95% CI], Se [95% CI], and Sp [95% CI], were 0.81 [0.72-0.87], 0.74 [0.61-0.84], and 0.74 [0.56-0.87] for ≥F1; 0.83 [0.77-0.89], 0.77 [0.65-0.85], and 0.77 [0.65-0.85] for ≥F2; 0.87 [0.80-0.92], 0.80 [0.68-0.88], and 0.80 [0.71-0.87] for ≥F3; 0.88 [0.79-0.94], 0.81 [0.66-0.91], and 0.81 [0.74-0.87] for F4, respectively. The optimal cut-offs in detecting ≥F1, ≥F2, ≥F3, and F4 were 6.792, 7.945, 9.040, and 11.614 kPa, respectively (**Table V, Figure 5**).

Table V. Sensitivity analysis of the diagnostic performance of 2D-SWE (kPa) for different stages of liver fibrosis by multi-level random effects model

Measurement in kPa						
Fibrosis stage	**No of studies/No of cut-offs**	**Cut-off**	**Se** [95%CI]	**Sp** [95%CI]	**sAUC for Se given Sp** [95%CI]	**sAUC for Sp given Se** [95%CI]
Asian population						
Mild fibrosis, ≥F1; F0 vs. F1-F4	8/10	6.953	0.76 [0.62 - 0.86]	0.76 [0.57 - 0.88]	0.83 [0.73 - 0.90]	0.83 [0.70 - 0.91]
Significant fibrosis, ≥F2; F0-F1 vs. F2-F4	11/16	8.561	0.74 [0.60 - 0.84]	0.74 [0.63 - 0.83]	0.80 [0.69 - 0.88]	0.80 [0.71 - 0.88]
Advanced fibrosis, ≥F3; F0-F2 vs. F3-F4	12/17	10.182	0.78 [0.60 - 0.89]	0.78 [0.68 - 0.85]	0.84 [0.43 - 0.96]	0.84 [0.47 - 0.96]
Cirrhosis, F4; F0-F3 vs. F4	9/12	12.466	0.83 [0.62 - 0.94]	0.83 [0.75 - 0.89]	0.90 [0.78 - 0.97]	0.90 [0.81 - 0.95]
Population with T2DM						
Significant fibrosis, ≥F2; F0-F1 vs. F2-F4	9/15	7.961	0.77 [0.64 - 0.87]	0.77 [0.63 - 0.87]	0.84 [0.77 - 0.90]	0.84 [0.76 - 0.90]
Advanced fibrosis, ≥F3; F0-F2 vs. F3-F4	10/16	9.010	0.81 [0.68 - 0.90]	0.81 [0.69 - 0.89]	0.88 [0.81 - 0.93]	0.88 [0.81 - 0.92]
Cirrhosis, F4; F0-F3 vs. F4	6/10	11.760	0.81 [0.67 - 0.90]	0.81 [0.73 - 0.87]	0.88 [0.81 - 0.93]	0.88 [0.83 - 0.91]
Population with obesity						
Mild fibrosis, ≥F1; F0 vs. F1-F4	7/11	6.792	0.74 [0.61 - 0.84]	0.74 [0.56 - 0.87]	0.81 [0.72 - 0.87]	0.81 [0.69 - 0.89]
Significant fibrosis, ≥F2; F0-F1 vs. F2-F4	13/23	7.945	0.77 [0.65 - 0.85]	0.77 [0.65 - 0.85]	0.83 [0.77 - 0.89]	0.83 [0.76 - 0.88]
Advanced fibrosis, ≥F3; F0-F2 vs. F3-F4	14/24	9.040	0.80 [0.68 - 0.88]	0.80 [0.71 - 0.87]	0.87 [0.80 - 0.92]	0.87 [0.81 - 0.91]
Cirrhosis, F4; F0-F3 vs. F4	9/15	11.614	0.81 [0.66 - 0.91]	0.81 [0.74 - 0.87]	0.88 [0.79 - 0.94]	0.88 [0.82 - 0.93]
Type of ultrasound manufacturer						
SuperSonic Imagine						
Mild fibrosis, ≥F1; F0 vs. F1-F4	3/5	7.305	0.73 [0.45 - 0.90]	0.73 [0.41 - 0.91]	0.79 [0.24 - 0.97]	0.79 [0.12 - 0.97]
Significant fibrosis, ≥F2; F0-F1 vs. F2-F4	9/17	8.284	0.75 [0.63 - 0.84]	0.75 [0.63 - 0.85]	0.82 [0.74 - 0.88]	0.82 [0.73 - 0.88]
Advanced fibrosis, ≥F3; F0-F2 vs. F3-F4	9/17	10.172	0.79 [0.67 - 0.88]	0.79 [0.70 - 0.86]	0.86 [0.76 - 0.93]	0.86 [0.76 - 0.92]
Cirrhosis, F4; F0-F3 vs. F4	7/15	11.848	0.81 [0.66 - 0.90]	0.81 [0.73 - 0.88]	0.88 [0.78 - 0.94]	0.88 [0.81 - 0.93]
Canon Medical Systems/Toshiba						
Significant fibrosis, ≥F2; F0-F1 vs. F2-F4	4/6	7.226	0.75 [0.45 - 0.91]	0.76 [0.61 - 0.86]	0.82 [0.26 - 0.96]	0.82 [0.38 - 0.96]
Advanced fibrosis, ≥F3; F0-F2 vs. F3-F4	4/6	7.831	0.80 [0.51 - 0.94]	0.80 [0.69 - 0.87]	0.86 [0.21 - 0.98]	0.86 [0.33 - 0.97]
General Electric Healthcare						
Significant fibrosis, ≥F2; F0-F1 vs. F2-F4	3/5	7.204	0.81 [0.56 - 0.94]	0.81 [0.56 - 0.94]	0.88 [0.74 - 0.95]	0.88 [0.76 - 0.95]
Advanced fibrosis, ≥F3; F0-F2 vs. F3-F4	4/6	8.060	0.84 [0.60 - 0.95]	0.84 [0.62 - 0.94]	0.90 [0.77 - 0.96]	0.90 [0.81 - 0.97]

Abbreviations: 95% CI, 95% confidence interval, F1 mild fibrosis, F2 significant fibrosis, F3 advanced fibrosis, F4 cirrhosis, kPa kilopascals, m/sec meters per second, No number, sAUC Summary Area Under ROC Curve, Se sensitivity, Sp specificity, T2DM type 2 diabetes mellitus

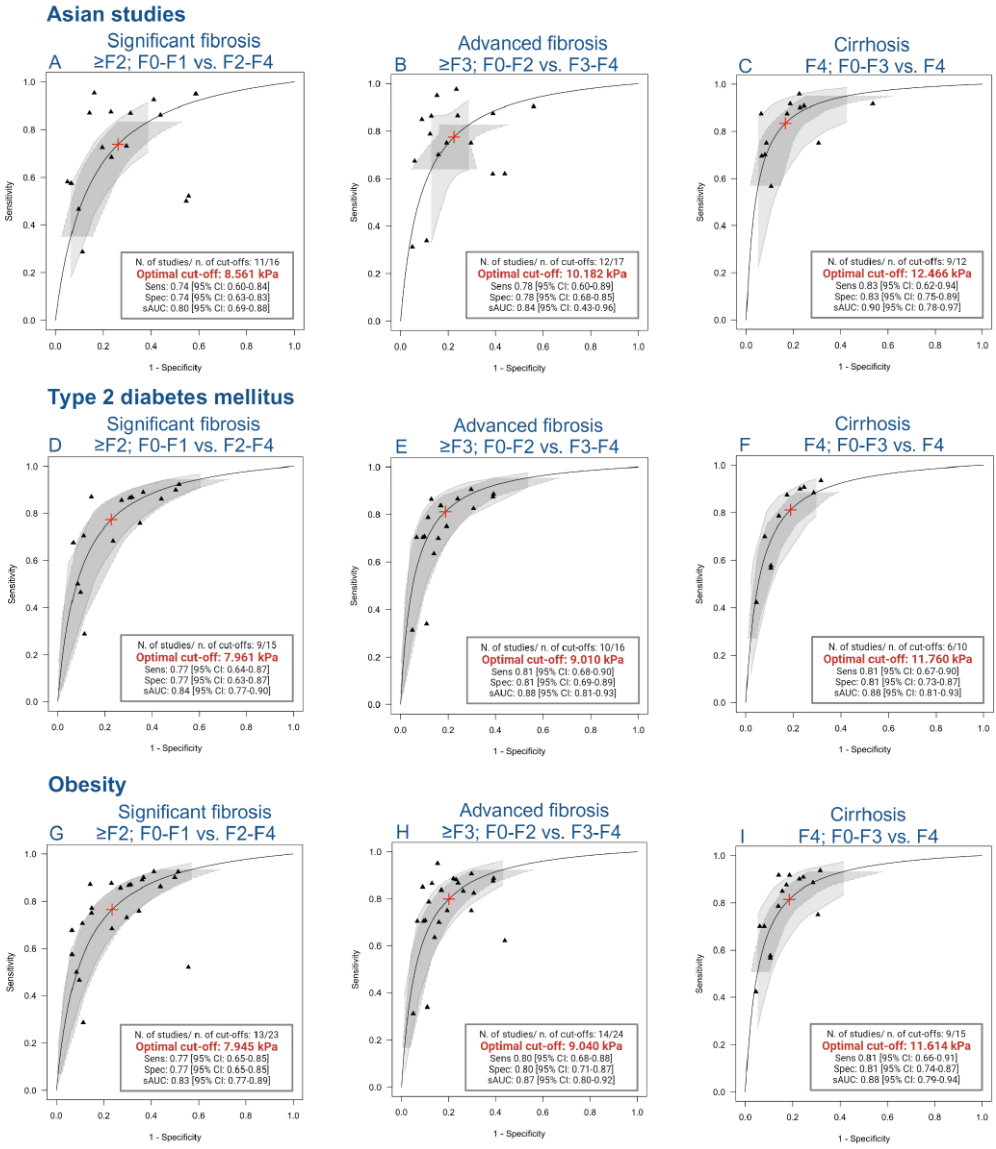

Figure 5. sAUC by multi-level random effects (CICS) model for multiple thresholds data for sensitivity analysis for different subpopulations (kPa)

Figure 5 legend: 95% CI, 95% confidence interval, CICS Common random intercept and common slope, F2 significant fibrosis, F3 advanced fibrosis, F4 cirrhosis, kPa kilopascals, N number, sAUC Summary Area Under ROC Curve, Sens sensitivity, Spec specificity, T2DM type 2 diabetes mellitus.

Type of ultrasound manufacturer

SuperSonic Imagine. The diagnostic accuracy in detecting ≥F1, ≥F2, ≥F3, and F4 by SuperSonic Imagine was investigated in 3 (15%), 9 (45%), 9 (45%) and 7 (35%) studies that reported the results in kPa, respectively. The sAUC [95% CI], Se [95% CI], and Sp [95% CI], were 0.79 [0.24-0.97], 0.73 [0.45-0.90], and 0.73 [0.41-0.91] for ≥F1; 0.82 [0.74-0.88], 0.75 [0.63-0.84], and 0.75 [0.63-0.85] for ≥F2; 0.86 [0.76-0.93], 0.79 [0.67-0.88], and 0.79 [0.70-0.86] for ≥F3; 0.88 [0.78-0.94], 0.81 [0.66-0.90], and 0.81 [0.73-0.88] for F4, respectively. The optimal cut-offs in detecting ≥F1, ≥F2, ≥F3, and F4 were 7.305, 8.284, 10.172, and 11.848 kPa, respectively (**Table V, Figure 6**).

Canon Medical Systems/Toshiba. The diagnostic accuracy in detecting ≥F2 and ≥F3 by Canon Medical Systems/Toshiba was investigated in 4 (20%) studies. The sAUC [95% CI], Se [95% CI], and Sp [95% CI] were 0.82 [0.26-0.96], 0.75 [0.45-0.91], 0.76 [0.61-0.86] for ≥F2; 0.86 [0.21-0.98], 0.80 [0.51-0.94], and 0.80 [0.69-0.87] for ≥F3, respectively. The optimal cut-offs in detecting ≥F2 and ≥F3 were 7.226 and 7.831 kPa, respectively (**Table V, Figure 6**).

General Electric Healthcare. The diagnostic accuracy in detecting ≥F2 and ≥F3 by General Electric Healthcare was investigated in 3 (15%) and 4 (20%) studies, respectively. The sAUC [95% CI], Se [95% CI], and Sp [95% CI] were 0.88 [0.74-0.95], 0.81 [0.56-0.94], and 0.81 [0.56-0.94] for ≥F2; 0.90 [0.77 - 0.96], 0.84 [0.60 - 0.95], and 0.84 [0.62 - 0.94] for ≥F3, respectively. The optimal cut-offs in detecting ≥F2 and ≥F3 were 7.204 and 8.060 kPa, respectively (**Table V, Figure 6**).

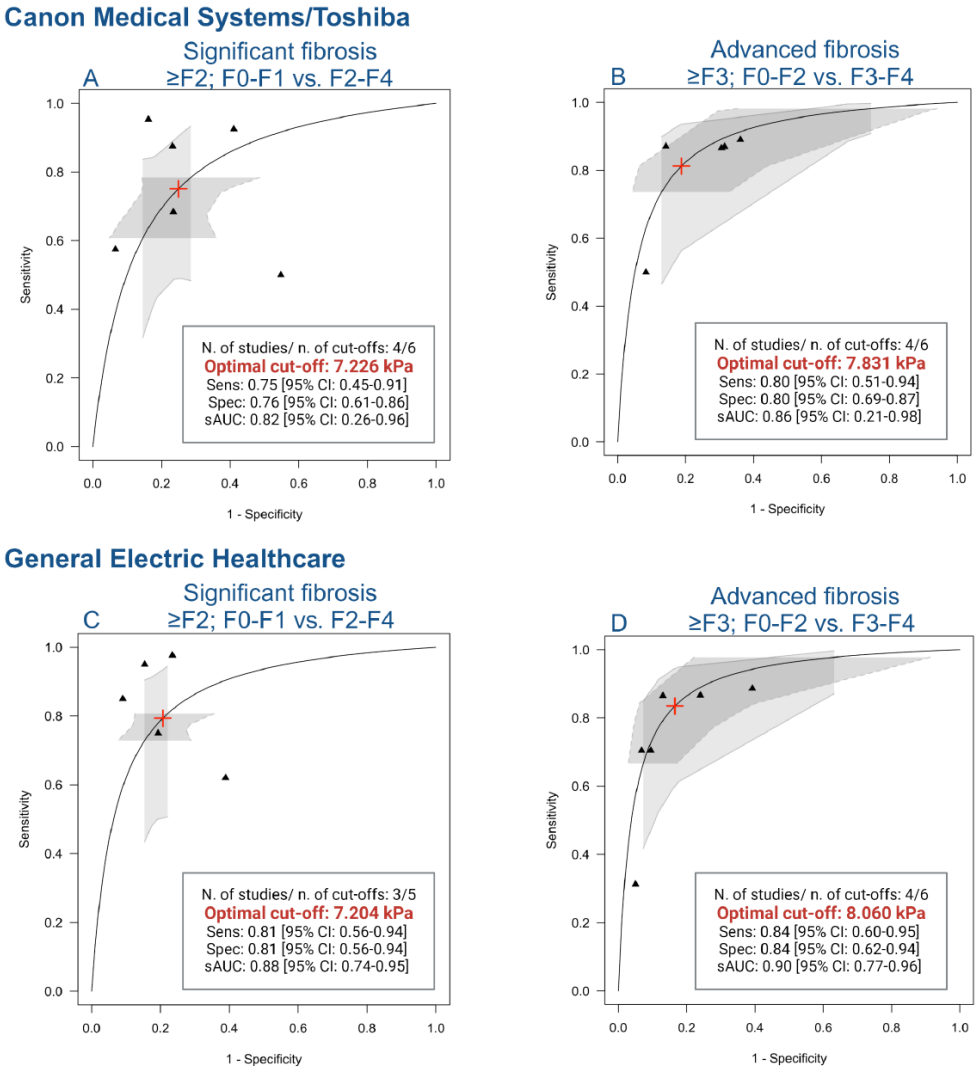

Figure 6. sAUC by multi-level random effects (CICS) model for multiple thresholds data for sensitivity analysis for Canon Medical Systems/Toshiba and General Electric Healthcare (kPa)

Figure 6 legend: 95% CI, 95% confidence interval, CICS Common random intercept and common slope, F2 significant fibrosis, F3 advanced fibrosis, kPa kilopascals, N number, sAUC Summary Area Under ROC Curve, Sens sensitivity, Spec specificity

Sensitivity analysis of the diagnostic performance of 2D-SWE (kPa) in different clinical scenarios.

We evaluated the accuracy of 2D-SWE cut-offs in two different disease prevalences representing different clinical scenarios. These scenarios include primary care settings (30% prevalence) and third-level hospitals (60% prevalence). We also calculated the negative and positive predictive values for different stages of liver

fibrosis (pre-test probability) in different subpopulations. The results of our analysis are found in **Table VI, Table VII, Table VIII, Table IX**.

Table VI. Negative and positive predictive values for 2D-SWE according to the prevalence of different stages of liver fibrosis (pre-test probability) by multi-level random effects model

Measurement in kPa						
Pre-test probability			Prevalence 30%		Prevalence 60%	
Scenario	**Cut-off**		**NPV**	**PPV**	**NPV**	**PPV**
All US device together						
Mild fibrosis, ≥F1; F0 vs. F1-F4						
	Best cut-off	6.432	0.879	0.572	0.824	0.675
	Rule-out cut-off	1.412	0.924	0.445	0.776	0.737
	Rule-in cut-off	29.306	0.813	0.690	0.555	0.886
Significant fibrosis, ≥F2; F0-F1 vs. F2-F4						
	Best cut-off	8.174	0.878	0.570	0.673	0.823
	Rule-out cut-off	6.030	0.923	0.443	0.775	0.736
	Rule-in cut-off	11.079	0.688	0.812	0.553	0.885
Advanced fibrosis, ≥F3; F0-F2 vs. F3-F4						
	Best cut-off	9.418	0.900	0.624	0.721	0.853
	Rule-out cut-off	6.505	0.936	0.507	0.806	0.782
	Rule-in cut-off	13.634	0.848	0.728	0.615	0.904
Cirrhosis, F4; F0-F3 vs. F4						
	Best cut-off	11.548	0.915	0.663	0.753	0.873
	Rule-out cut-off	8.632	0.942	0.562	0.824	0.818
	Rule-in cut-off	15.450	0.875	0.750	0.667	0.913
SuperSonic Imagine						
Mild fibrosis, ≥F1; F0 vs. F1-F4						
	Best cut-off	7.305	0.862	0.533	0.640	0.800
	Rule-out cut-off	5.209	0.912	0.408	0.746	0.707
	Rule-in cut-off	10.244	0.790	0.654	0.518	0.869
Significant fibrosis, ≥F2; F0-F1 vs. F2-F4						
	Best cut-off	8.284	0.876	0.565	0.669	0.820
	Rule-out cut-off	6.337	0.922	0.438	0.771	0.732
	Rule-in cut-off	10.829	0.809	0.684	0.548	0.884
Advanced fibrosis, ≥F3; F0-F2 vs. F3-F4						
	Best cut-off	10.172	0.899	0.622	0.719	0.852
	Rule-out cut-off	7.370	0.935	0.504	0.805	0.780
	Rule-in cut-off	14.040	0.847	0.727	0.612	0.903
Cirrhosis, F4; F0-F3 vs. F4						
	Best cut-off	11.848	0.909	0.648	0.741	0.866
	Rule-out cut-off	9.005	0.940	0.541	0.818	0.805
	Rule-in cut-off	15.590	0.865	0.742	0.647	0.910
Measurement in m/sec						
Pre-test probability			Prevalence 30%		Prevalence 60%	
Scenario	**Cut-off**		**NPV**	**PPV**	**NPV**	**PPV**
All US device together						
Significant fibrosis, ≥F2; F0-F1 vs. F2-F4						
	Best cut-off	1.481	0.879	0.572	0.675	0.824
	Rule-out cut-off	1.391	0.924	0.445	0.776	0.737
	Rule-in cut-off	1.578	0.814	0.690	0.555	0.886
Advanced fibrosis, ≥F3; F0-F2 vs. F3-F4						
	Best cut-off	1.633	0.886	0.588	0.689	0.833
	Rule-out cut-off	1.341	0.928	0.462	0.786	0.750
	Rule-in cut-off	1.988	0.824	0.703	0.572	0.892
Cirrhosis, F4; F0-F3 vs. F4						
	Best cut-off	1.748	0.915	0.663	0.754	0.873
	Rule-out cut-off	1.532	0.942	0.564	0.824	0.819
	Rule-in cut-off	1.995	0.876	0.750	0.668	0.913

Abbreviations: F1 mild fibrosis, F2 significant fibrosis, F3 advanced fibrosis, F4 cirrhosis, kPa kilopascals, m/sec meters per second, NPV negative predictive value, PPV positive predictive value, T2DM type 2 diabetes mellitus, US ultrasound

Table VII. Negative and positive predictive values for 2D-SWE according to the prevalence of different stages of liver fibrosis (pre-test probability) among different subpopulations by multi-level random effects model

Measurement in kPa						
Pre-test probability			Prevalence 30%		Prevalence 60%	
Scenario	**Cut-off**		**NPV**	**PPV**	**NPV**	**PPV**
Mild fibrosis, ≥F1; F0 vs. F1-F4						
Asian studies	*Best cut-off*	6.953	0.880	0.573	0.676	0.825
	Rule-out cut-off	5.396	0.924	0.447	0.777	0.738
	Rule-in cut-off	8.959	0.815	0.691	0.557	0.887
Obesity	*Best cut-off*	6.792	0.870	0.551	0.656	0.811
	Rule-out cut-off	5.361	0.918	0.424	0.761	0.721
	Rule-in cut-off	8.605	0.801	0.671	0.534	0.877
Significant fibrosis, ≥F2; F0-F1 vs. F2-F4						
Asian studies	*Best cut-off*	8.561	0.868	0.547	0.652	0.808
	Rule-out cut-off	4.616	0.916	0.420	0.757	0.717
	Rule-in cut-off	15.880	0.798	0.667	0.530	0.875
T2DM	*Best cut-off*	7.961	0.888	0.594	0.694	0.836
	Rule-out cut-off	6.404	0.929	0.469	0.790	0.756
	Rule-in cut-off	9.895	0.828	0.707	0.579	0.894
Obesity	*Best cut-off*	7.945	0.884	0.582	0.684	0.830
	Rule-out cut-off	6.158	0.927	0.456	0.783	0.746
	Rule-in cut-off	10.251	0.821	0.699	0.566	0.890
Advanced fibrosis, ≥F3; F0-F2 vs. F3-F4						
Asian studies	*Best cut-off*	10.182	0.890	0.597	0.697	0.838
	Rule-out cut-off	3.100	0.930	0.473	0.792	0.758
	Rule-in cut-off	33.447	0.830	0.709	0.582	0.895
T2DM	*Best cut-off*	9.010	0.910	0.649	0.742	0.866
	Rule-out cut-off	7.699	0.940	0.541	0.818	0.805
	Rule-in cut-off	10.545	0.865	0.743	0.647	0.910
Obesity	*Best cut-off*	9.040	0.903	0.631	0.727	0.857
	Rule-out cut-off	6.997	0.937	0.516	0.810	0.789
	Rule-in cut-off	11.680	0.853	0.732	0.624	0.906
Cirrhosis, F4; F0-F3 vs. F4						
Asian studies	*Best cut-off*	12.466	0.922	0.683	0.770	0.883
	Rule-out cut-off	9.519	0.945	0.595	0.831	0.837
	Rule-in cut-off	16.326	0.889	0.760	0.696	0.917
T2DM	*Best cut-off*	11.760	0.910	0.649	0.742	0.866
	Rule-out cut-off	9.594	0.940	0.542	0.818	0.805
	Rule-in cut-off	14.416	0.866	0.743	0.648	0.910
Obesity	*Best cut-off*	11.614	0.911	0.653	0.745	0.868
	Rule-out cut-off	8.253	0.941	0.548	0.820	0.809
	Rule-in cut-off	16.343	0.868	0.745	0.653	0.911

Abbreviations: F1 mild fibrosis, F2 significant fibrosis, F3 advanced fibrosis, F4 cirrhosis, kPa kilopascals, m/sec meters per second, NPV negative predictive value, PPV positive predictive value, T2DM type 2 diabetes mellitus, US ultrasound

Table VIII. Negative and positive predictive values for 2D-SWE according to the prevalence of different stages of liver fibrosis (pre-test probability) among other subpopulations by multi-level random effects model

Measurement in kPa						
Pre-test probability			Prevalence 30%		Prevalence 60%	
Scenario	**Cut-off**		**NPV**	**PPV**	**NPV**	**PPV**
Mild fibrosis, ≥F1; F0 vs. F1-F4						
Non-T2DM	*Best cut-off*	5.824	0.886	0.588	0.689	0.833
	Rule-out cut-off	4.805	0.928	0.462	0.786	0.751
	Rule-in cut-off	6.843	0.824	0.703	0.572	0.892
Significant fibrosis, ≥F2; F0-F1 vs. F2-F4						
Non-Asian studies	*Best cut-off*	7.401	0.895	0.610	0.709	0.846
	Rule-out cut-off	6.301	0.933	0.489	0.799	0.770
	Rule-in cut-off	8.693	0.839	0.719	0.599	0.900
Non-T2DM	*Best cut-off*	8.077	0.903	0.632	0.728	0.857
	Rule-out cut-off	6.793	0.937	0.518	0.810	0.790
	Rule-in cut-off	9.604	0.854	0.733	0.626	0.906
Advanced fibrosis, ≥F3; F0-F2 vs. F3-F4						
Non-Asian studies	*Best cut-off*	8.481	0.914	0.663	0.753	0.873
	Rule-out cut-off	7.541	0.942	0.562	0.824	0.818
	Rule-in cut-off	9.539	0.875	0.750	0.667	0.913
Non-T2DM	*Best cut-off*	9.315	0.921	0.681	0.768	0.882
	Rule-out cut-off	8.052	0.945	0.591	0.830	0.835
	Rule-in cut-off	10.775	0.887	0.759	0.692	0.917
Cirrhosis, F4; F0-F3 vs. F4						
Non-Asian studies	*Best cut-off*	10.914	0.908	0.644	0.737	0.863
	Rule-out cut-off	8.027	0.939	0.534	0.816	0.801
	Rule-in cut-off	14.840	0.862	0.740	0.641	0.909
Non-T2DM	*Best cut-off*	10.656	0.921	0.682	0.770	0.883
	Rule-out cut-off	8.973	0.945	0.594	0.831	0.837
	Rule-in cut-off	12.655	0.888	0.759	0.695	0.917

Abbreviations: F1 mild fibrosis, F2 significant fibrosis, F3 advanced fibrosis, F4 cirrhosis, kPa kilopascals, m/sec meters per second, NPV negative predictive value, PPV positive predictive value, T2DM type 2 diabetes mellitus, US ultrasound

Table IX. Negative and positive predictive values for 2D-SWE according to the prevalence of different stages of liver fibrosis (pre-test probability) for other types of ultrasound machines by multi-level random effects model

Measurement in kPa						
Pre-test probability			Prevalence 30%		Prevalence 60%	
Scenario	**Cut-off**		**NPV**	**PPV**	**NPV**	**PPV**
Significant fibrosis, ≥F2; F0-F1 vs. F2-F4						
Canon/Toshiba	*Best cut-off*	7.226	0.876	0.564	0.668	0.819
	Rule-out cut-off	3.191	0.921	0.437	0.770	0.731
	Rule-in cut-off	16.363	0.809	0.683	0.547	0.883
GE	*Best cut-off*	7.204	0.910	0.650	0.743	0.867
	Rule-out cut-off	6.665	0.940	0.543	0.818	0.806
	Rule-in cut-off	7.787	0.866	0.743	0.649	0.910
Advanced fibrosis, ≥F3; F0-F2 vs. F3-F4						
Canon/Toshiba	*Best cut-off*	7.831	0.900	0.622	0.719	0.852
	Rule-out cut-off	2.500	0.936	0.505	0.806	0.781
	Rule-in cut-off	24.531	0.847	0.727	0.613	0.903
GE	*Best cut-off*	8.060	0.922	0.684	0.771	0.883
	Rule-out cut-off	7.578	0.945	0.596	0.831	0.838
	Rule-in cut-off	8.574	0.890	0.760	0.697	0.917

Abbreviations: F2 significant fibrosis, F3 advanced fibrosis, kPa kilopascals, m/sec meters per second, NPV negative predictive value, PPV positive predictive value, T2DM type 2 diabetes mellitus, US ultrasound

4.5. Discussions

Our study utilizes a multi-threshold approach within the meta-analysis to provide robust evidence on the applicability of 2D-SWE for identifying various stages of liver fibrosis. Additionally, it aims to contribute to the standardization of 2D-SWE cut-off values. This potential standardization represents a promising avenue for future developments in the field, offering researchers a clear direction for advancing their work.

The 2017 EFSUMB Guidelines state that 2D-SWE technology has measurement bias depending on the software method (19). However, advancements in technology have contributed to a reduction in variance in fibrosis staging across ultrasound systems, mainly due to the efforts of the Quantitative Image Biomarker Alliance (QIBA) (162, 163). Cut-off values for non-VCTE elastography methods lack robust validation and should be approached cautiously.

The Society of Radiologists in Ultrasound (SRU) consensus statement (47) has highlighted that the considerable liver stiffness value overlap of METAVIR scores (47), more significant than the measurement variability between elastography devices (164), suggests that distinct cut-off values for each company might not be necessary (47). Nevertheless, when comparing different manufacturers, discrepancies in cut-off values exist and tend to be more pronounced among patients above the threshold for cACLD (164). In this context, the current guidelines and position papers advocate method standardisation (19, 47, 48, 165-167). Until further validation is conducted, the proposed cut-off values should be interpreted with caution (165). SRU and WFUMB recommend the "rule of four" for ARFI techniques to diagnose cACLD (47, 48). In MASLD, the cut-off values for cACLD may be lower, and follow-up or additional testing is recommended for those with values between 7 and 9 kPa (47). According to the AASLD practice guidelines on portal hypertension management, 2D-SWE values below 7-8 kPa may rule out compensated advanced chronic liver disease (cACLD). Cut-offs ranging from 13-16 kPa are suggested for diagnosing cACLD, while values of 17-20 kPa or higher could indicate the presence of varices and potential decompensation (165). Compared to VCTE, 2D-SWE (mainly SSI) shows similar accuracy (19) but potentially higher applicability, as a considerable number of ultrasound machines from almost all manufacturers are equipped with elastography software nowadays (168).

We have provided cut-off values for pre-test probabilities, as these thresholds can vary depending on the prevalence of the condition within the target population (165). The prevalence of advanced fibrosis in high-risk populations for having MASLD varies between 4-33% (166). Similarly, the prevalence of advanced fibrosis in our population was 17.9%. In this regard, we have provided cut-off values for different stages of liver fibrosis at pre-test probabilities of 30% and 60%, mimicking different clinical scenarios.

Overall Diagnostic Performance of 2D-SWE. We determined optimized cut-off values for each stage of liver fibrosis, achieving excellent sAUC, sensitivity (Se), and specificity (Sp). When aggregating data from all ultrasound manufacturers, 2D-SWE demonstrated strong sensitivity and specificity across all stages of fibrosis, with optimal cut-offs ranging from 6.432 to 11.548 kPa. Although there were minor differences in optimal cut-off values based on ethnicity and comorbidities, these differences were not statistically significant. In studies involving Asian populations, the optimal cut-offs were generally higher for each stage of liver fibrosis, likely due to population-specific factors. However, sub-analyses confirmed that these variations did not significantly impact the cut-off values.

After optimising the cut-off values, advanced fibrosis (≥F3) could be ruled-out with high Se and NPV for all US devices together (7.4 kPa), T2DM subpopulation (7.7 kPa), the subgroup with prevalent obesity (7 kPa), non-Asian studies (7.5 kPa), thresholds that do not vary significantly and closely align with the 8 kPa cut-off proposed for LSM-VCTE (94). Similarly, the rule-in cut-offs for advanced fibrosis (≥F3) with high Sp and PPV by all US devices together (13.6 kPa), among the T2DM subpopulation (10.6 kPa), the subpopulation with prevalent obesity (11.7 kPa) closely to the 12 kPa cut-off proposed for LSM-VCTE (94).

Type of ultrasound manufacturer. The optimized cut-off values provided by SuperSonic Imagine for diagnosing different stages of liver fibrosis were 7.3 kPa for ≥F1, 8.3 kPa for ≥F2, 10.2 kPa for ≥F3, and 11.9 kPa for F4. These values closely resembled those obtained when analyzing all ultrasound devices collectively. In contrast, the cut-off values from Canon Medical Systems/Toshiba were lower, at 7.3 kPa for ≥F2 and 7.8 kPa for ≥F3, while General Electric Healthcare provided values of 7.2 kPa for ≥F2 and 8.1 kPa for ≥F3, aligning with some previous comparative studies (131). The variation in cut-off values could be explained by the fact that a considerable proportion of the studies included in the meta-analysis (9 out of 20, 45%) reported using SSI. Nevertheless, ultrasound machines from all manufacturers show excellent performance in diagnosing various stages of liver fibrosis, though there are slight variations in sensitivity and specificity. These differences may be attributed to the technical aspects of the machines, underscoring the need for standardization in reporting and validation across different ultrasound modules (47).

Comparison with similar published meta-analyses. Our meta-analysis stands out from previous studies in its application of a multi-level random effects model on biopsy-proven MASLD, a novel approach that has not been used before. While other studies have evaluated the diagnostic performance of 2D-SWE in mixed liver disease etiologies or small biopsy-proven MASLD cohorts, none have taken this unique approach. Only Selvaraj et al. (18) and Herrmann et al. (169) have meta-analysed data from four SuperSonic Imagine with comparable results regarding sAUC values and proposed cut-off ranges.

Strengths and limitations. Our meta-analysis boasts several significant strengths. Firstly, by employing a multi-level random effects model, we enhanced robustness and efficacy, offering improved performance over the traditional diagnostic meta-analysis methods (170, 171). Secondly, we conducted a comprehensive literature search without imposing restrictions on gender, race, ethnicity, or language of publications. Thirdly, we determined the optimized cut-offs for fibrosis staging using the largest cohort of biopsy-proven MASLD patients. Despite these strengths, the study has some limitations. The variability in study designs and ultrasound manufacturers may account for differences in results. Moreover, reliance on published data limited our ability to control for potential confounders and to perform consistent analyses across studies. An individual patient data (IPD) meta-analysis would have been ideal to reduce variability bias. However, to minimize bias in our analysis, we included only studies that used histology as the reference standard.

The methodological quality of the studies included in our meta-analysis was not consistently optimal. Many studies did not employ the "intention to diagnose" (ITD) method when assessing QUADAS-2, which means that selection bias related to flow and timing could not be fully excluded. The absence of an ITD approach in these studies reflects a relatively low quality in some of the published research on this topic. Therefore, researchers and publishers should consider adopting the ITD method in future studies on 2D-SWE to improve the quality and reliability of the findings.

4.6. Conclusions

This study demonstrates that 2D-SWE is a reliable tool for assessing liver fibrosis across various stages and patient populations. However, it highlights the importance of accounting for individual patient factors and differences in machine performance when interpreting results, reporting examinations, and determining optimal cut-offs.

By including over 2,000 patients with biopsy-confirmed MASLD from diverse settings, this meta-analysis aims to support clinicians in making more informed decisions and enhancing patient risk stratification, potentially integrating 2D-SWE into referral pathways.

The use of a multi-level random effects model provides strong evidence of 2D-SWE's effectiveness in identifying stages of liver fibrosis in MASLD and offers valuable insights into standardizing cut-off values for clinical use. The study emphasizes the need to consider patient-specific factors and variations between ultrasound machines when interpreting liver stiffness measurements with 2D-SWE.

In conclusion, the study supports the broad applicability of 2D-SWE for liver fibrosis assessment but underscores the necessity of considering individual patient

factors and machine performance variations to ensure the most accurate non-invasive evaluation for patients with metabolic fatty liver disease.

Some of the preliminary results were presented at the EASL Congress 2024, Milan, Italy – Taru MG, Leucuta DC, Ferri S, Hashim A, Orasan O, Procopet B et all. Diagnostic accuracy of two-dimensional shear wave elastography (2D-SWE) for non-invasive assessment of liver fibrosis in biopsy-proven metabolic dysfunction-associated steatotic liver disease (MASLD). Systematic-review and multi-level random effects model meta-analysis. EASL Congress 2024. Milan, Italy. 5-8 June 2024.

The full text manuscript was submitted to journal, and it is currently under revision.

5. The effectiveness of non-selective ß-blockers in preventing the first decompensation event in patients with compensated cirrhosis enduring clinically significant portal-hypertension (CSPH) after etiological treatment. Diabetes mellitus as independent risk factor for first decompensation event

5.1. Introduction

Portal hypertension (PH) plays a key role in the shift from compensated to decompensated cirrhosis, which are two stages of liver disease characterized by distinct symptoms and survival outcomes (172). Decompensation, according to the last Baveno VII consensus (41), is defined by the occurrence of ascites at least grade II, variceal bleeding and/or hepatic encephalopathy (HE) at least grade II.

When the portal pressure gradient, (indirectly measured as hepatic venous pressure gradient – HVPG) arises to 10 mmHg and above, clinical decompensation may develop (41). This condition is known as clinically significant portal hypertension (CSPH), as patients who advance to decompensation face an increased risk of mortality (172). The identification of CSPH by HVPG has been mostly validated in patients with alcohol-related and active-viral cirrhosis (173), while concerns exist in patients with other etiologies, such as MASLD (103, 104).

Over the past forty years, non-selective beta-blockers (NSBB) have been fundamental in the treatment and prevention of variceal bleeding, both as a primary and secondary measure (174, 175). Subsequent evidence broadened the target population to all patients with cirrhosis and CSPH (176) since their use can mitigate the development of any decompensating event (99). The landmark study by Villanueva (99), that demonstrated the benefit of NSBB in preventing any decompensating event, was conducted in patients with compensated cirrhosis and CSPH (defined by an HVPG≥ 10 mmHg) before the era of DAA-treatment for HCV.

Concerns were then raised (177) whether: 1) NSBB benefit applies also to patients with *clinical* evidence of CSPH (presence of gastroesophageal varices -GEV- of any size and/or spontaneous portosystemic collaterals -SPSS) without HVPG measurement, and whether 2) NSBB treatment remains beneficial in patients whose etiological factor has been removed. In patients with cirrhosis and CSPH, HCV treatment is able, in fact, to reduce the HVPG for up to two years post-treatment (178). However, even in this cohort (178), up to 53-65% of patients still present CSPH after two years from DAA treatment, remaining at risk of decompensation.

5.2. Working hypothesis/objectives

Our study primarily aimed to evaluate the impact of non-selective beta-blockers (NSBB) on the occurrence of the first decompensation event in patients with cirrhosis who have clinical signs of persistent clinically significant portal hypertension (CSPH) two years after initiating etiological treatment. Additionally, we sought to identify independent risk factors that might trigger this initial decompensation event.

5.3. Material and methods

Study population. This was a monocentric observational study involving consecutive patients with compensated cirrhosis who had no prior history of decompensation and exhibited persistent clinical signs of clinically significant portal hypertension (CSPH) two years after receiving etiological treatment. The patients were assessed at the Internal Medicine Unit for the Treatment of Severe Organ Failure at IRCCS Azienda Ospedaliero-Universitaria di Bologna, Italy, during the period from 2017 to 2020.

The diagnosis of cirrhosis was established using clinical, biochemical, imaging, and/or histological criteria, with histological confirmation required for MASLD-related cirrhosis. Clinical evidence of clinically significant portal hypertension (CSPH) was defined by the presence of gastroesophageal varices (GEV) observed during upper gastrointestinal endoscopy and/or splenomegaly with portal system collateralization (SPSS) identified through cross-sectional imaging. Both cirrhosis and clinical signs of CSPH had to be present at the time of inclusion in the study.

In order to minimize the potential long-term benefit of etiological treatment on PH (178), we used the timeframe of 2017-2020 for patients enrollment since in our center the majority of patients with HCV-related cirrhosis were treated with DAA between 2015-2017 and therefore, by 2017-2020, patients enrolled in this study were expected to be included after two years following etiological treatment. We subsequently applied identical selection criteria to all patients with cirrhosis of different etiologies.

Currently, there is no definitive etiological treatment for MASLD-related cirrhosis. Despite this, we chose not to exclude these patients to provide a current perspective on the benefits of non-selective beta-blockers (NSBB) in contemporary populations. However, the effectiveness of NSBB remains a subject of debate for both groups of patients (177).

Selection criteria For etiologies other than HCV: patients with HBV were included only if they were on nucleos(t)ide analogues (NUC) and had achieved undetectable HBV-DNA levels for at least two years. Patients with alcohol-related cirrhosis had to maintain abstinence for a minimum of two years before being included. Those with autoimmune liver disease were included after achieving stable

remission under specific treatment for at least two years. Patients with MASLD were required to be undergoing treatment for diabetes, hypercholesterolemia, and/or arterial hypertension, if clinically indicated, and were included in the study two years after the initiation of these treatments to align as closely as possible with the other patient groups.

Exclusion criteria. age under 18 or over 80 years, cirrhosis without evidence of gastroesophageal varices (GEV) or splenomegaly with portal system collateralization (SPSS), complete portal vein thrombosis (PVT) or partial PVT under anticoagulant therapy, previous transjugular intrahepatic portosystemic shunt (TIPS) or surgical shunt, splenectomy, previous episode of hepatic decompensation, active hepatocellular carcinoma (HCC) or HCC previously classified as beyond Milan criteria, histological diagnosis of vascular liver disease, heart failure, hepatopulmonary syndrome, portopulmonary hypertension, any medical condition with an expected survival of less than six months, neurological or psychiatric disorders affecting the assessment of hepatic encephalopathy (HE), and lack of essential information. The inclusion date was the date of the first visit occurring between 2017 and 2020, but only after a minimum of two years following the initiation of etiological treatment.

Patient evaluation. Data on the etiology of cirrhosis, comorbidities, and pharmacological treatments were gathered both at enrollment and throughout follow-up. Routine laboratory tests were performed at enrollment, and MELD, MELD-Na, and Child-Pugh scores were calculated. Ultrasounds for hepatocellular carcinoma (HCC) surveillance and portal vein thrombosis (PVT) assessment were conducted every six months, or sooner if clinically necessary, as part of standard clinical practice; these data were subsequently reviewed for the study. Abdominal CT and MRI scans were assessed by radiologists with expertise in hepatic diseases. Porto-systemic collaterals were defined as spontaneous connections between the spleno-mesenteric-portal axis and the systemic venous system, excluding gastroesophageal varices (GEV), and were classified based on the site of connection (179). Upper gastrointestinal endoscopy was performed in all patients with cirrhosis regardless the non-invasive criteria to avoid endoscopy (180) and GEV, when present, classified as small or medium-large with or without red wall marks (41).

Use of non-selective ß-blockers. The initial evidence supporting the use of non-selective beta-blockers (NSBB) to prevent decompensating events in patients with cirrhosis and clinically significant portal hypertension (CSPH) was presented at the International Liver Congress in 2017. Following this, our center began initiating NSBB treatment for some patients based on clinical evidence of CSPH, even if they had only small gastroesophageal varices (GEV) or splenomegaly with portal system collateralization (SPSS) without GEV. The decision to prescribe NSBB was made by clinicians, considering the patient's clinical and hemodynamic characteristics as well as potential contraindications. For primary prophylaxis of variceal bleeding in patients

with medium to large GEV, NSBB were the first-line treatment, while endoscopic variceal ligation (EVL) was used for patients who could not tolerate NSBB or had contraindications. NSBB dosages were adjusted to the highest tolerable level, up to 120 mg/day for propranolol and 12.5 mg/day for carvedilol. Some patients received higher doses of carvedilol due to concurrent cardiological conditions, primarily arterial hypertension.

Outcomes and follow-up. The primary endpoint was the occurrence of first hepatic decompensation, defined per Baveno VII criteria (41) as the development of variceal bleeding, ascites and/or overt HE in patients on-NSBB vs those off-NSBB. During follow-up, surveillance ultrasonography was performed every six months (or sooner if indicated) following international guidelines, with any development of hepatocellular carcinoma (HCC) or portal vein thrombosis (PVT) confirmed by CT scans. Complications such as acute kidney injury (AKI), hepatorenal syndrome, and bacterial infections were also documented. Bacterial infections were diagnosed and managed according to both international and local guidelines. To investigate the relationship between bacterial infections and the occurrence of the first decompensation event, only infections that occurred prior to decompensation were considered. Consequently, episodes of spontaneous bacterial peritonitis, which require the presence of ascites, were excluded from this analysis.

The follow-up period concluded in June 2023. For patients who experienced decompensation, follow-up was terminated at the point when decompensation was first observed. Since the occurrence of portal vein thrombosis (PVT) and/or hepatocellular carcinoma (HCC) — and their associated treatments — could independently influence decompensation, these were treated as competing risk events. Therefore, follow-up for these patients was censored (considered as compensated) at the time of PVT or HCC diagnosis.

Ethical approval. The study was conducted following the principles outlined in the Helsinki Declaration and received approval from our institutional review boards (MITIGO study - 405/2023). Informed consent was obtained from all participants who were still alive and under follow-up, while consent was waived for participants who had dropped out or had passed away.

Statistical analysis. Continuous variables were assessed for homogeneity using Levene's test and were presented as mean ± standard deviation; comparisons were made using the Student's t-test. Categorical variables were expressed as frequencies and compared using the chi-square test. The cumulative incidence of decompensation was estimated with portal vein thrombosis (PVT) and hepatocellular carcinoma (HCC) treated as competing events, and cumulative incidence curves were compared using Gray's test. Predictors of decompensation and bacterial infections were identified through multivariable Cox regression analysis with a stepwise backward selection method, reporting hazard ratios (HR) and 95% confidence intervals (CI) for each predictor. Receiver operating characteristic (ROC) curve

analysis was conducted for continuous parameters of interest. A p-value of <0.05 was considered statistically significant. Statistical analyses were performed using IBM SPSS (Version 27, NY, USA) and the cmprsk package in R (R Foundation for Statistical Computing, Vienna, Austria).

5.4. Results

A total of 406 patients were included in the final analysis. **Figure 1** illustrates the flow of patients during the study.

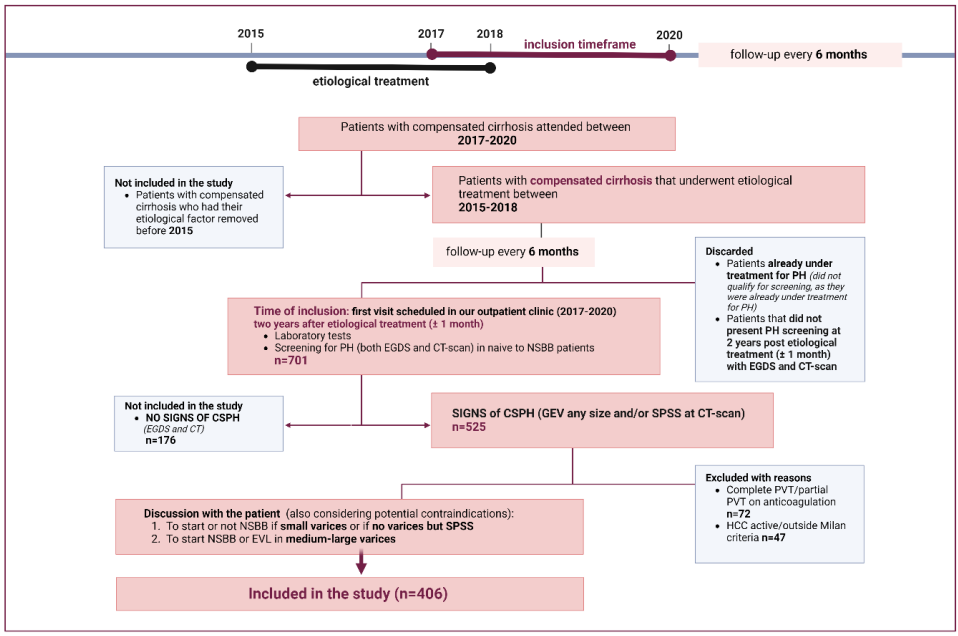

Figure 1. Study flow and patient selection

Baseline characteristics are outlined in **Table I.** The mean age of the entire cohort was 62.2 years (± 11.26), with 262 patients (64.5%) being male. The predominant etiology of cirrhosis was viral, accounting for 59%, followed by alcohol-related cirrhosis at 14%. Most patients were classified as Child-Pugh A (85%), with the remaining patients classified as Child-Pugh B7. Baseline diabetes was present in 34% of patients, all of whom were receiving specific treatment. A history of hepatocellular carcinoma (HCC), not active at the time of inclusion, was observed in 4% of patients, and portal vein thrombosis (PVT), which was partial and affected only intrahepatic branches without anticoagulant therapy, was found in 3% of patients.

The majority of patients (n=299, 74%) exhibited gastroesophageal varices (GEV), with 206 of these patients having small GEV (51% of the total cohort); none of these had associated red wall marks. Additionally, 281 patients (69%) had

splenomegaly with portal system collateralization (SPSS), with most of these (58%) showing recanalization of the paraumbilical vein. Among the patients with SPSS, 107 (26%) had SPSS without accompanying GEV.

Table I. Patient characteristics at inclusion and outcomes of interest

	NSBB-on (n=187)	NSBB-off (n=219)	p
Baseline characteristics			
Gender, M	122 (65,2%)	140 (63,9%)	0,783
Age, yrs*	62,24 ± 11,26	61,57 ± 11,29	0,770
Etiology			0,223
Alcohol related	20 (10,7%)	37 (16,9%)	
HCV-SVR	86 (46,0%)	93 (42,4%)	
HBV on NUC	32 (17,1%)	28 (12,8%)	
MASLD	28 (15,0%)	26 (11,9%)	
Miscellanea	21 (11,2%)	35 (16,0%)	
Arterial Hypertension	84 (44,9%)	93 (42,5%)	0,677
Diabetes	69 (36,7%)	69 (31,5%)	0,253
White blood Count (x10^3/mmc)*	4842,80 ± 1871,26	5191,20 ± 1947,83	0,068
Hemoglobin, (g/dl)*	13,03 ± 1,93	12,85 ± 1,85	0,348
Platelets count (x10^3/mmc)*	***102,32 ±51,51***	***118,96 ±56,15***	***0,002***
AST (IU/L)*	37,31 ± 16,43	39,57 ± 16,83	0,173
ALT (IU/L)*	29,66 ± 15,44	31,43 ± 15,88	0,258
Bilirubin (mg/dL) *	1,31 ± 0,56	1,25 ± 0,55	0,300
Albumin (g/L)*	3,82 ± 0,49	3,77 ± 0,50	0,337
INR*	1,20 ± 0,11	1,19 ± 0,14	0,670
Creatinine (mg/dL)*	0,82 ± 0,21	0,80 ± 0,21	0,299
Sodium (mmol/L) *	139,42 ± 2,80	138,93 ± 2,88	0,083
Child-Pugh score*	5,51 ± 0,73	5,57 ± 0,75	0,410
Child-Pugh score, class			0,667
Child-Pugh class A	160 (85,6%)	184 (84,0%)	
Child-Pugh class B (all B7)	27 (14,4%)	35 (16,0%)	
MELD*	9,77 ± 1,89	9,60 ± 1,95	0,383
MELD- Na*	10,81 ± 2,44	10,94 ± 2,61	0,616
Gastroesophageal Varices (GEV)			***<0.0001***
No GEV (SPSS only)	***24 (12,8%)***	***83 (37,9%)***	
Small GEV	***99 (52,9%)***	***107 (48,9%)***	
Medium-Large GEV	***64 (34,3%)***	***29 (13,2%)***	
HCC	7 (3,7%)	9 (4,1%)	0,850
PVT	7 (3,7%)	5 (2,3%)	0,757
Treatments			
Non-selective beta-blocker			NA
Propranolol	144 (77,0%)	NA	
Propranolol Mean dose (mg/day)	61,9 ± 9,1	NA	
Carvedilol	43 (23,0%)	NA	
Carvedilol Mean dose (mg/day)	12,3 ± 4,2	NA	
Endoscopic Variceal Ligation	NA	29 (13,2%)	NA
Statins	30 (16,0%)	32 (14,6%)	0,690
Outcomes			
Decompensation-overall	***30 (16,0%)***	***97 (44,3%)***	***<0,0001***
Decompensation-type			***<0,0001***
Ascites	***22 (11,8%)***	***76 (34,7%)***	
Bleeding	***5 (2,7%)***	***8 (3,7%)***	
Hepatic encephalopathy	***3 (1,6%)***	***13 (5,9%)***	
PVT (new or worsening)	17 (9,1%)	14 (6,4%)	0,314
HCC (new diagnosis)	26 (13,9%)	20 (9,1%)	0,131
Bacterial Infections	***25 (13,4%)***	***59 (26,9%)***	***0,001***

*Abbreviations: ALT: alanine aminotransferase; AST: aspartate aminotransferase; HBV: hepatitis B virus; HCC: hepatocellular carcinoma; HCV: hepatitis C virus; GEV: gastroesophageal varices; INR: International Normalized Ratio; MASLD: metabolic dysfunction-associated steatotic liver disease; MELD: model for end stage liver disease; NUC: nucleos(t)ide analogue; NSBB: non selective beta-blockers; PVT: portal vein thrombosis; SPSS: spontaneous porto-systemic shunts; SVR: sustained virological response; *Data are expressed as mean ± SD, absolute frequency and percentage (%) when appropriate. Comparisons between groups were performed by means of Student's t test or the X^2 test when appropriate*

A total of 187 (46%) patients were on NSBB, the majority of them (77%) on propranolol with a median dose of 62 mg per day. The two groups (on-NSBB and off-NSBB) had comparable baseline characteristics (**Table I**) regarding etiology of liver disease, comorbidities (both arterial hypertension and diabetes), blood tests and the relative liver score. Patients on-NSBB had a significantly lower mean platelet count and higher rate of GEV.

Outcomes. During a mean follow-up period of 32 ± 22 months, 127 patients (31%) experienced decompensation. Among these, 98 patients (24%) developed ascites, accounting for 77% of all decompensating events, 13 patients (3%) had variceal bleeding, and 16 patients (4%) experienced hepatic encephalopathy (HE). The average time to decompensation was 27 ± 20 months. No patients developed acute-on-chronic liver failure (ACLF). Only one patient developed acute kidney injury (AKI), which was diagnosed on the same day as ascites decompensation. During the follow-up period, 31 patients developed portal vein thrombosis (PVT) and 46 developed hepatocellular carcinoma (HCC) before experiencing decompensation; follow-up for these patients was terminated on the day of PVT or HCC diagnosis, and they were censored as compensated, with these conditions analyzed as competing risk events. No transjugular intrahepatic portosystemic shunts (TIPS) were implanted, as follow-up was stopped at the time of PVT diagnosis, and no patients died or underwent liver transplantation before decompensation (or HCC diagnosis, as follow-up was stopped at that point).

Patients on-NSBB had a significantly lower rate of decompensation (ascites, variceal bleeding, or HE) than patients off-NSBB: 16% vs 44% respectively (HR 0,28, 95% CI 0,19–0,43; p by Gray-test <0,0001) (**Table I**).

Among patients with gastroesophageal varices (GEV) of any size (n=299), decompensation rates were 28 out of 163 (17%) for those on non-selective beta-blockers (NSBB) versus 61 out of 136 (45%) for those not on NSBB (HR 0.30, 95% CI 0.19–0.48; p < 0.0001 by Gray's test). For patients with small GEV (n=206), decompensation rates were 17 out of 99 (17%) for those on NSBB versus 46 out of 107 (43%) for those not on NSBB (HR 0.31, 95% CI 0.18–0.55; p < 0.0001 by Gray's test). In patients with medium-large GEV (n=93), decompensation rates were 11 out of 64 (17%) for those on NSBB compared to 15 out of 29 (52%) for those undergoing endoscopic variceal ligation (EVL) (HR 0.26, 95% CI 0.12–0.58; p < 0.0001 by Gray's test). Among patients with splenomegaly with portal system collateralization (SPSS) only (n=107), decompensation occurred in 2 out of 24 (8%) for those on NSBB versus 36 out of 83 (43%) for those not on NSBB (HR 0.15, 95% CI 0.05–0.64; p = 0.002 by Gray's test).

Decompensation according to etiology of cirrhosis. Patients with viral-treated etiology experienced lower rate of decompensation than patients with alcohol- or MASLD-related etiology (HCV-SVR accounted for the 21% of the decompensation

rate, HBV on NUC 26%, Alcohol 44%, MASLD 46%; p<0.0001). Despite different rates of decompensation among groups, the benefit of NSBB in lowering first decompensation was significant in each different etiology, including patients with HCV-SVR cirrhosis (n=179) (HR 0,24, 95% CI 0,11–0,52; p by Gray-test <0,0001) and those with MASLD-related cirrhosis (n=54) (HR 0,30, 95% CI 0,13–0,71; p by Gray-test =0,004) (**Figure 2**).

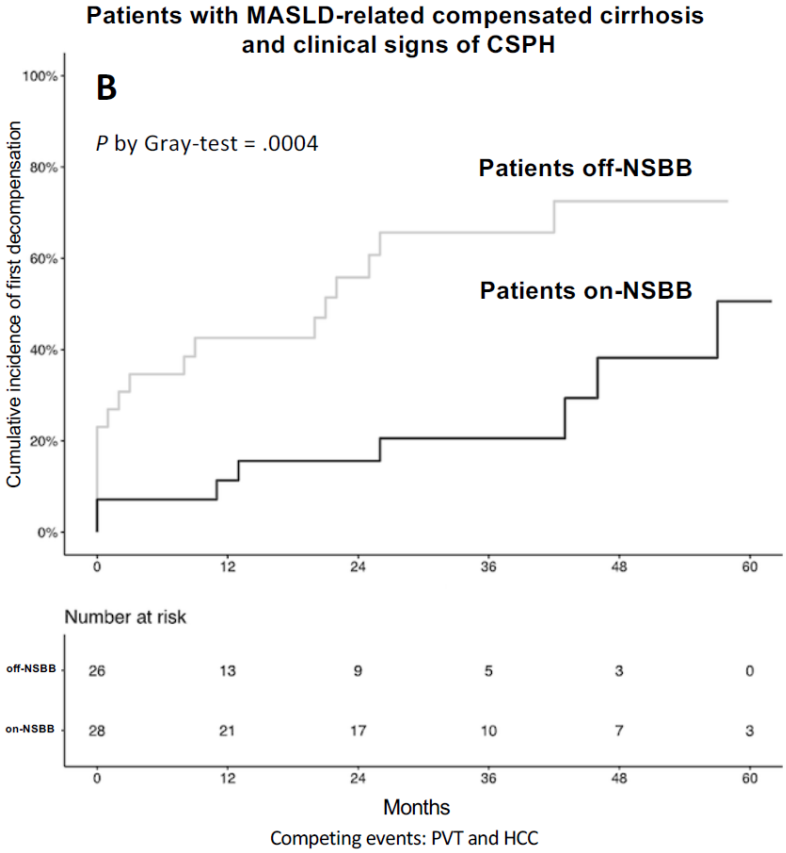

Figure 2. NSBB benefit in patients with compensated MASLD-cirrhosis and clinical signs of CSPH
Figure 2 legend: NSBB – non-selective beta-blockers, PVT – portal vein thrombosis, HCC – hepatocellular carcinoma

Predictors of first decompensation. Patients who decompensated had lower levels of hemoglobin and platelets count and higher Child-Pugh, MELD and MELD-Na score (Table 2). The rate of patients with diabetes was significantly higher in patients who decompensated (45% vs 30%; p=0,014) (**Table II, Table III**).

Table II. Cox regression analysis on predictors of first decompensation

	No decompensation during follow-up (n=279)	Decompensation during follow-up (n=127)	p
Gender, M	184 (65,9 %)	78 (71,4%)	0,376
Age, yrs*	61,15 ± 11,41	62,02 ± 10,97	0,476
Etiology			***<0,0001***
Alcohol	***32 (11,5%)***	***25 (19,7%)***	
HCV-SVR	***141 (50,5%)***	***38 (29,9%)***	
HBV on NUC	***43 (15,4%)***	***17 (13,4%)***	
MASLD	***29 (10,4%)***	***25 (19,7%)***	
Miscellanea	***34 (12,2%)***	***22 (17,3%)***	
Arterial Hypertension	115 (41,2%)	62 (48,8%)	0,141
Diabetes	***84 (30,1%)***	***54 (45,2%)***	***0,014***
White blood Count (x10^3/mmc)*	5034,31 ± 1860,26	5022,80 ± 2048,21	0,955
Hemoglobin, (g/dl)*	***13,24 ±1,82***	***12,25 ±1,88***	***<0,0001***
Platelets count (x10^3/mmc)*	***115,34 ±55,91***	***102,41 ±50,82***	***<0,0001***
AST (IU/L)*	***35,39 ±15,56***	***45,43 ±16,99***	***<0,0001***
ALT (IU/L)*	***28,49 ±15,31***	***35,28 ±15,54***	***<0,0001***
Bilirubin (mg/dL) *	***1,21 ±0,55***	***1,41 ±0,53***	***0,001***
Albumin (g/L)*	***3,92 ±0,46***	***3,51 ±0,46***	***<0,0001***
INR*	***1,18 ±0,13***	***1,23 ±0,11***	***<0,0001***
Creatinine (mg/dL)*	0,81 ± 0,20	0,82 ± 0,25	0,843
Sodium (mmol/L) *	***139,45 ±2,72***	***138,52 ±3,02***	***0,002***
Child-Pugh score*	***5,41 ±0,67***	***5,85 ±0,81***	***<0,0001***
Child-Pugh score, class			***<0,0001***
Child class A	***251 (90,0%)***	***93 (73,2%)***	
Child class B (all B7)	***28 (10,0%)***	***34 (26,8%)***	
MELD*	***9,38 ±1,93***	***10,35 ±1,75***	***<0,0001***
MELD- Na*	***10,42 ±2,46***	***11,91 ±2,41***	***<0,0001***
Gastroesophageal Varices - any size	210 (75,3%)	89 (70,1%)	0,271
Gastroesophageal Varices			0,492
No Varices (SPSS only)	69 (24,7%)	38 (29,9%)	
Small varices	143 (51,3%)	63 (49,6%)	
Medium-Large varices	67 (24,0%)	26 (20,5%)	
HCC at baseline	8 (2,9%)	8 (6,3%)	0,099
PVT at baseline	7 (2,5%)	5 (3,9%)	0,431
Non-selective beta-blocker	***157 (56,2%)***	***30 (23,6%)***	***<0,0001***
Statins	47 (16,8%)	15 (11,8%)	0,191
Bacterial Infections	***28 (10,0%)***	***56 (44,1%)***	***<0,0001***

*Abbreviations: ALT: alanine aminotransferase; AST: aspartate aminotransferase; HBV: hepatitis B virus; HCC: hepatocellular carcinoma; HCV: hepatitis C virus; GEV: gastroesophageal varices; INR: International Normalized Ratio; MASLD: metabolic dysfunction-associated steatotic liver disease; MELD: model for end stage liver disease; NUC: nucleos(t)ide analogue; NSBB: non selective beta-blockers; PVT: portal vein thrombosis; SPSS: spontaneous porto-systemic shunts; SVR: sustained virological response; *Data are expressed as mean ± SD, absolute frequency and percentage (%) when appropriate. Comparisons between groups were performed by means of Student's t test or the X2 test when appropriate*

At univariate analysis (**Table III**) treated viral etiology and NSBB use were protective factors for first decompensation.

Table III. Cox regression analysis on predictors of first decompensation

	Univariate		Multivariate	
	HR (95% CI)	**p**	**HR (95% CI)**	**p**
Etiology- Viral	**0,511 (0,360 – 0,726)**	**<0,0001**	0,974 (0,660 – 1,438)	0,895
Diabetes	**1,619 (1,138 – 2,302)**	**0,007**	**1,587 (1,071 – 2,352)**	**0,021**
Hemoglobin	**0,771 (0,705 – 0,834)**	**<0,0001**	**0,850 (0,770 – 0,939)**	**0,001**
Platelets count	**0,996 (0,993 – 1,000)**	**0,037**	**0,996 (0,992 – 1,000)**	**0,031**
AST	**1,027 (1,018 – 1,036)**	**<0,0001**	0,997 (0,983 – 1,011)	0,635
ALT	**1,023 (1,013 – 1,033)**	**<0,0001**	**1,019 (1,004 – 1,034)**	**0,014**
Child-Pugh score	**1,964 (1,594 – 2,418)**	**<0,0001**	**1,774 (1,114 – 2,825)**	**0,016**
Child-Pugh B (vs A)	**2,735 (1,841– 4,062)**	**<0,0001**	0,584 (0,270 – 1,263)	0,172
MELD	**1,261 (1,150– 1,383)**	**<0,0001**	0,947 (0,806 – 1,112)	0,506
MELD- Na	**1,258 (1,174– 1,347)**	**<0,0001**	**1,121 (1,004 – 1,252)**	**0,043**
Non-selective beta-blocker	**0,282 (0,187 – 0,426)**	**<0,0001**	**0,320 (0,208 – 0,492)**	**<0,0001**
Infections during Follow-up	**3,595 (2,520 – 5,128)**	**<0,0001**	**2,432 (1,652 – 3,581)**	**<0,0001**

Abbreviations: ALT: alanine aminotransferase; AST: aspartate aminotransferase; CI: confidence interval; HR: hazard ratio; MELD: model for end stage liver disease.

Multivariable Cox regression analysis (**Table III**) showed that diabetes, ALT, Child-Pugh score, MELD-Na and bacterial infections were independent predictors of decompensation, while higher hemoglobin levels, higher platelets count, and NSBB-use were independent protective factors. The ROC analysis identified 12,5 g/dl as the best discriminating cut-off for Hemoglobin in predicting first decompensation.

Bacterial infections. During follow-up, 84 patients (21%) experienced a total of 101 episodes of bacterial infections. The most common types of infections were spontaneous bacteremia (24%), urinary tract infections (18%), and pneumonia (16%). Patients on non-selective beta-blockers (NSBB) had a significantly lower rate of bacterial infections compared to those not on NSBB (13% vs 27%, p = 0.001) (**Table I**). Multivariable Cox regression analysis (**Table IV**) identified that only hemoglobin levels, Child-Pugh score, and NSBB use were independently associated with the development of bacterial infections.

Table IV. Cox regression analysis on predictors of first decompensation

	Univariate		Multivariate	
	HR (95% CI)	**p**	**HR (95% CI)**	**p**
Etiology- Viral	**0,579 (0,3677 – 0,889)**	**0,013**	0,955 (0,602 – 1,513)	0,844
Diabetes	1,181 (0,748 – 1,863)	0,475		
Gastroesophageal Varices	0,647 (0,409 – 1,023)	0,067		
Hemoglobin	**0,839 (0,751 – 0,938)**	**0,002**	**0,868 (0,767 – 0,983)**	**0,026**
Platelets count	1 (0,995 – 1,004)	0,829		
Child-Pugh score	**2,245 (1,741 – 2,896)**	**<0,0001**	**2,100 (1,490 – 2,960)**	**<0,0001**
MELD	**1,261 (1,127– 1,410)**	**<0,0001**	1,022 (0,887 – 1,178)	0,760
Non-selective beta-blocker	**0,347 (0,217 – 0,556)**	**<0,0001**	**0,363 (0,225 – 0,586)**	**<0,0001**

Abbreviations: CI: confidence interval; HR: hazard ratio; MELD: model for end stage liver disease.

Patients who decompensated had a significant higher rate of bacterial infections than those that remained compensated (44% vs 10%, p<0,0001) (**Table II**). The competing risk factor analysis investigating the relationship between bacterial infections, NSBB use, and the first decompensation event revealed that patients not on NSBB, who had at least one episode of bacterial infection, presented a significantly higher rate of decompensation (73%). In contrast, patients on NSBB who did not experience bacterial infections had a much lower decompensation rate of 10% (HR 2.08, 95% CI 1.73–2.49; p < 0.0001 by Gray's test).

Relationship between Liver Stiffness Measurement, NSBB-use and rate of decompensation.

Among 406 patients included, 91 (22,4% of the population) had their liver stiffness measurement (LSM) performed in the 12 months before the enrollment in the study. Fifty-three patients had LSM ≥ 25 kPa (17 with medium-large GEV, 25 with small GEV, 11 presenting with SPSS only), 28 (53%) of them were started on NSBB. During follow-up, 15 (28%) patients decompensated: 4/28 (14%) in the on-NSBB group and 11/25 (44%) in the off-NSBB group (p=0,01).

5.5. Discussions

Our study demonstrates that non-selective beta-blockers (NSBB) are effective in preventing the onset of the first decompensation event in a real-world population of patients with cirrhosis and clinically significant portal hypertension (CSPH) who have undergone treatment for their underlying etiological factors. Recent findings have

already shown that NSBB can prevent first hepatic decompensation (99, 174), but the landmark study (99), was conducted before the availability of DAA treatment for HCV. Moreover, the HVPG (by which patients in the PREDESCI trial were selected) is not universally available. Similar accessibility challenges stand in some peripheral centers for non-invasive surrogate tools of PH like transient elastography.

We therefore investigated the role of non-selective beta-blockers (NSBB) in preventing the first decompensation event specifically in patients with compensated cirrhosis who exhibited persistent clinical features of clinically significant portal hypertension (CSPH) following etiological treatment.

Main finding. We gathered data from a large monocentric cohort of patients with compensated cirrhosis, which included comprehensive baseline characteristics and outcomes, and our sample size exceeded that of previous trials on non-selective beta-blockers (NSBB). After a mean follow-up period of nearly three years, patients on non-selective beta-blockers (NSBB), despite showing more pronounced signs of portal hypertension (PH), had a significantly lower rate of first hepatic decompensation. Similarly to the PREDESCI trial (99), the main decompensating event was ascites with an incidence of 24% in our cohort, higher than the one reported in the PREDESCI trial. This confirms, in a cohort of patients with treated or with metabolic etiology, the benefit of NSBB in reducing the onset of all decompensating event including ascites (9). When stratified by clinical signs of portal hypertension (PH), the benefit of non-selective beta-blockers (NSBB) remained consistent across all subgroups, including those without gastroesophageal varices (GEV). We believe these findings are particularly noteworthy as they provide the first evidence of a potential benefit of non-selective beta-blockers (NSBB) in patients with splenomegaly with portal system collateralization (SPSS) even in the absence of gastroesophageal varices (GEV).

The benefit of non-selective beta-blockers (NSBB) in preventing the first decompensation event was significant across all cirrhosis etiologies. We confirmed that patients with HCV who achieved sustained virologic response (SVR) or those with HBV managed with nucleos(t)ide analogues (NUC) experienced a significantly lower rate of decompensation compared to patients with alcohol-related or MASLD-related cirrhosis. However, those patients in whom CSPH persists after etiological treatment remain at risk of decompensation (although lower) with still significant benefit from NSBB.

In addition to the established predictors of decompensation, our study identified that non-selective beta-blocker (NSBB) use was independently associated with a reduced risk of first decompensation. Conversely, bacterial infections, diabetes, and low hemoglobin levels were found to be associated with an increased risk of decompensation. Bacterial infections were found to be the strongest trigger of first decompensation, confirming the results by Villanueva et al (181). We further explored whether this impact can be mitigated by the NSBB use. NSBB were previously shown to reduce the incidence of bacterial infections-related hospital admission in patients with

decompensated cirrhosis (182) and of SBP in patients with ascites (183), but were not associated with a lower risk of bacterial infections in compensated cirrhosis (181). In our cohort, likely due to a larger sample size compared to the Villanueva cohort, patients on non-selective beta-blockers (NSBB) experienced a lower rate of bacterial infections

Interestingly, diabetes emerged as an independent risk factor for decompensation, regardless of the etiology of cirrhosis. O'Beirne and colleagues (184) recently demonstrated that diabetes leads to a progression of liver disease up to decompensated cirrhosis in patients with MASLD. We found that the negative impact of diabetes applies to patients of any etiology of cirrhosis. Patients with diabetes had worse outcomes independently from NSBB use, and this confirms (in a larger cohort), recent findings (119) that diabetes impairs the hemodynamic response of NSBB, triggering decompensation.

Surprisingly, hemoglobin levels were identified as an independent predictor of decompensation. Low hemoglobin levels have previously been reported as predictors of poorer outcomes in patients with cirrhosis (185, 186). We found a significant impact of low hemoglobin levels in patients with strictly compensated cirrhosis, where a cut-off of 12,5 g/dl discriminates patients more prone to decompensate. Given the independency from platelets count, the impact of low hemoglobin levels on decompensation might not just be explained with hypersplenism, but probably by a broader impact of PH on hemoglobin combining spleen destructions, portal hypertensive gastropathy, lower absorption of iron and vitamins, increasing, in turn, cardiac output and triggering decompensation. Given the observational nature of our study, we can only speculate on the mechanisms through which hemoglobin levels affect outcomes. However, to our knowledge, this is the first evidence showing that relatively low hemoglobin levels can negatively impact outcomes even in patients with strictly compensated cirrhosis.

Strengths and limits of our study. We confirmed the benefit of non-selective beta-blockers (NSBB) in a large monocentric cohort of patients with compensated cirrhosis, incorporating predictors and triggers for the first decompensation. Due to our selection criteria, these findings are applicable to centers that do not have access to hepatic venous pressure gradient (HVPG) measurements or liver stiffness measurements (LSM).

Limitations of our study stem from its observational nature. For instance, some key data, such as body mass index (BMI), were not consistently collected, which limited our ability to explore the impact of obesity on decompensation. Additionally, data on nutritional status were not available for all patients, which hindered a thorough understanding of the role of hemoglobin levels. Although the proportion of patients with alcohol-related cirrhosis was low, we could not adequately assess alcohol consumption for some patients. Alcohol abstinence was monitored at each visit, and

laboratory tests were checked for consistency, but the data were largely self-reported and lacked uniform collection of quantitative biomarkers. Finally, as our study was based on clinical practice, there was no placebo group for comparison. In patients with medium-large GEV, the NSBB group was compared to those receiving endoscopic variceal ligation (EVL), which, while effective in reducing the incidence of first variceal bleeding, did not impact other decompensation events.

5.6. Conclusions

Our findings have significant clinical implications. We confirmed the benefit of non-selective beta-blockers (NSBB) in preventing all types of decompensating events within a large, population-based cohort of patients with cirrhosis, including MASLD-related cirrhosis, and persistent clinically significant portal hypertension (CSPH) after etiological treatment.

We also explored the interaction between NSBB and decompensation triggers such as bacterial infections, revealing an interconnection that suggests the benefits of NSBB might extend beyond their hemodynamic effects on portal hypertension.

Additionally, we identified new predictors of decompensation, which could inform future prospective studies on the impact of overall nutritional status on the occurrence of first decompensation events.

Some of the preliminary results from this study were presented at the AISF Congress 2023, Rome, Italy – Turco L, Taru MG, Vitale G, Cappa FM, Berardi S, Baldan A, Di Donato R, Pianta P, Vero V, Vizioli L, Morelli MC. Non-selective beta-blockers lower the risk of first decompensation in patients with cirrhosis and enduring clinically significant portal hypertension after etiological treatment. Digestive and Liver Disease. 2024 Feb 1;56:S2. Rome, Italy. 14-15 March 2024.

Subsequently, the results were published in full text - Turco L*, Taru MG*, Vitale G, Stefanescu H, Mirici Cappa F, Berardi S, Baldan A, Di Donato R, Pianta P, Vero V, Vizioli L, Procopciuc LM, Procopet B, Morelli MC, Piscaglia F. β-blockers lower first decompensation in patients with cirrhosis and enduring portal hypertension after etiological treatment. Clin Gastroenterol Hepatol. 2024 Aug 27:S1542-3565(24)00780-8. doi: 10.1016/j.cgh.2024.08.012. Epub ahead of print. PMID: 39209198 (ISI IF 11.6, Q1) *Observation: Turco L (Internal Medicine Unit for the Treatment of Severe Organ Failure, IRCCS Azienda Ospedaliero-Universitaria di, Bologna, Italy, and Taru MG (Faculty of Medicine, "Iuliu Hatieganu" University of Medicine and Pharmacy, Cluj-Napoca, Romania) share first autorship

6. General Discussions

The validation of non-invasive scoring systems such as Agile 3+, Agile 4, and the FAST score, within Study 1 (187), marks a significant advancement in the management of patients with metabolic dysfunction-associated steatotic liver disease (MASLD). In our study encompassing 246 biopsy-confirmed NAFLD patients meeting MASLD criteria, we rigorously assessed these scores' efficacy in distinguishing advanced fibrosis, cirrhosis, and fibrotic MASH. The findings affirm the utility of these scores, aligning with previous research (116), and offering promising avenues for clinical application. Developed specifically for individuals with MASLD (63), Agile 3+ and Agile 4 scores serve multifaceted purposes. They not only identify advanced fibrosis and cirrhosis with commendable accuracy but also optimize positive predictive values, reducing the indeterminate "grey zone" (63). Our assessment revealed that the AUROC for Agile 3+ in detecting advanced fibrosis (≥F3) was excellent, albeit slightly lower than LSM-VCTE alone. However, Agile 3+ significantly curtailed the number of patients with indeterminate results, enhancing diagnostic accuracy. Similarly, Agile 4 demonstrated exceptional performance in discriminating cirrhosis (F4), with an AUROC marginally superior to LSM-VCTE. The application of a dual cut-off approach resulted in only 11.4% of patients remaining in the grey zone, underscoring the score's efficacy. Notably, both Agile scores outperformed the FIB-4 index, reinforcing their superiority. Nevertheless, we acknowledge the limitations of our study, that are primarily inherent in its retrospective nature.

By applying a multi-threshold approach within the meta-analysis (137, 138, 171) from Study 2 (188), we provided robust evidence on the applicability of two-dimensional shear wave elastography (2D-SWE) for identifying various stages of liver fibrosis in biopsy-proven MASLD. This methodology is significant in advancing the understanding of 2D-SWE's diagnostic capabilities and its potential for contributing to the standardization of cut-off values, a crucial step towards improving the consistency and reliability of liver fibrosis assessment in different clinical settings. The standardization of cut-off values could pave the way for broader consensus in clinical practice. According to the 2017 EFSUMB Guidelines (19), 2D-SWE technology has measurement biases that vary depending on the software method used. However, technological advancements, particularly efforts led by the Quantitative Image Biomarker Alliance (QIBA) (47), have contributed to a reduction in this variance, thereby improving the reliability of fibrosis staging across different ultrasound systems. Nevertheless, the cut-off values for non-VCTE (vibration-controlled transient elastography) elastography methods, such as 2D-SWE, still lack robust validation and should be interpreted cautiously in clinical practice. In this respect, our analysis also considered the impact of various patient demographics and clinical conditions on the diagnostic performance of 2D-SWE. Notably, our study determined optimized cut-off

values for different stages of liver fibrosis, achieving excellent sensitivity and specificity across all stages, with slight variations based on ethnicity, comorbidities and type of ultrasound machine. When analyzing the performance of 2D-SWE across different ultrasound manufacturers, we observed minor differences in the optimized cut-off values for fibrosis staging. For instance, SuperSonic Imagine's values closely aligned with the collective data from all ultrasound devices, whereas Canon Medical Systems/Toshiba and General Electric Healthcare reported slightly lower values. These variations underscore the importance of standardizing reporting and validation across different ultrasound modules to ensure consistent diagnostic outcomes. Our study distinguishes itself from previous meta-analyses (18, 169) through the application of a multi-level random effects model. Despite these strengths, we acknowledge certain limitations, such as variability in study designs and the reliance on published data only, which may have introduced some degree of bias. Future research should consider individual patient data meta-analyses to further refine these findings. Additionally, adopting the "intention to diagnose" method in future studies could improve the methodological quality and reliability of research in this field of non-invasive testing.

Study 3 (189) underscored the efficacy of non-selective beta-blockers (NSBB) in preventing the first decompensation event in a real-world cohort of patients with compensated cirrhosis and clinically significant portal hypertension (CSPH), who have already received treatment for their underlying etiologies, including MASLD-related cirrhosis. These findings align with previous research, which suggested the potential benefits of NSBB in this context. However, our study extended this knowledge by demonstrating that NSBB are beneficial across various etiologies of compensated cirrhosis with treated etiology, including MASLD-related cirrhosis and across different subgroups, such as patients with small GEV and SPSS only. We found that patients with persistent CSPH, despite etiological treatment, continue to benefit from NSBB, showing a lower rate of first hepatic decompensation, particularly in the prevention of ascites. Furthermore, our study highlighted the significance of certain risk factors in precipitating decompensation events. In particular, type 2 diabetes mellitus and low hemoglobin levels were identified as independent predictors of poor outcomes, underscoring the need for careful monitoring and management of these conditions in cirrhotic patients.

7.General Conclussions

In conclusion, Study 1 provides a comprehensive evaluation of several non-invasive diagnostic tests (NITs) in the context of metabolic dysfunction-associated fatty liver disease (MASLD). The validation of Agile 3+, Agile 4, and FAST scores in distinguishing various stages of liver fibrosis in Caucasian patients with biopsy-confirmed MASLD highlights their potential utility in clinical practice, particularly in enhancing diagnostic accuracy and reducing indeterminate results. Additionally, Study 2 supports the broad applicability of two-dimensional shear wave elastography (2D-SWE) for assessing different stages of liver fibrosis in biopsy-proven MASLD, emphasizing the need for careful consideration of individual patient factors and machine performance variations to ensure accurate evaluations. The findings presented in Study 3 underscore the clinical significance of non-selective beta-blockers (NSBB) in preventing decompensating events in patients with compensated cirrhosis, including those with MASLD-related cirrhosis and persistent clinically significant portal hypertension (CSPH). Study 3 also underscores the significance of factors included in the new definition of MASLD, such as type 2 diabetes mellitus, and their impact on disease progression and the risk of decompensation, regardless etiology. The interaction between NSBB and decompensation triggers, such as the presence of T2DM, or bacterial infections, suggest potential benefits that extend beyond their primary hemodynamic effects.

These conclusions collectively enhance our understanding of MASLD and its management, paving the way for improved patient outcomes through more informed clinical decision-making.

8. The originality and innovative contributions of the thesis

All the studies were conducted for the first time in Romania and represent some of the few studies conducted worldwide in this field.

The thesis has multiple original aspects, of which we highlight the following:

- Conducting the first study in the world that validated the utility of Agile 3+, Agile 4, and FAST scores in identifying different stages of liver fibrosis in biopsy-proven MASLD patients, primarily of Caucasian origin. It is important to highlight that previous studies were conducted on different populations, emphasizing the originality and significance of this research.
    - We validated the previously proposed cut-off values in the Caucasian population:
        - Using the cut-off of 0.451, Agile 3+ presented a Se = 90.41%, Sp = 79.77%, PPV = 65.35%, NPV = 95.17% and Acc = 82.93% for ruling out advanced fibrosis
        - Using the cut-off of 0.679, Agile 3+ presented a Se=76.71%, Sp=91.91%, PPV=80%, NPV=90.34% and Acc=87.40% for ruling-in advanced fibrosis
        - Using the cut-off of 0.251, Agile 4 presented a Se=96.55%, Sp=84.79%, PPV=45.90%, NPV=99.46%, and Acc=86.18% in ruling-out cirrhosis
        - Using the cut-off of 0.565, Agile 4 presented a Se=72.41%, Sp=94.47%, PPV=63.64%, NPV=96.24%, and Acc=91.87% in ruling-in cirrhosis
    - We set specific cut-off values for the Caucasian population:
        - Using the cut-off of 0.480, Agile 3+ presented a Se=90.41%, Sp=82.66%, PPV=68.75%, NPV=95.33%, and Acc=84.96% for ruling out advanced fibrosis
        - Using the cut-off of 0.680, Agile 3+ presented a Se=76.71%, Sp=92.49%, PPV=81.17%, NPV=90.40%, and Acc=87.81% for ruling-in advanced fibrosis
        - Using the cut-off of 0.380, Agile 4 presented a Se=93.10%, Sp=90.78%, PPV=57.44%, NPV=98.99%, and Acc=91.05% for ruling-out cirrhosis

        - Using the cut-off of 0.520, Agile 4 presented a Se=75.86%, Sp=94.01%, PPV=62.86%, NPV=96.68%, and Acc=91.87% in ruling-in cirrhosis
    - Agile 3+ and Agile 4 scores significantly reduced the number of patients remained in the so-called "grey zone" (indeterminate results), wile exhibiting excellent diagnostic accuracy
        - By using Agile 3+ standard cut-offs for advanced fibrosis, 0.451 and 0.679 and LSM-VCTE standard cut-offs of 8 kPa and 12 kPa, the proportion of patients that were left unclassified were 12.6% versus 21.9%
        - By using Agile 4 standard cut-ffs for cirrhosis, namely 0.251 and 0.565, and the LSM-VCTE cut-offs of 8 kPa and 20 kPa, then 10 kPa and 20 kPa, the proportion of patients that were left unclassified were 11.4%, versus 39.4% and 26.8%, respectively
    - The FAST score exhibited an acceptable performance for depicting fibrotic MASH in the Caucasian population. It outperformed simple scores such as FIB-4 and APRI, but was not significantly superior than LSM-VCTE alone
- Performing the first multi-level random effects model meta-analysis of 2D-SWE for assessing liver fibrosis in biopsy-proven MASLD, demonstrating excellent diagnostic accuracy based on evidence from the largest cohort of biopsy-proven MASLD patients (2,223 subjects). This study was crucial in establishing cut-off values, as prior to this analysis, the performance of 2D-SWE in MASLD was not standardized. This study will enhance the role of 2D-SWE in assessing liver fibrosis, and our proposed cut-off values may be included in future practice guidelines.
    - When all ultrasound devices were considered together:
        - The optimal cut-off for depicting mild fibrosis was 6.432 kPa
        - The optimal cut-off for depicting significant fibrosis was 8.174 kPa
        - The optimal cut-off for depicting advanced fibrosis was 9.418 kPa
        - The optimal cut-off for depicting cirrhosis was 11.548 kPa
    - When SSI ultrasound devices were considered:
        - The optimal cut-off for depicting mild fibrosis was 7.305 kPa
        - The optimal cut-off for depicting significant fibrosis was 8.284 kPa
        - The optimal cut-off for depicting advanced fibrosis was 10.172 kPa
        - The optimal cut-off for depicting cirrhosis was 11.848 kPa

- Obtaining, for the first time, results that demonstrated the potential for cut-off standardization of 2D-SWE, offering promising directions for future advancements in the field. However, it is essential to consider individual patient factors and variations in machine performance when interpreting these results.
- We evaluated the accuracy of 2D-SWE cut-off values in different disease prevalences of different clinical scenarios and we calculated the NPV and PPV for different stages of liver fibrosis (pre-test probability) in different subpopulations
    - When all ultrasound devices were considered together, at a pre-test probability of 30%, the cut-off of 6.030 kPa presented a NPV of 0.923 for ruling-out significant fibrosis
    - When all ultrasound devices were considered together, at a pre-test probability of 30%, the cut-off of 9.418 kPa presented a NPV of 0.900 for ruling-out advanced fibrosis
    - When all ultrasound devices were considered together, at a pre-test probability of 60%, the cut-off of 13.634 kPa presented a PPV of 0.904 for ruling-in advanced fibrosis
    - When only SSI ultrasound devices were considered, at a pre-test probability of 30%, a cut-off value of 6.337 kPa presented a NPV of 0.922 for ruling-out significant fibrosis
    - When only SSI ultrasound devices were considered, at a pre-test probability of 30%, a cut-off value of 7.370 kPa presented a NPV of 0.935 for ruling-out advanced fibrosis
    - When only SSI ultrasound devices were considered, at a pre-test probability of 60%, a cut-off value of 15.590 kPa presented a PPV of 0.935 for ruling-in cirrhosis
- We highlighted the potential of a widespread applicability of 2D-SWE for assessing liver fibrosis
- Demonstrating that non-selective beta-blockers (NSBB) lower the risk of the first decompensation event in patients with compensated cirrhosis and clinically significant portal hypertension (CSPH) with treated etiology, two years following etiological treatment, including MASLD-related compensated cirrhosis. The benefit of NSBB on decompensation was maintained in patients with small gastroesophageal varices (GEV), in those with significant portal hypertension even without GEV, and across various etiologies. This finding could significantly impact clinical practice regarding the initiation of NSBB treatment.
    - Patients on-NSBB had a significantly lower rate of first decompensation than patients off-NSBB: 16% vs 44%

  - In patients with small GEV, first decompensation occurred in 17/99 (17%) vs 46/10 (43%) for on-NSBB and off-NSBB
  - In patients with SPSS only, first decompensation occurred in 2/24 (8%) vs 36/83 (43%) for on-NSBB and off-NSBB
- We objectively assessed the critical role of metabolic factors, such as type 2 diabetes mellitus, in driving liver disease progression and triggering the first decompensation event.
  - Presence of type 2 diabetes mellitus was significantly higher in patients who presented the first decompensation event, 45% vs 30%
  - At univariate and multivariate cox regression-analysis, type 2 diabetes melitus was an independent predictor of first decompensation
- We objectively assessed the critical role of other factors in driving liver disease progression and in triggering the first decompensation event
  - Patients with compensated cirrhosis who presented the first decompensation event had a significant higher rate of bacterial infections than those that remained compensated 44% vs 10%
  - We discovered that low hemoglobin levels had a significant impact on patients with strictly compensated cirrhosis. Specifically, a hemoglobin threshold of 12.5 g/dL effectively distinguished patients at risk of presenting the first decompensation event

REFERENCES

1. Rinella ME, Lazarus JV, Ratziu V, Francque SM, Sanyal AJ, Kanwal F, et al. A multi-society Delphi consensus statement on new fatty liver disease nomenclature. Hepatology. 2023.
2. Riazi K, Azhari H, Charette JH, Underwood FE, King JA, Afshar EE, et al. The prevalence and incidence of NAFLD worldwide: a systematic review and meta-analysis. Lancet Gastroenterol Hepatol. 2022;7(9):851-61.
3. Le MH, Yeo YH, Li X, Li J, Zou B, Wu Y, et al. 2019 Global NAFLD Prevalence: A Systematic Review and Meta-analysis. Clin Gastroenterol Hepatol. 2022;20(12):2809-17 e28.
4. Younossi ZM, Koenig AB, Abdelatif D, Fazel Y, Henry L, Wymer M. Global epidemiology of nonalcoholic fatty liver disease-Meta-analytic assessment of prevalence, incidence, and outcomes. Hepatology. 2016;64(1):73-84.
5. Pimpin L, Cortez-Pinto H, Negro F, Corbould E, Lazarus JV, Webber L, et al. Burden of liver disease in Europe: Epidemiology and analysis of risk factors to identify prevention policies. J Hepatol. 2018;69(3):718-35.
6. Garcia-Tsao G. Nonalcoholic Steatohepatitis - Opportunities and Challenges. N Engl J Med. 2021;385(17):1615-7.
7. Loomba R, Friedman SL, Shulman GI. Mechanisms and disease consequences of nonalcoholic fatty liver disease. Cell. 2021;184(10):2537-64.
8. Allen AM, Therneau TM, Ahmed OT, Gidener T, Mara KC, Larson JJ, et al. Clinical course of non-alcoholic fatty liver disease and the implications for clinical trial design. J Hepatol. 2022;77(5):1237-45.
9. Diehl AM, Day C. Cause, Pathogenesis, and Treatment of Nonalcoholic Steatohepatitis. N Engl J Med. 2017;377(21):2063-72.
10. Kleiner DE, Brunt EM, Van Natta M, Behling C, Contos MJ, Cummings OW, et al. Design and validation of a histological scoring system for nonalcoholic fatty liver disease. Hepatology. 2005;41(6):1313-21.
11. Zhou JH, Cai JJ, She ZG, Li HL. Noninvasive evaluation of nonalcoholic fatty liver disease: Current evidence and practice. World J Gastroenterol. 2019;25(11):1307-26.
12. Ratziu V, Charlotte F, Heurtier A, Gombert S, Giral P, Bruckert E, et al. Sampling variability of liver biopsy in nonalcoholic fatty liver disease. Gastroenterology. 2005;128(7):1898-906.
13. Dulai PS, Singh S, Patel J, Soni M, Prokop LJ, Younossi Z, et al. Increased risk of mortality by fibrosis stage in nonalcoholic fatty liver disease: Systematic review and meta-analysis. Hepatology. 2017;65(5):1557-65.
14. Taylor RS, Taylor RJ, Bayliss S, Hagström H, Nasr P, Schattenberg JM, et al. Association Between Fibrosis Stage and Outcomes of Patients With Nonalcoholic Fatty Liver Disease: A Systematic Review and Meta-Analysis. Gastroenterology. 2020;158(6):1611-25.e12.
15. Sanyal AJ, Van Natta ML, Clark J, Neuschwander-Tetri BA, Diehl A, Dasarathy S, et al. Prospective Study of Outcomes in Adults with Nonalcoholic Fatty Liver Disease. N Engl J Med. 2021;385(17):1559-69.
16. Ng CH, Lim WH, Hui Lim GE, Hao Tan DJ, Syn N, Muthiah MD, et al. Mortality Outcomes by Fibrosis Stage in Nonalcoholic Fatty Liver Disease: A Systematic Review and Meta-analysis. Clinical Gastroenterology and Hepatology. 2022.
17. Lazarus JV, Mark HE, Anstee QM, Arab JP, Batterham RL, Castera L, et al. Advancing the global public health agenda for NAFLD: a consensus statement. Nat Rev Gastroenterol Hepatol. 2022;19(1):60-78.
18. Selvaraj EA, Mozes FE, Jayaswal ANA, Zafarmand MH, Vali Y, Lee JA, et al. Diagnostic accuracy of elastography and magnetic resonance imaging in patients with NAFLD: A systematic review and meta-analysis. J Hepatol. 2021;75(4):770-85.
19. Dietrich CF, Bamber J, Berzigotti A, Bota S, Cantisani V, Castera L, et al. EFSUMB Guidelines and Recommendations on the Clinical Use of Liver Ultrasound Elastography, Update 2017 (Long Version). Ultraschall Med. 2017;38(4):e16-e47.
20. Ferraioli G, Wong VW, Castera L, Berzigotti A, Sporea I, Dietrich CF, et al. Liver Ultrasound Elastography: An Update to the World Federation for Ultrasound in Medicine and Biology Guidelines and Recommendations. Ultrasound Med Biol. 2018;44(12):2419-40.

21. Mikolasevic I, Orlic L, Franjic N, Hauser G, Stimac D, Milic S. Transient elastography (FibroScan(®)) with controlled attenuation parameter in the assessment of liver steatosis and fibrosis in patients with nonalcoholic fatty liver disease - Where do we stand? World J Gastroenterol. 2016;22(32):7236-51.
22. Sandrin L, Fourquet B, Hasquenoph JM, Yon S, Fournier C, Mal F, et al. Transient elastography: a new noninvasive method for assessment of hepatic fibrosis. Ultrasound Med Biol. 2003;29(12):1705-13.
23. Xia B, Wang F, Friedrich-Rust M, Zhou F, Zhu J, Yang H, et al. Feasibility and Efficacy of Transient Elastography using the XL probe to diagnose liver fibrosis and cirrhosis: A meta-analysis. Medicine (Baltimore). 2018;97(39):e11816.
24. Arieira C, Monteiro S, Xavier S, Dias de Castro F, Magalhães J, Marinho C, et al. Transient elastography: should XL probe be used in all overweight patients? Scand J Gastroenterol. 2019;54(8):1022-6.
25. Sigrist RMS, Liau J, Kaffas AE, Chammas MC, Willmann JK. Ultrasound Elastography: Review of Techniques and Clinical Applications. Theranostics. 2017;7(5):1303-29.
26. Srinivasa Babu A, Wells ML, Teytelboym OM, Mackey JE, Miller FH, Yeh BM, et al. Elastography in Chronic Liver Disease: Modalities, Techniques, Limitations, and Future Directions. Radiographics. 2016;36(7):1987-2006.
27. Papatheodoridi M, Cholongitas E. Diagnosis of Non-alcoholic Fatty Liver Disease (NAFLD): Current Concepts. Curr Pharm Des. 2018;24(38):4574-86.
28. Kettaneh A, Marcellin P, Douvin C, Poupon R, Ziol M, Beaugrand M, et al. Features associated with success rate and performance of FibroScan measurements for the diagnosis of cirrhosis in HCV patients: a prospective study of 935 patients. J Hepatol. 2007;46(4):628-34.
29. Boursier J, Konate A, Guilluy M, Gorea G, Sawadogo A, Quemener E, et al. Learning curve and interobserver reproducibility evaluation of liver stiffness measurement by transient elastography. Eur J Gastroenterol Hepatol. 2008;20(7):693-701.
30. Wong GL, Wong VW, Chim AM, Yiu KK, Chu SH, Li MK, et al. Factors associated with unreliable liver stiffness measurement and its failure with transient elastography in the Chinese population. J Gastroenterol Hepatol. 2011;26(2):300-5.
31. Myers RP, Pomier-Layrargues G, Kirsch R, Pollett A, Duarte-Rojo A, Wong D, et al. Feasibility and diagnostic performance of the FibroScan XL probe for liver stiffness measurement in overweight and obese patients. Hepatology. 2012;55(1):199-208.
32. Coco B, Oliveri F, Maina AM, Ciccorossi P, Sacco R, Colombatto P, et al. Transient elastography: a new surrogate marker of liver fibrosis influenced by major changes of transaminases. J Viral Hepat. 2007;14(5):360-9.
33. Sagir A, Erhardt A, Schmitt M, Häussinger D. Transient elastography is unreliable for detection of cirrhosis in patients with acute liver damage. Hepatology. 2008;47(2):592-5.
34. Arena U, Vizzutti F, Corti G, Ambu S, Stasi C, Bresci S, et al. Acute viral hepatitis increases liver stiffness values measured by transient elastography. Hepatology. 2008;47(2):380-4.
35. Millonig G, Reimann FM, Friedrich S, Fonouni H, Mehrabi A, Büchler MW, et al. Extrahepatic cholestasis increases liver stiffness (FibroScan) irrespective of fibrosis. Hepatology. 2008;48(5):1718-23.
36. Millonig G, Friedrich S, Adolf S, Fonouni H, Golriz M, Mehrabi A, et al. Liver stiffness is directly influenced by central venous pressure. J Hepatol. 2010;52(2):206-10.
37. Petta S, Maida M, Macaluso FS, Di Marco V, Cammà C, Cabibi D, et al. The severity of steatosis influences liver stiffness measurement in patients with nonalcoholic fatty liver disease. Hepatology. 2015;62(4):1101-10.
38. Lupşor-Platon M, Feier D, Stefănescu H, Tamas A, Botan E, Sparchez Z, et al. Diagnostic accuracy of controlled attenuation parameter measured by transient elastography for the non-invasive assessment of liver steatosis: a prospective study. J Gastrointestin Liver Dis. 2015;24(1):35-42.
39. Gaia S, Carenzi S, Barilli AL, Bugianesi E, Smedile A, Brunello F, et al. Reliability of transient elastography for the detection of fibrosis in non-alcoholic fatty liver disease and chronic viral hepatitis. J Hepatol. 2011;54(1):64-71.
40. Wong VW, Irles M, Wong GL, Shili S, Chan AW, Merrouche W, et al. Unified interpretation of liver stiffness measurement by M and XL probes in non-alcoholic fatty liver disease. Gut. 2019;68(11):2057-64.
41. de Franchis R, Bosch J, Garcia-Tsao G, Reiberger T, Ripoll C. Baveno VII - Renewing consensus in portal hypertension. J Hepatol. 2022;76(4):959-74.
42. Lazarus JV, Castera L, Mark HE, Allen AM, Adams LA, Anstee QM, et al. Real-world evidence on non-invasive tests and associated cut-offs used to assess fibrosis in routine clinical practice. JHEP Rep. 2023;5(1):100596.
43. Sasso M, Beaugrand M, de Ledinghen V, Douvin C, Marcellin P, Poupon R, et al. Controlled attenuation parameter (CAP): a novel VCTE™ guided ultrasonic attenuation measurement for the evaluation of

hepatic steatosis: preliminary study and validation in a cohort of patients with chronic liver disease from various causes. Ultrasound Med Biol. 2010;36(11):1825-35.
44. Karlas T, Petroff D, Sasso M, Fan J-G, Mi Y-Q, de Lédinghen V, et al. Individual patient data meta-analysis of controlled attenuation parameter (CAP) technology for assessing steatosis. Journal of hepatology. 2017;66(5):1022-30.
45. Muller M, Gennisson JL, Deffieux T, Tanter M, Fink M. Quantitative viscoelasticity mapping of human liver using supersonic shear imaging: preliminary in vivo feasibility study. Ultrasound Med Biol. 2009;35(2):219-29.
46. Ferraioli G, Tinelli C, Zicchetti M, Above E, Poma G, Di Gregorio M, et al. Reproducibility of real-time shear wave elastography in the evaluation of liver elasticity. Eur J Radiol. 2012;81(11):3102-6.
47. Barr RG, Wilson SR, Rubens D, Garcia-Tsao G, Ferraioli G. Update to the Society of Radiologists in Ultrasound Liver Elastography Consensus Statement. Radiology. 2020;296(2):263-74.
48. Ferraioli G, Barr RG, Berzigotti A, Sporea I, Wong VWS, Reiberger T, et al. WFUMB Guideline/Guidance on Liver Multiparametric Ultrasound: Part 1. Update to 2018 Guidelines on Liver Ultrasound Elastography. Ultrasound in Medicine & Biology. 2024.
49. Cassinotto C, Lapuyade B, Mouries A, Hiriart J-B, Vergniol J, Gaye D, et al. Non-invasive assessment of liver fibrosis with impulse elastography: comparison of Supersonic Shear Imaging with ARFI and FibroScan®. Journal of hepatology. 2014;61(3):550-7.
50. Barr RG, Ferraioli G, Palmeri ML, Goodman ZD, Garcia-Tsao G, Rubin J, et al. Elastography Assessment of Liver Fibrosis: Society of Radiologists in Ultrasound Consensus Conference Statement. Radiology. 2015;276(3):845-61.
51. Cassinotto C, Anselme S, Jacq T, Irles-Depe M, Belgour A, Hermida M, et al. Inter-platform Variability of Liver Elastography: Pairwise Comparisons of Four Devices. Ultrasound in Medicine & Biology. 2022;48(11):2258-66.
52. Cassinotto C, Lapuyade B, Guiu B, Marraud des Grottes H, Piron L, Merrouche W, et al. Agreement Between 2-Dimensional Shear Wave and Transient Elastography Values for Diagnosis of Advanced Chronic Liver Disease. Clin Gastroenterol Hepatol. 2020;18(13):2971-9.e3.
53. Ferraioli G, Maiocchi L, Raciti MV, Tinelli C, De Silvestri A, Nichetti M, et al. Detection of Liver Steatosis With a Novel Ultrasound-Based Technique: A Pilot Study Using MRI-Derived Proton Density Fat Fraction as the Gold Standard. Clin Transl Gastroenterol. 2019;10(10):e00081.
54. Jeon SK, Lee JM, Joo I, Yoon JH, Lee DH, Lee JY, et al. Prospective Evaluation of Hepatic Steatosis Using Ultrasound Attenuation Imaging in Patients with Chronic Liver Disease with Magnetic Resonance Imaging Proton Density Fat Fraction as the Reference Standard. Ultrasound Med Biol. 2019;45(6):1407-16.
55. Sporea I, Bâldea V, Lupușoru R, Bende F, Mare R, Lazăr A, et al. Quantification of Steatosis and Fibrosis using a new system implemented in an ultrasound machine. Med Ultrason. 2020;22(3):265-71.
56. Jang JK, Lee ES, Seo JW, Kim YR, Kim SY, Cho YY, et al. Two-dimensional Shear-Wave Elastography and US Attenuation Imaging for Nonalcoholic Steatohepatitis Diagnosis: A Cross-sectional, Multicenter Study. Radiology. 2022;305(1):118-26.
57. Fujiwara Y, Kuroda H, Abe T, Ishida K, Oguri T, Noguchi S, et al. The B-Mode Image-Guided Ultrasound Attenuation Parameter Accurately Detects Hepatic Steatosis in Chronic Liver Disease. Ultrasound Med Biol. 2018;44(11):2223-32.
58. Kuroda H, Abe T, Fujiwara Y, Nagasawa T, Takikawa Y. Diagnostic accuracy of ultrasound-guided attenuation parameter as a noninvasive test for steatosis in non-alcoholic fatty liver disease. J Med Ultrason (2001). 2021;48(4):471-80.
59. Ogino Y, Wakui N, Nagai H, Igarashi Y. The ultrasound-guided attenuation parameter is useful in quantification of hepatic steatosis in non-alcoholic fatty liver disease. JGH Open. 2021;5(8):947-52.
60. Sugimoto K, Moriyasu F, Oshiro H, Takeuchi H, Yoshimasu Y, Kasai Y, et al. Clinical utilization of shear wave dispersion imaging in diffuse liver disease. Ultrasonography. 2020;39(1):3-10.
61. Zhang X-q, Zheng R-q, Jin J-y, Wang J-f, Zhang T, Zeng J. US shear-wave elastography dispersion for characterization of chronic liver disease. Radiology. 2022;305(3):597-605.
62. Lee DH, Lee JY, Bae JS, Yi NJ, Lee KW, Suh KS, et al. Shear-Wave Dispersion Slope from US Shear-Wave Elastography: Detection of Allograft Damage after Liver Transplantation. Radiology. 2019;293(2):327-33.
63. Sanyal AJ, Foucquier J, Younossi ZM, Harrison SA, Newsome PN, Chan WK, et al. Enhanced diagnosis of advanced fibrosis and cirrhosis in individuals with NAFLD using FibroScan-based Agile scores. J Hepatol. 2023;78(2):247-59.

64. Pennisi G, Enea M, Pandolfo A, Celsa C, Antonucci M, Ciccioli C, et al. AGILE 3+ Score for the Diagnosis of Advanced Fibrosis and for Predicting Liver-related Events in NAFLD. Clin Gastroenterol Hepatol. 2023;21(5):1293-302.e5.
65. Newsome PN, Sasso M, Deeks JJ, Paredes A, Boursier J, Chan WK, et al. FibroScan-AST (FAST) score for the non-invasive identification of patients with non-alcoholic steatohepatitis with significant activity and fibrosis: a prospective derivation and global validation study. Lancet Gastroenterol Hepatol. 2020;5(4):362-73.
66. Pandyarajan V, Gish RG, Alkhouri N, Noureddin M. Screening for Nonalcoholic Fatty Liver Disease in the Primary Care Clinic. Gastroenterol Hepatol (N Y). 2019;15(7):357-65.
67. Younossi ZM, Henry L. Epidemiology of non-alcoholic fatty liver disease and hepatocellular carcinoma. JHEP Rep. 2021;3(4):100305.
68. Zoller H, Tilg H. Nonalcoholic fatty liver disease and hepatocellular carcinoma. Metabolism. 2016;65(8):1151-60.
69. Berkan-Kawińska A, Piekarska A. Hepatocellular carcinoma in non-alcohol fatty liver disease - changing trends and specific challenges. Curr Med Res Opin. 2020;36(2):235-43.
70. Chettouh H, Lequoy M, Fartoux L, Vigouroux C, Desbois-Mouthon C. Hyperinsulinaemia and insulin signalling in the pathogenesis and the clinical course of hepatocellular carcinoma. Liver Int. 2015;35(10):2203-17.
71. Nyberg LM, Cheetham TC, Patton HM, Yang SJ, Chiang KM, Caparosa SL, et al. The Natural History of NAFLD, a Community-Based Study at a Large Health Care Delivery System in the United States. Hepatol Commun. 2021;5(1):83-96.
72. Villanueva A. Hepatocellular Carcinoma. N Engl J Med. 2019;380(15):1450-62.
73. Stine JG, Wentworth BJ, Zimmet A, Rinella ME, Loomba R, Caldwell SH, et al. Systematic review with meta-analysis: risk of hepatocellular carcinoma in non-alcoholic steatohepatitis without cirrhosis compared to other liver diseases. Aliment Pharmacol Ther. 2018;48(7):696-703.
74. Björkström K, Widman L, Hagström H. Risk of hepatic and extrahepatic cancer in NAFLD: A population-based cohort study. Liver Int. 2022;42(4):820-8.
75. Simon TG, Roelstraete B, Sharma R, Khalili H, Hagström H, Ludvigsson JF. Cancer Risk in Patients With Biopsy-Confirmed Nonalcoholic Fatty Liver Disease: A Population-Based Cohort Study. Hepatology. 2021;74(5):2410-23.
76. Younossi ZM, Golabi P, Paik JM, Henry A, Van Dongen C, Henry L. The global epidemiology of nonalcoholic fatty liver disease (NAFLD) and nonalcoholic steatohepatitis (NASH): a systematic review. Hepatology. 2023;77(4):1335-47.
77. Michelotti A, de Scordilli M, Palmero L, Guardascione M, Masala M, Roncato R, et al. NAFLD-Related Hepatocarcinoma: The Malignant Side of Metabolic Syndrome. Cells. 2021;10(8).
78. Shah PA, Patil R, Harrison SA. NAFLD-related hepatocellular carcinoma: The growing challenge. Hepatology. 2023;77(1):323-38.
79. Ioannou GN. Epidemiology and risk-stratification of NAFLD-associated HCC. J Hepatol. 2021;75(6):1476-84.
80. Han J, Wang B, Liu W, Wang S, Chen R, Chen M, et al. Declining disease burden of HCC in the United States, 1992-2017: A population-based analysis. Hepatology. 2022;76(3):576-88.
81. Younossi Z, Stepanova M, Ong JP, Jacobson IM, Bugianesi E, Duseja A, et al. Nonalcoholic Steatohepatitis Is the Fastest Growing Cause of Hepatocellular Carcinoma in Liver Transplant Candidates. Clin Gastroenterol Hepatol. 2019;17(4):748-55.e3.
82. Haldar D, Kern B, Hodson J, Armstrong MJ, Adam R, Berlakovich G, et al. Outcomes of liver transplantation for non-alcoholic steatohepatitis: A European Liver Transplant Registry study. J Hepatol. 2019;71(2):313-22.
83. Hagström H, Nasr P, Ekstedt M, Hammar U, Stål P, Hultcrantz R, et al. Fibrosis stage but not NASH predicts mortality and time to development of severe liver disease in biopsy-proven NAFLD. J Hepatol. 2017;67(6):1265-73.
84. Moran-Lev H, Cohen S, Webb M, Yerushalmy-Feler A, Amir A, Gal DL, et al. Higher BMI predicts liver fibrosis among obese children and adolescents with NAFLD - an interventional pilot study. BMC Pediatr. 2021;21(1):385.
85. Correa-Rodríguez M, Izquierdo M, García-Hermoso A, Ramírez-Vélez R. Discriminatory capacity of obesity indicators as predictors of high liver fat in US adolescents. Eur J Clin Invest. 2022;52(1):e13654.
86. Visseren FLJ, Mach F, Smulders YM, Carballo D, Koskinas KC, Bäck M, et al. 2021 ESC Guidelines on cardiovascular disease prevention in clinical practice. Eur Heart J. 2021;42(34):3227-337.

87. Piscaglia F, Svegliati-Baroni G, Barchetti A, Pecorelli A, Marinelli S, Tiribelli C, et al. Clinical patterns of hepatocellular carcinoma in nonalcoholic fatty liver disease: a multicenter prospective study. Hepatology. 2016;63(3):827-38.
88. Loomba R, Lim JK, Patton H, El-Serag HB. AGA Clinical Practice Update on Screening and Surveillance for Hepatocellular Carcinoma in Patients With Nonalcoholic Fatty Liver Disease: Expert Review. Gastroenterology. 2020;158(6):1822-30.
89. Llovet JM, Willoughby CE, Singal AG, Greten TF, Heikenwälder M, El-Serag HB, et al. Nonalcoholic steatohepatitis-related hepatocellular carcinoma: pathogenesis and treatment. Nat Rev Gastroenterol Hepatol. 2023;20(8):487-503.
90. Pons M, Rivera-Esteban J, Manzano R, Banares J, Bermudez M, Vargas V, et al. Non-Invasive Tests of Liver Fibrosis Help in Predicting the Development of Hepatocellular Carcinoma among Patients with NAFLD. J Clin Med. 2022;11(9).
91. Dhar D, Baglieri J, Kisseleva T, Brenner DA. Mechanisms of liver fibrosis and its role in liver cancer. Exp Biol Med (Maywood). 2020;245(2):96-108.
92. Valery PC, Laversanne M, Clark PJ, Petrick JL, McGlynn KA, Bray F. Projections of primary liver cancer to 2030 in 30 countries worldwide. Hepatology. 2018;67(2):600-11.
93. Kanwal F, Kramer JR, Mapakshi S, Natarajan Y, Chayanupatkul M, Richardson PA, et al. Risk of Hepatocellular Cancer in Patients With Non-Alcoholic Fatty Liver Disease. Gastroenterology. 2018;155(6):1828-37.e2.
94. Berzigotti A, Tsochatzis E, Boursier J, Castera L, Cazzagon N, Friedrich-Rust M, et al. EASL Clinical Practice Guidelines on non-invasive tests for evaluation of liver disease severity and prognosis – 2021 update. Journal of Hepatology. 2021;75(3):659-89.
95. Johnson AL, Hayward KL, Patel P, Horsfall LU, Cheah AEZ, Irvine KM, et al. Predicting Liver-Related Outcomes in People With Nonalcoholic Fatty Liver Disease: The Prognostic Value of Noninvasive Fibrosis Tests. Hepatol Commun. 2022;6(4):728-39.
96. Petta S, Sebastiani G, Viganò M, Ampuero J, Wai-Sun Wong V, Boursier J, et al. Monitoring Occurrence of Liver-Related Events and Survival by Transient Elastography in Patients With Nonalcoholic Fatty Liver Disease and Compensated Advanced Chronic Liver Disease. Clin Gastroenterol Hepatol. 2021;19(4):806-15.e5.
97. Boursier J, Hagström H, Ekstedt M, Moreau C, Bonacci M, Cure S, et al. Non-invasive tests accurately stratify patients with NAFLD based on their risk of liver-related events. J Hepatol. 2022;76(5):1013-20.
98. Ripoll C, Groszmann R, Garcia-Tsao G, Grace N, Burroughs A, Planas R, et al. Hepatic venous pressure gradient predicts clinical decompensation in patients with compensated cirrhosis. Gastroenterology. 2007;133(2):481-8.
99. Villanueva C, Albillos A, Genescà J, Garcia-Pagan JC, Calleja JL, Aracil C, et al. β blockers to prevent decompensation of cirrhosis in patients with clinically significant portal hypertension (PREDESCI): a randomised, double-blind, placebo-controlled, multicentre trial. Lancet. 2019;393(10181):1597-608.
100. Rabiee A, Deng Y, Ciarleglio M, Chan JL, Pons M, Genesca J, et al. Noninvasive predictors of clinically significant portal hypertension in NASH cirrhosis: Validation of ANTICIPATE models and development of a lab-based model. Hepatol Commun. 2022;6(12):3324-34.
101. Jachs M, Hartl L, Simbrunner B, Bauer D, Paternostro R, Scheiner B, et al. The Sequential Application of Baveno VII Criteria and VITRO Score Improves Diagnosis of Clinically Significant Portal Hypertension. Clin Gastroenterol Hepatol. 2023;21(7):1854-63.e10.
102. Dajti E, Ravaioli F, Marasco G, Alemanni LV, Colecchia L, Ferrarese A, et al. A Combined Baveno VII and Spleen Stiffness Algorithm to Improve the Noninvasive Diagnosis of Clinically Significant Portal Hypertension in Patients With Compensated Advanced Chronic Liver Disease. Am J Gastroenterol. 2022;117(11):1825-33.
103. Ferrusquía-Acosta J, Bassegoda O, Turco L, Reverter E, Pellone M, Bianchini M, et al. Agreement between wedged hepatic venous pressure and portal pressure in non-alcoholic steatohepatitis-related cirrhosis. J Hepatol. 2021;74(4):811-8.
104. Bassegoda O, Olivas P, Turco L, Mandorfer M, Serra-Burriel M, Tellez L, et al. Decompensation in Advanced Nonalcoholic Fatty Liver Disease May Occur at Lower Hepatic Venous Pressure Gradient Levels Than in Patients With Viral Disease. Clin Gastroenterol Hepatol. 2022;20(10):2276-86.e6.
105. Sanyal AJ, Van Natta ML, Clark J, Neuschwander-Tetri BA, Diehl A, Dasarathy S, et al. Prospective Study of Outcomes in Adults with Nonalcoholic Fatty Liver Disease. N Engl J Med. 2021;385(17):1559-69.
106. Brunt EM, Clouston AD, Goodman Z, Guy C, Kleiner DE, Lackner C, et al. Complexity of ballooned hepatocyte feature recognition: Defining a training atlas for artificial intelligence-based imaging in NAFLD. J Hepatol. 2022;76(5):1030-41.

107.Selvaraj EA, Mózes FE, Jayaswal ANA, Zafarmand MH, Vali Y, Lee JA, et al. Diagnostic accuracy of elastography and magnetic resonance imaging in patients with NAFLD: A systematic review and meta-analysis. J Hepatol. 2021;75(4):770-85.
108. Sanyal AJ, Castera L, Wong VW-S. Noninvasive Assessment of Liver Fibrosis in NAFLD. Clinical Gastroenterology and Hepatology. 2023;21(8):2026-39.
109.EAS L Clinical Practice Guidelines on non-invasive tests for evaluation of liver disease severity and prognosis - 2021 update. J Hepatol. 2021;75(3):659-89.
110. Chalasani N, Younossi Z, Lavine JE, Diehl AM, Brunt EM, Cusi K, et al. The diagnosis and management of non-alcoholic fatty liver disease: practice Guideline by the American Association for the Study of Liver Diseases, American College of Gastroenterology, and the American Gastroenterological Association. Hepatology. 2012;55(6):2005-23.
111. Bedossa P. Utility and appropriateness of the fatty liver inhibition of progression (FLIP) algorithm and steatosis, activity, and fibrosis (SAF) score in the evaluation of biopsies of nonalcoholic fatty liver disease. Hepatology. 2014;60(2):565-75.
112. Sterling RK, Lissen E, Clumeck N, Sola R, Correa MC, Montaner J, et al. Development of a simple noninvasive index to predict significant fibrosis in patients with HIV/HCV coinfection. Hepatology. 2006;43(6):1317-25.
113. Wai CT, Greenson JK, Fontana RJ, Kalbfleisch JD, Marrero JA, Conjeevaram HS, et al. A simple noninvasive index can predict both significant fibrosis and cirrhosis in patients with chronic hepatitis C. Hepatology. 2003;38(2):518-26.
114. Liver EAftSot. EASL-ALEH Clinical Practice Guidelines: Non-invasive tests for evaluation of liver disease severity and prognosis. Journal of hepatology. 2015;63(1):237-64.
115. Mózes FE, Lee JA, Selvaraj EA, Jayaswal ANA, Trauner M, Boursier J, et al. Diagnostic accuracy of non-invasive tests for advanced fibrosis in patients with NAFLD: an individual patient data meta-analysis. Gut. 2022;71(5):1006-19.
116. Dalbeni A, Lombardi R, Henrique M, Zoncapè M, Pennisi G, Petta S, et al. Diagnostic accuracy of AGILE3+ score for advanced fibrosis in patients with non-alcoholic fatty liver disease: A systematic review and meta-analysis. Hepatology. 2023.
117. Pons M, Augustin S, Scheiner B, Guillaume M, Rosselli M, Rodrigues SG, et al. Noninvasive Diagnosis of Portal Hypertension in Patients With Compensated Advanced Chronic Liver Disease. Am J Gastroenterol. 2021;116(4):723-32.
118. Miura K, Hayashi H, Kamada Y, Fujii H, Takahashi H, Oeda S, et al. Agile 3+ and Agile 4, noninvasive tests for liver fibrosis, are excellent formulae to predict liver-related events in nonalcoholic fatty liver disease. Hepatol Res. 2023;53(10):978-88.
119. Paternostro R, Jachs M, Hartl L, Simbrunner B, Scheiner B, Bauer D, et al. Diabetes impairs the haemodynamic response to non-selective betablockers in compensated cirrhosis and predisposes to hepatic decompensation. Aliment Pharmacol Ther. 2023;58(8):805-13.
120. Ravaioli F, Dajti E, Mantovani A, Newsome PN, Targher G, Colecchia A. Diagnostic accuracy of FibroScan-AST (FAST) score for the non-invasive identification of patients with fibrotic non-alcoholic steatohepatitis: a systematic review and meta-analysis. Gut. 2023;72(7):1399-409.
121. Kanwal F, Shubrook JH, Adams LA, Pfotenhauer K, Wai-Sun Wong V, Wright E, et al. Clinical Care Pathway for the Risk Stratification and Management of Patients With Nonalcoholic Fatty Liver Disease. Gastroenterology. 2021;161(5):1657-69.
122. Hashida R, Nakano D, Kawaguchi M, Younossi ZM, Kawaguchi T. Changing from NAFLD to MASLD: The Implications for health related quality of life data. Journal of Hepatology. 2024.
123. Tracey GS, Bjorn R, Hannes H, Johan S, Jonas FL. Non-alcoholic fatty liver disease and incident major adverse cardiovascular events: results from a nationwide histology cohort. Gut. 2022;71(9):1867.
124. Lazarus JV, Mark HE, Anstee QM, Arab JP, Batterham RL, Castera L, et al. Advancing the global public health agenda for NAFLD: a consensus statement. Nat Rev Gastroenterol Hepatol. 2022;19(1):60-78.
125. Taru MG, Neamti L, Taru V, Procopciuc LM, Procopet B, Lupsor-Platon M. How to Identify Advanced Fibrosis in Adult Patients with Non-Alcoholic Fatty Liver Disease (NAFLD) and Non-Alcoholic Steatohepatitis (NASH) Using Ultrasound Elastography-A Review of the Literature and Proposed Multistep Approach. Diagnostics (Basel). 2023;13(4).
126. Harrison SA, Taub R, Neff GW, Lucas KJ, Labriola D, Moussa SE, et al. Resmetirom for nonalcoholic fatty liver disease: a randomized, double-blind, placebo-controlled phase 3 trial. Nature Medicine. 2023;29(11):2919-28.
127. Boursier J, Vergniol J, Guillet A, Hiriart JB, Lannes A, Le Bail B, et al. Diagnostic accuracy and prognostic significance of blood fibrosis tests and liver stiffness measurement by FibroScan in non-alcoholic fatty liver disease. Journal of Hepatology. 2016;65(3):570-8.

128. Mulazzani L, Salvatore V, Ravaioli F, Allegretti G, Matassoni F, Granata R, et al. Point shear wave ultrasound elastography with Esaote compared to real-time 2D shear wave elastography with supersonic imagine for the quantification of liver stiffness. Journal of Ultrasound. 2017;20(3):213-25.
129. Liu F, Bi M, Jing X, Ding H, Zeng J, Zheng R, et al. Multiparametric US for Identifying Metabolic Dysfunction–associated Steatohepatitis: A Prospective Multicenter Study. Radiology. 2024;310(3):e232416.
130. Kaplan DE, Ripoll C, Thiele M, Fortune BE, Simonetto DA, Garcia-Tsao G, et al. AASLD Practice Guidance on risk stratification and management of portal hypertension and varices in cirrhosis. Hepatology. 9900.
131. Piscaglia F, Salvatore V, Mulazzani L, Cantisani V, Colecchia A, Di Donato R, et al. Differences in liver stiffness values obtained with new ultrasound elastography machines and Fibroscan: A comparative study. Dig Liver Dis. 2017;49(7):802-8.
132. Kjaergaard M, Lindvig KP, Thorhauge KH, Andersen P, Hansen JK, Kastrup N, et al. Using the ELF test, FIB-4 and NAFLD fibrosis score to screen the population for liver disease. Journal of Hepatology. 2023.
133. Moher D, Liberati A, Tetzlaff J, Altman DG, Group P. Preferred reporting items for systematic reviews and meta-analyses: the PRISMA statement. PLoS Med. 2009;6(7):e1000097.
134. Cohen JF, Deeks JJ, Hooft L, Salameh JP, Korevaar DA, Gatsonis C, et al. Preferred reporting items for journal and conference abstracts of systematic reviews and meta-analyses of diagnostic test accuracy studies (PRISMA-DTA for Abstracts): checklist, explanation, and elaboration. BMJ. 2021;372:n265.
135. Salameh JP, Bossuyt PM, McGrath TA, Thombs BD, Hyde CJ, Macaskill P, et al. Preferred reporting items for systematic review and meta-analysis of diagnostic test accuracy studies (PRISMA-DTA): explanation, elaboration, and checklist. BMJ. 2020;370:m2632.
136. Whiting PF, Rutjes AW, Westwood ME, Mallett S, Deeks JJ, Reitsma JB, et al. QUADAS-2: a revised tool for the quality assessment of diagnostic accuracy studies. Ann Intern Med. 2011;155(8):529-36.
137. Steinhauser S, Schumacher M, Rücker G. Modelling multiple thresholds in meta-analysis of diagnostic test accuracy studies. BMC Medical Research Methodology. 2016;16(1):97.
138. Schneider A, Linde K, Reitsma JB, Steinhauser S, Rücker G. A novel statistical model for analyzing data of a systematic review generates optimal cutoff values for fractional exhaled nitric oxide for asthma diagnosis. J Clin Epidemiol. 2017;92:69-78.
139. Organization WH. The Asia-Pacific perspective: redefining obesity and its treatment. 2000.
140. Haam J-H, Kim BT, Kim EM, Kwon H, Kang J-H, Park JH, et al. Diagnosis of obesity: 2022 update of clinical practice guidelines for obesity by the Korean Society for the Study of Obesity. Journal of obesity & metabolic syndrome. 2023;32(2):121.
141. Obesity: preventing and managing the global epidemic. Report of a WHO consultation. World Health Organ Tech Rep Ser. 2000;894:i-xii, 1-253.
142. Bürkner PC, Doebler P. Testing for publication bias in diagnostic meta-analysis: a simulation study. Stat Med. 2014;33(18):3061-77.
143. Lee MS, Bae JM, Joo SK, Woo H, Lee DH, Jung YJ, et al. Prospective comparison among transient elastography, supersonic shear imaging, and ARFI imaging for predicting fibrosis in nonalcoholic fatty liver disease. PLoS One. 2017;12(11):e0188321.
144. Takeuchi H, Sugimoto K, Oshiro H, Iwatsuka K, Kono S, Yoshimasu Y, et al. Liver fibrosis: noninvasive assessment using supersonic shear imaging and FIB4 index in patients with non-alcoholic fatty liver disease. J Med Ultrason (2001). 2018;45(2):243-9.
145. Jamialahmadi T, Nematy M, Jangjoo A, Goshayeshi L, Rezvani R, Ghaffarzadegan K, et al. Measurement of Liver Stiffness with 2D-Shear Wave Elastography (2D-SWE) in Bariatric Surgery Candidates Reveals Acceptable Diagnostic Yield Compared to Liver Biopsy. Obes Surg. 2019;29(8):2585-92.
146. Chen G, Yang JC, Zhang GX, Cheng Z, Du X. Evaluation of Six Noninvasive Methods for the Detection of Fibrosis in Chinese Patients with Obesity and Nonalcoholic Fatty Liver Disease. Obes Surg. 2022;32(11):3619-26.
147. Zhou J, Yan F, Xu J, Lu Q, Zhu X, Gao B, et al. Diagnosis of steatohepatitis and fibrosis in biopsy-proven nonalcoholic fatty liver diseases: including two-dimension real-time shear wave elastography and noninvasive fibrotic biomarker scores. Quant Imaging Med Surg. 2022;12(3):1800-14.
148. Kuroda H, Fujiwara Y, Abe T, Nagasawa T, Oguri T, Noguchi S, et al. Two-dimensional shear wave elastography and ultrasound-guided attenuation parameter for progressive non-alcoholic steatohepatitis. PLoS One. 2021;16(4):e0249493.
149. Imajo K, Honda Y, Kobayashi T, Nagai K, Ozaki A, Iwaki M, et al. Direct Comparison of US and MR Elastography for Staging Liver Fibrosis in Patients With Nonalcoholic Fatty Liver Disease. Clin Gastroenterol Hepatol. 2022;20(4):908-17.e11.

150. Kalaiyarasi K, Sanchalika A, Hsien Min L, Wei Ming Y, Vishalkumar S, Kuo Chao Y, et al. Transient Elastography Is the Best-Performing Non-Invasive Test of Liver Fibrosis in Obese Asian Patients with Non-Alcoholic Fatty Liver Disease: A Pilot, Cross-Sectional Study. Medicina (Kaunas). 2024;60(1).
151. Lee DH, Cho EJ, Bae JS, Lee JY, Yu SJ, Kim H, et al. Accuracy of Two-Dimensional Shear Wave Elastography and Attenuation Imaging for Evaluation of Patients With Nonalcoholic Steatohepatitis. Clin Gastroenterol Hepatol. 2021;19(4):797-805.e7.
152. Laroia ST, Vellore Srinivasan S, Yadav K, Rastogi A, Kumar S, Kumar G, et al. Performance of shear wave elastography: A single centre pilot study of mixed etiology liver disease patients with normal BMI. Australas J Ultrasound Med. 2021;24(3):120-36.
153. Kim JW, Lee CH, Kim B-H, Lee Y-S, Hwang S-Y, Park BN, et al. Ultrasonographic index for the diagnosis of non-alcoholic steatohepatitis in patients with non-alcoholic fatty liver disease. Quantitative Imaging in Medicine and Surgery. 2021;12(3):1815-29.
154. Ogino Y, Wakui N, Nagai H, Matsuda T. Comparison of strain elastography and shear wave elatography in diagnosis of fibrosis in nonalcoholic fatty liver disease. J Med Ultrason (2001). 2023;50(2):187-95.
155. Sugimoto K, Moriyasu F, Oshiro H, Takeuchi H, Abe M, Yoshimasu Y, et al. The role of multiparametric US of the liver for the evaluation of nonalcoholic steatohepatitis. Radiology. 2020;296(3):532-40.
156. Ozturk A, Mohammadi R, Pierce TT, Kamarthi S, Dhyani M, Grajo JR, et al. Diagnostic Accuracy of Shear Wave Elastography as a Non-invasive Biomarker of High-Risk Non-alcoholic Steatohepatitis in Patients with Non-alcoholic Fatty Liver Disease. Ultrasound Med Biol. 2020;46(4):972-80.
157. Sharpton SR, Tamaki N, Bettencourt R, Madamba E, Jung J, Liu A, et al. Diagnostic accuracy of two-dimensional shear wave elastography and transient elastography in nonalcoholic fatty liver disease. Therap Adv Gastroenterol. 2021;14:17562848211050436.
158. Furlan A, Tublin ME, Yu L, Chopra KB, Lippello A, Behari J. Comparison of 2D Shear Wave Elastography, Transient Elastography, and MR Elastography for the Diagnosis of Fibrosis in Patients With Nonalcoholic Fatty Liver Disease. AJR Am J Roentgenol. 2020;214(1):W20-w6.
159. Zhang YN, Fowler KJ, Boehringer AS, Montes V, Schlein AN, Covarrubias Y, et al. Comparative diagnostic performance of ultrasound shear wave elastography and magnetic resonance elastography for classifying fibrosis stage in adults with biopsy-proven nonalcoholic fatty liver disease. Eur Radiol. 2022;32(4):2457-69.
160. Cassinotto C, Boursier J, de Lédinghen V, Lebigot J, Lapuyade B, Cales P, et al. Liver stiffness in nonalcoholic fatty liver disease: A comparison of supersonic shear imaging, FibroScan, and ARFI with liver biopsy. Hepatology. 2016;63(6):1817-27.
161. Mendoza YP, Rodrigues SG, Delgado MG, Murgia G, Lange NF, Schropp J, et al. Inflammatory activity affects the accuracy of liver stiffness measurement by transient elastography but not by two-dimensional shear wave elastography in non-alcoholic fatty liver disease. Liver Int. 2022;42(1):102-11.
162. Hall TJ, Milkowski A, Garra B, Carson P, Palmeri M, Nightingale K, et al., editors. RSNA/QIBA: Shear wave speed as a biomarker for liver fibrosis staging. 2013 IEEE International Ultrasonics Symposium (IUS); 2013: IEEE.
163. Palmeri M, Nightingale K, Fielding S, Rouze N, Deng Y, Lynch T, et al., editors. RSNA QIBA ultrasound shear wave speed Phase II phantom study in viscoelastic media. 2015 IEEE International Ultrasonics Symposium (IUS); 2015: IEEE.
164. Ferraioli G, De Silvestri A, Lissandrin R, Maiocchi L, Tinelli C, Filice C, et al. Evaluation of Inter-System Variability in Liver Stiffness Measurements. Ultraschall Med. 2019;40(1):64-75.
165. Kaplan DE, Bosch J, Ripoll C, Thiele M, Fortune BE, Simonetto DA, et al. AASLD practice guidance on risk stratification and management of portal hypertension and varices in cirrhosis. Hepatology. 2023.
166. Rinella ME, Neuschwander-Tetri BA, Siddiqui MS, Abdelmalek MF, Caldwell S, Barb D, et al. AASLD Practice Guidance on the clinical assessment and management of nonalcoholic fatty liver disease. Hepatology. 2023;77(5):1797-835.
167. Ferraioli G, Barr RG, Berzigotti A, Sporea I, Wong VWS, Reiberger T, et al. WFUMB Guidelines/Guidance on Liver Multiparametric Ultrasound. Part 2: Guidance on Liver Fat Quantification. Ultrasound in medicine & biology. 2024.
168. Cassinotto C, Charrie A, Mouries A, Lapuyade B, Hiriart JB, Vergniol J, et al. Liver and spleen elastography using supersonic shear imaging for the non-invasive diagnosis of cirrhosis severity and oesophageal varices. Dig Liver Dis. 2015;47(8):695-701.
169. Herrmann E, de Lédinghen V, Cassinotto C, Chu WC, Leung VY, Ferraioli G, et al. Assessment of biopsy-proven liver fibrosis by two-dimensional shear wave elastography: An individual patient data-based meta-analysis. Hepatology. 2018;67(1):260-72.
170. Rosenberger KJ, Chu H, Lin L. Empirical comparisons of meta-analysis methods for diagnostic studies: a meta-epidemiological study. BMJ Open. 2022;12(5):e055336.

171. Hamza TH, Arends LR, van Houwelingen HC, Stijnen T. Multivariate random effects meta-analysis of diagnostic tests with multiple thresholds. BMC Medical Research Methodology. 2009;9(1):73.
172. D'Amico G, Morabito A, D'Amico M, Pasta L, Malizia G, Rebora P, et al. Clinical states of cirrhosis and competing risks. J Hepatol. 2018;68(3):563-76.
173. Perelló A, Escorsell A, Bru C, Gilabert R, Moitinho E, García-Pagán JC, et al. Wedged hepatic venous pressure adequately reflects portal pressure in hepatitis C virus-related cirrhosis. Hepatology. 1999;30(6):1393-7.
174. Turco L, Villanueva C, La Mura V, García-Pagán JC, Reiberger T, Genescà J, et al. Lowering Portal Pressure Improves Outcomes of Patients With Cirrhosis, With or Without Ascites: A Meta-Analysis. Clin Gastroenterol Hepatol. 2020;18(2):313-27.e6.
175. Turco L, García-Tsao G. Portal pressure reductions induced by nonselective beta-blockers improve outcomes and decrease mortality in patients with cirrhosis with and without ascites. Clin Liver Dis (Hoboken). 2022;20(1):1-4.
176. Turco L, Reiberger T, Vitale G, La Mura V. Carvedilol as the new non-selective beta-blocker of choice in patients with cirrhosis and portal hypertension. Liver Int. 2023;43(6):1183-94.
177. Tosetti G, Degasperi E, Farina E, Primignani M, Lampertico P. Carvedilol to reduce the risk of decompensation in patients with compensated cirrhosis: Is it really needed in patients with cured HCV or suppressed HBV? Journal of Hepatology. 2023;79(5):e200-e2.
178. Lens S, Baiges A, Alvarado-Tapias E, E LL, Martinez J, Fortea JI, et al. Clinical outcome and hemodynamic changes following HCV eradication with oral antiviral therapy in patients with clinically significant portal hypertension. J Hepatol. 2020;73(6):1415-24.
179. Nardelli S, Riggio O, Turco L, Gioia S, Puzzono M, Bianchini M, et al. Relevance of Spontaneous Portosystemic Shunts Detected with CT in Patients with Cirrhosis. Radiology. 2021;299(1):133-40.
180. Jangouk P, Turco L, De Oliveira A, Schepis F, Villa E, Garcia-Tsao G. Validating, deconstructing and refining Baveno criteria for ruling out high-risk varices in patients with compensated cirrhosis. Liver Int. 2017;37(8):1177-83.
181. Villanueva C, Albillos A, Genescà J, Garcia-Pagan JC, Brujats A, Calleja JL, et al. Bacterial infections adversely influence the risk of decompensation and survival in compensated cirrhosis. J Hepatol. 2021;75(3):589-99.
182. Sasso R, Rockey DC. Non-selective beta-blocker use in cirrhotic patients is associated with a reduced likelihood of hospitalisation for infection. Aliment Pharmacol Ther. 2021;53(3):418-25.
183. Senzolo M, Cholongitas E, Burra P, Leandro G, Thalheimer U, Patch D, et al. beta-Blockers protect against spontaneous bacterial peritonitis in cirrhotic patients: a meta-analysis. Liver Int. 2009;29(8):1189-93.
184. O'Beirne J, Skoien R, Leggett BA, Hartel GF, Gordon LG, Powell EE, et al. Diabetes mellitus and the progression of non-alcoholic fatty liver disease to decompensated cirrhosis: a retrospective cohort study. Med J Aust. 2023;219(8):358-65.
185. Scheiner B, Semmler G, Maurer F, Schwabl P, Bucsics TA, Paternostro R, et al. Prevalence of and risk factors for anaemia in patients with advanced chronic liver disease. Liver Int. 2020;40(1):194-204.
186. Pompili E, Baldassarre M, Zaccherini G, Tufoni M, Iannone G, Pratelli D, et al. Low haemoglobin level predicts early hospital readmission in patients with cirrhosis and acute decompensation. JHEP Rep. 2023;5(5):100698.
187. Taru M-G, Tefas C, Neamti L, Minciuna I, Taru V, Maniu A, et al. FAST and Agile–the MASLD drift: Validation of Agile 3+, Agile 4 and FAST scores in 246 biopsy-proven NAFLD patients meeting MASLD criteria of prevalent caucasian origin. Plos one. 2024;19(5):e0303971.
188. Taru M-G, Leucuta D-C, Ferri S, Hashim A, Orasan O, Procopet B, et al. WED-232-YI Diagnostic accuracy of two-dimensional shear wave elastography (2D-SWE) for non-invasive assessment of liver fibrosis in biopsy-proven metabolic dysfunction-associated steatotic liver disease (MASLD). Systematic-review and multi-level random effects model meta-analysis. Journal of Hepatology. 2024;80:S521.
189. Turco L, Taru M, Vitale G, Cappa FM, Berardi S, Baldan A, et al. Non-selective beta-blockers lower the risk of first decompensation in patients with cirrhosis and enduring clinically significant portal hypertension after etiological treatment. Digestive and Liver Disease. 2024;56:S2.

ANNEXES

Articles published in full text as a result of doctoral research, FIRST AUTHOR:

1. **Taru MG**, Neamti L, Taru V, Procopciuc LM, Procopet B, Lupsor-Platon M. How to Identify Advanced Fibrosis in Adult Patients with Non-Alcoholic Fatty Liver Disease (NAFLD) and Non-Alcoholic Steatohepatitis (NASH) Using Ultrasound Elastography—A Review of the Literature and Proposed Multistep Approach. Diagnostics. 2023 Feb 19;13(4):788. DOI:10.3390/diagnostics13040788 (ISI IF 3, Q1; WOS:000939326200001) (Chapter 1, The current state of knowledge)
2. **Taru MG**, Lupsor-Platon M. Exploring Opportunities to Enhance the Screening and Surveillance of Hepatocellular Carcinoma in Non-Alcoholic Fatty Liver Disease (NAFLD) through Risk Stratification Algorithms Incorporating Ultrasound Elastography. Cancers. 2023 Aug 14;15(16):4097. DOI:10.3390/cancers15164097 (ISI IF 4.5, Q1; WOS:001057069300001) (Chapter 1, The current state of knowledge)
3. **Taru MG**, Tefas C, Neamti L, Minciuna I, Taru V, Maniu A, Rusu I, Petrushev B, Procopciuc LM, Leucuta DC, Procopet B, Ferri S, Lupsor-Platon M, Stefanescu H. FAST and Agile–the MASLD drift: Validation of Agile 3+, Agile 4 and FAST scores in 246 biopsy-proven NAFLD patients meeting MASLD criteria of prevalent caucasian origin. PloS one. 2024 May 23;19(5): e0303971. DOI:10.1371/journal.pone.0303971 (ISI IF 2.9, Q1; WOS:001231237700084) (Personal contribution, Chapter 3)
4. Turco L*, **Taru MG***, Vitale G, Stefanescu H, Mirici Cappa F, Berardi S, Baldan A, Di Donato R, Pianta P, Vero V, Vizioli L, Procopciuc LM, Procopet B, Morelli MC, Piscaglia F. β-blockers lower first decompensation in patients with cirrhosis and enduring portal hypertension after etiological treatment. Clin Gastroenterol Hepatol. 2024 Aug 27:S1542-3565(24)00780-8. doi: 10.1016/j.cgh.2024.08.012. Epub ahead of print. PMID: 39209198 (ISI IF 11.6, Q1) **Observation: Turco L (Internal Medicine Unit for the Treatment of Severe Organ Failure, IRCCS Azienda Ospedaliero-Universitaria di, Bologna, Italy, and Taru MG (Faculty of Medicine, "Iuliu Hatieganu" University of Medicine and Pharmacy, Cluj-Napoca, Romania) share first autorship*
5. **Taru MG,** Leucuta DC, Lupsor-Platon M, Turco L, Ferri S, Hashim A, Orasan OH, Procopet B, Stefanescu H, Morelli MC, Piscaglia F. Diagnostic accuracy of 2D-SWE ultrasound for liver fibrosis assessment in MASLD: A multi-level random effects model meta-analysis. Hepatology.:10-97.

AWARDS and SCHOLARSHIPS received for contributions in the field of the doctoral thesis:

1. **Young Investigator Scholarship** – Free registration for EASL Congress 2024. Milan, Italy. 5-8 June 2024 for the abstract entitled "Diagnostic accuracy of two-dimensional shear wave elastography (2D-SWE) for non-invasive assessment of liver fibrosis in biopsy-proven metabolic dysfunction-associated steatotic liver disease (MASLD). Systematic-review and multi-level random effects model meta-analysis".
2. **Scholarship (H.G. no. 118/2023)** offered by The Study Loans and Scholarships Agency, The Ministry of Education, Romania (15000 EUR).

Abstracts presented at international conferences as a result of doctoral research, FIRST AUTHOR:

1. **Taru MG**, Leucuta DC, Neamti L, Maniu A, Taru V, Petrushev B, Rusu I, Tefas C, Fischer P, Terec AI, Procopciuc LM. Diagnostic accuracy of VCTE and 2D-SWE in biopsy-proven nafld and performance of two-step approaches to predict advanced fibrosis. In Hepatology 2023 oct 1 (vol. 78, pp. s791-s792). Two Commerce sq, 2001 Market st, Philadelphia, PA 19103 USA: Lippincott Williams & Wilkins. The Liver Meeting. Boston, Massachusetts. 10-14 November 2023.
2. **Taru MG**, Taru V, Minciuna I, Petrushev B, Rusu I, Fischer P et all. The controlled attenuation parameter has limited value in assessing the degree of steatosis in different stages of compensated chronic liver disease. EASL NAFLD SUMMIT. Dublin, Ireland. 15-17 September 2022.
3. **Taru MG**, Tefas C, Neamti L, Minciuna I, Taru V, Maniu A et all. FAST and Agile – the MASLD Drift: validation of Agile 3+, Agile 4 and FAST scores in 246 biopsy-proven MASLD patients of prevalent caucasian origin. EASL Congress 2024. Milan, Italy. 5-8 June 2024.
4. **Taru MG**, Leucuta DC, Ferri S, Hashim A, Orasan O, Procopet B et all. Diagnostic accuracy of two-dimensional shear wave elastography (2D-SWE) for non-invasive assessment of liver fibrosis in biopsy-proven metabolic dysfunction-associated steatotic liver disease (MASLD). Systematic-review and multi-level random effects model meta-analysis. EASL Congress 2024. Milan, Italy. 5-8 June 2024.

Articles published in full text as a result of doctoral research, CO-AUTHOR:

1. Minciuna I, **Taru MG**, Procopet B, Stefanescu H. The Interplay between Liver Sinusoidal Endothelial Cells, Platelets, and Neutrophil Extracellular Traps in the Development and Progression of Metabolic Dysfunction-Associated Steatotic Liver Disease. Journal of Clinical Medicine. 2024 Feb 29;13(5):1406. https://doi.org/10.3390/jcm13051406 (**IF=3.9, Q2**)
2. Minciuna I, **Taru M**, Fodor A, Farcau ON, Fischer P, Radu C, Lupsor-Platon M, Stefanescu H, Procopet B. Multiparametric ultrasound evaluation of liver fibrosis,

steatosis, and viscosity in patients with chronic liver disease. Medical Ultrasonography. 2024 Jun 21;26(2):117-24. (**IF=2.7, Q3**)

3. Paternostro, R., Kwanten, W. J., Hofer, B. S., Semmler, G., Bagdadi, A., Luzko, I., Hernández-Gea, V., Graupera, I., García-Pagán, J. C., Saltini, D., Indulti, F., Schepis, F., Moga, L., Rautou, P.-E., Llop, E., Téllez, L., Albillos, A., Fortea, J. I., Puente, A., Tosetti, G., Primignani, M., Zipprich, A., Vuille-Lessard, E., Berzigotti, A., Taru, **M.-G., Taru**, V., Procopet, B., Jansen, C., Praktiknjo, M., Gu, W., Trebicka, J., Ibanez-Samaniego, L., Bañares, R., Rivera-Esteban, J., Pericas, J. M., Genesca, J., Alvarado, E., Villanueva, C., Larrue, H., Bureau, C., Laleman, W., Ardevol, A., Masnou, H., Vanwolleghem, T., Trauner, M., Mandorfer, M., Francque, S., Reiberger, T., a study by the Baveno Cooperation: an EASL consortium. (2024). Hepatic venous pressure gradient predicts risk of hepatic decompensation and liver-related mortality in patients with MASLD. Journal of Hepatology. Published: May 30, 2024. DOI: https://doi.org/10.1016/j.jhep.2024.05.033 (**IF=25.7, Q1**)

Abstracts presented at international conferences as a result of doctoral research, CO-AUTHOR:

1. Turco L, **Taru MG**, Vitale G, Cappa FM, Berardi S, Baldan A, Di Donato R, Pianta P, Vero V, Vizioli L, Morelli MC. Non-selective beta-blockers lower the risk of first decompensation in patients with cirrhosis and enduring clinically significant portal hypertension after etiological treatment. Digestive and Liver Disease. 2024 Feb 1;56:S2. Rome, Italy. 14-15 March 2024.
2. Taru V, **Taru MG**, Petrushev B, Ioana R, Stefanescu H, Fodor A, Ignat MD, Petra F, Nicoara-Farcau O, Platon M, Procopet B. Recently validated non-invasive tests for liver fibrosis assessment have great performance in identifying NASH patients at risk for decompensation. Journal of Hepatology. 2023 Jun 1;78:S295-6. Viena, Austria. 21-24 June 2023.
3. Paternostro R, Kwanten WJ, Hofer BS, Semmler G, Bagdadi A, Luzko I, Hernandez-Gea V, Graupera I, **M Taru**, Saltini D, Indulti F. Natural history of patients with NAFLD-associated compensated advanced chronic liver disease stratified according to severity of portal hypertension. Zeitschrift für Gastroenterologie. 2023 May;61(05):P31.
4. Minciuna I, **Taru M**, Farcau ON, Platon-Lupsor M, Stefanescu H, Procopet B. Multiparametric ultrasound evaluation of liver fibrosis, steatosis and viscosity in patients with chronic liver disease. Ultrasound in Medicine and Biology. 2022 Jan 1;48:S16. Timisoara, Romania. 25-28 May 2022.
5. Cozma A, Terec IA, **Taru MG**, Orasan O, Procopciuc LM. Correlation between metabolic-associated fatty liver disease and cardiovascular pathology: Insights from arterial stiffness, cardiac dysfunction, and atherosclerosis. Bonn, Germany. 5-7 October 2023.

Other contributions:

1. **Co-Speaker** (skills learning centre) – Liver and spleen elastography at the EASL Congress 2024, Milan, Italy, 5-8 June 2024.